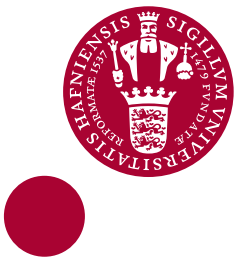

Microscopic and spectroscopic characterisation of waterlogged archaeological softwood from anoxic environments

Pedersen, Nanna Bjerregaard

Publication date:
2015

DEPARTMENT OF GEOSCIENCES AND
NATURAL RESOURCE MANAGEMENT

UNIVERSITY OF COPENHAGEN

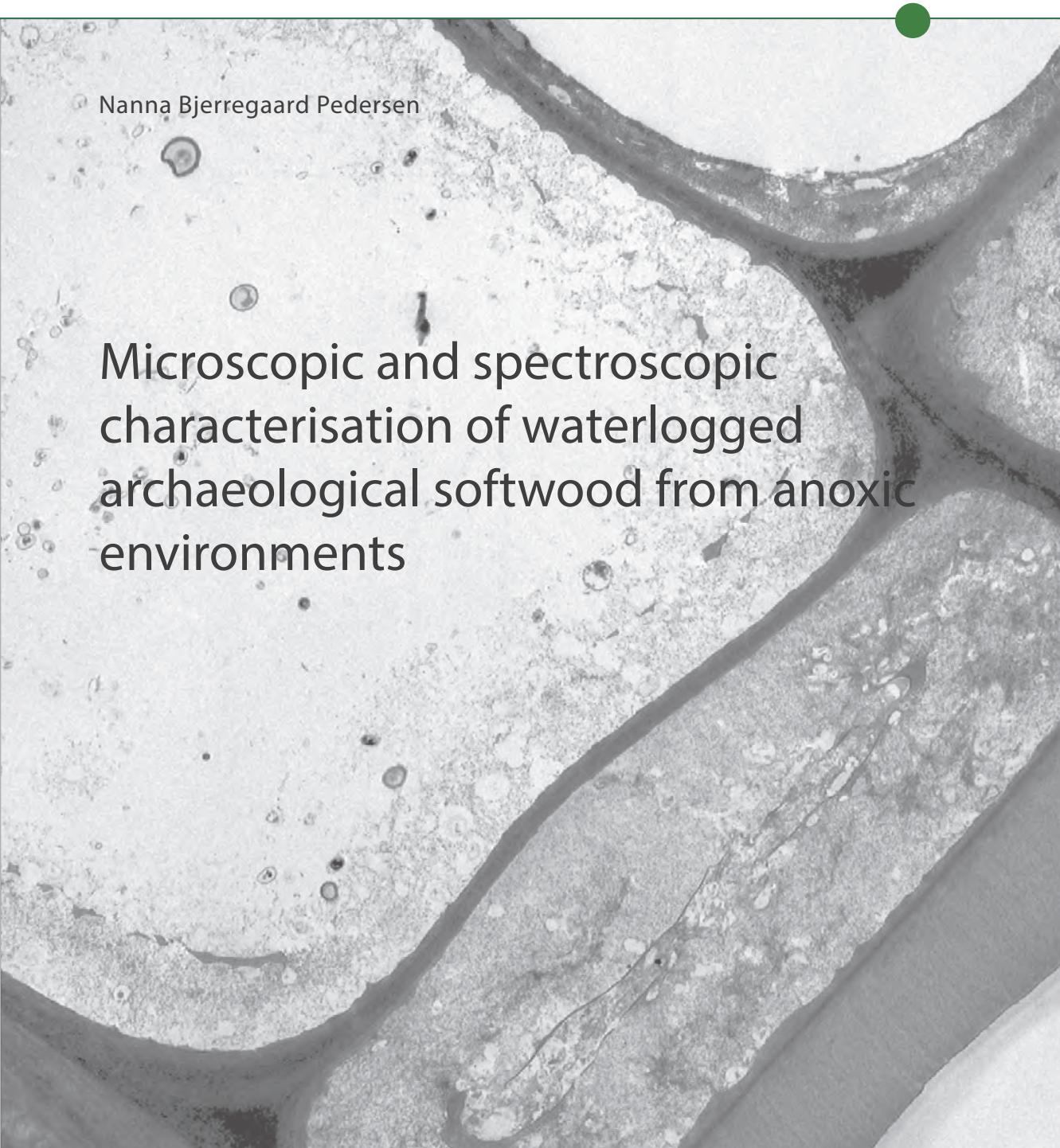

Nanna Bjerregaard Pedersen

Microscopic and spectroscopic characterisation of waterlogged archaeological softwood from anoxic environments

DEPARTMENT OF GEOSCIENCES AND
NATURAL RESOURCE MANAGEMENT

UNIVERSITY OF COPENHAGEN

Nanna Bjerregaard Pedersen

Microscopic and spectroscopic characterisation of waterlogged archaeological softwood from anoxic environments

Title	Microscopic and spectroscopic characterisation of waterlogged archaeological softwood from anoxic environments
Author	Nanna Bjerregaard Pedersen
Citation	Pedersen, N.B. (2015): Microscopic and spectroscopic characterisation of waterlogged archaeological softwood from anoxic environments. IGN PhD Thesis May 2015. Department of Geosciences and Natural Resource Management, University of Copenhagen, Frederiksberg. 125 pp.
Publisher	Department of Geosciences and Natural Resource Management University of Copenhagen Rolighedsvej 23 DK-1958 Frederiksberg C +45 353 31500 ign@ign.ku.dk www.ign.ku.dk
Responsible under the press law	Gertrud Jørgensen
ISBN	978-87-7903-707-6 (paper) 978-87-7903-708-3 (internet)
Lay-out	Inger Grønkjær Ulrich
Printed by	Novagraf A/S
Number printed	50
Order	Single issues are available from Department of Geosciences and Natural Resource Management Also published at www.ign.ku.dk.

Academic advisor

Professor Claus Felby
University of Copenhagen, Faculty of Science,
Department of Geosciences and Natural Resource Management

Co-advised by

Senior researcher Lisbeth Garbrecht Thygesen
University of Copenhagen, Faculty of Science,
Department of Geosciences and Natural Resource Management

Senior researcher Poul Jensen
National Museum of Denmark, Conservation Department

Professor Charlotte Gjelstrup Björdal
University of Gothenburg, Faculty of Science, Department of Conservation

The PhD thesis was defended 8th of October 2014 at University of Copenhagen, Faculty of Science, Department of Geosciences and Natural Resource Management with the following assessment committee

Senior Researcher Søren Barsberg (chair)
Department of Geosciences and Natural Resource Management, Faculty of Science,
University of Copenhagen, Denmark

Professor David Gregory
National Museum of Denmark, Environmental Archaeology and Materials Science,
Copenhagen, Denmark

Senior Researcher Gry Alfredsen
Norwegian Forest and Landscape Institute, Section for Wood Technology, Ås, Norway

Preface

Cycling of materials in nature is fascinating. It is amazing how a soil matrix and the abiotic and biotic factors acting there are able to turn highly complex materials into small molecules which will then again form part of larger organisms or materials. It is even more fascinating how extreme natural environments are able to supress the normal catabolic processes, and thereby preserve objects from past human cultures for centuries or millennia. I have had the chance to work with this aspect within wood decay and conservation in this PhD study.

My approach to studying wood decay is as a conservator. I have been fortunate to perform my PhD work within the research group Biomass Science and Technology at the University of Copenhagen, Department of Geosciences and Natural Resource Management, Section for Forest, Nature and Biomass. Studying waterlogged archaeological wood in a research group working with fundamental and applied aspects of biomass science have opened my eyes to the fact that other fields may benefit from the knowledge obtained in this study. In addition, I have realised that studying the chemistry of a material is a highly cross disciplinary task. It is essential to understand the complex nature of wood as a material to be able to combine chemical analysis and interpretation of this with the morphological characteristics of the wood.

Acknowledgements

I would like to thank Poul Jensen for setting up the initial contact to the research group Biomass Science and Technology at University of Copenhagen and to Claus Felby for giving me the opportunity to conduct a PhD study with the curiosity: Waterlogged archaeological wood. I would like to thank all my supervisors for helping me through the process from conservator to researcher; with a special thanks to Lisbeth Garbrecht Thygesen who has given me academic advice on a daily basis. In addition I would like to thank all my colleagues in the biomass group and at The National Museum for academic advice, technical help, and a great time over the years.

I would also like to thank my co-authors Notburger Gierlinger, Uwe Schmitt, and Gerald Koch for giving me the opportunity to perform measurements on my waterlogged poles. In this connection I would also like to thank the Thünen Institute and Johannes Kepel University for hosting me and Cost Action FP0802 for financial support.

The project would not have been possible without appropriate sample material, and I would like to thank the Museum of Copenhagen for hosting me for several days at Kongens Nytorv while the Norway spruce poles were retrieved, and for letting me use the material for research. I would also like to thank my colleague Hanne Billeschou Juhl at Bevaringscenter Nordjylland for obtaining several Scots pine poles. I would like to thank René Klaassen, SHR Timber Research (The Netherlands) and Madelene Skogbert, Studio Västsvensk Konservering for help in retrieving sample material that unfortunately turned out not to be suitable sample material in this context.
Last but not least, I would like to thank my wonderful family for going through this with me; with a special thanks to my husband who has supported me all way through this project both mentally and practically. Thanks to my two great sons who are very much a part of this project as they were born into it. Thanks to my very supportive parents in law who have done a great job in taking care of my family while I was taking care of my dead and smelly wood.

Table of contents

Preface **4**

Acknowledgements **5**

Table of contents **6**

Summary **8**

Dansk resumé **10**

List of publications **12**

List of conference contributions **14**

1 Introduction **15**

1.1 Background 15

1.2 Objective and hypothesis 17

1.3 Outline of thesis 18

2 Softwood ultrastructure and chemical composition **19**

2.1 Xylem composition 19

2.2 Chemical composition 20

2.3 Ultrastructure 22

2.4 Organisation of the biopolymers 24

3 Wood decay under oxygen restricted conditions **26**

3.1 Biotic versus abiotic decay 26

3.2 Biotic decay mechanisms 28

3.3 Wood decay under oxygen restricted conditions 29

4 Sample material **32**

4.1 Criteria for selection of sample material 32

4.2 Norway spruce poles from Kongens Nytorv 33

4.3 Scots pine pole from Nibe 40

5 Morphological decay pattern 42
5.1 Macroscopic appearance 42
5.2 Microscopic decay pattern in cross section 42
5.3 Decay viewed in longitudinal direction 51
5.4 Decay resistance 54
6 Chemical analysis of waterlogged wood 58
6.1 Chemical composition 58
6.2 Traditional analytical methods 58
6.3 Chemical imaging 67
7 Carbohydrate distribution and decay 69
7.1 Determination of polysaccharide degradation 69
7.2 Sound cell wall compartments 69
7.3 Erosion bacteria decay 71
8 Lignin distribution and decay 77
8.1 Determination of lignin degradation 77
8.2 Sound cell wall compartments 78
8.3 Erosion bacteria decay 79
9 Conclusions and perspectives 96
9.1 Conclusions 96
9.2 Significance for conservation 98
9.3 Significance for anaerobic biomass degradation 101
10 References 105
Appendix A 118
Appendix B 123
PAPER I-III 125

Summary

Waterlogged anoxic environments are extreme ecosystems with little support for wood degrading organisms and very slow abiotic decay mechanisms. Highly specialised facultative anaerobic erosion bacteria consortia are able to decay several different wood species in a great span of waterlogged (near) anoxic ecosystems. The decay is slow and incomplete which makes it possible for archaeological wooden objects to be preserved for millennia. The archaeological wood is rich in cultural information due to the unique degradation pattern that preserves original dimensions and surface details. However, the wood xylem is often soft and spongy with no strength and conservation treatments are needed. To understand the mechanical behaviour of the residual wood structure and how potential impregnation agents interact with it, chemical characterisation at the ultrastructural level is essential. This will improve the ability to develop suitable and cost effective conservations treatments for waterlogged archaeological wooden objects. Furthermore, waterlogged archaeological wood is well suited for studying slow and incomplete anaerobic degradation of lignocellulosic biomass, which has not been widely studied. This might improve the understanding of carbon release from waterlogged anaerobic environments acting as sinks in the global carbon cycle and uncover new enzymatic pathways within usage of biomass for fuels and chemicals (PAPER I).

Ultrastructural morphology, chemical composition, and spatial resolved chemical information were studied at the sub-cellular level on waterlogged archaeological Norway spruce [*Picea abies* (L.) Karst] and Scots pine [*Pinus sylvestris* L.]. The material was retrieved from anoxic waterlogged sites and solely decayed by erosion bacteria. Confocal Raman imaging, UV-microspectrophotometry, light microscopy, scanning electron microscopy, transmission electron microscopy, compositional analysis, ATR-FTIR spectroscopy, and size exclusion chromatography were applied to improve the understanding of the residual wood structure left after erosion bacteria decay in waterlogged anoxic environments (PAPER II and PAPER III).

Morphological analyses showed typical erosion bacteria decay patterns in the residual wood structure. Tracheids were decayed in preference to parenchyma and epithelia cells. Cross sections of intermediate decayed wood show a random mixture of decayed and sound tracheids adjacent to each other. This may very well lead to the interpretation that sound and decayed tracheids are randomly mixed in the wood xylem. However, in the longitudinal direction individual tracheids contained alternating decayed and sound cell wall regions. Within tracheids the secondary cell wall was degraded in preference to the compound middle lamella and cell corners. The S2 cell wall layer was decayed in preference to the S1 layer, and the S3 layer was often only partly decayed even when the S2 cell wall was completely decayed. The highly lignified outer S2 layer in mild compression wood was not decayed by erosion bacteria. Bordered pits had a greater decay resistance than the S2 layer. The decay resistance of some cell types and cell wall compartments is most likely explained not only by elevated lignin content but also

differences in chemical composition and supramolecular structure of the biopolymers in the cell wall (PAPER II).

Compositional analyses and ATR-FTIR spectroscopy showed higher lignin and lower carbohydrate contents in the residual xylem of waterlogged wood compared to reference xylem. In addition, the relative increase in lignin content and decrease in carbohydrate content correlated with the degree of degradation. This was expected. The presence of carbohydrates in totally disintegrated xylem is consistent with the ultrastructural studies showing intact parenchyma and epithelia cells, intact compound middle lamella and S1 layer, and partly preserved S3 layer (PAPER III). An amorphous residual material was left after decay of the secondary cell wall. This residual material varied in appearance with two distinct types in light microscope and three distinct types in transmission electron microscopy (PAPER II).

Spatial resolved chemical information obtained with confocal Raman imaging and UV-microspectrophotometry showed that the residual material always contained lignin or lignin-like substances. The lignin concentration varied from levels lower to levels higher than native S2 layer concentrations; often within cross sections of single tracheids. The residual material showed strong depletion of carbohydrates and an abrupt border between intact cell wall regions and regions with residual material. This is an indication of effective polysaccharide degradation by erosion bacteria consortia (PAPER II and III). The two types of residual material observed in light microscope do not show differences in the carbohydrate content of the residual material; both types show a very low/non-existing carbohydrate content.

The chemical composition of lignin in the residual material was similar to the chemical composition of sound waterlogged S2 layers. However, depolymerisation cannot be ruled out with Raman spectroscopy and UV-spectrophotometry (PAPER II and III). An initial size exclusion chromatography analysis points toward partly depolymerisation of the lignin polymer in the residual material. As a whole the results show a high degree of lignin conservation in the residual wood structure and points to the theory that the lignin substances in the residual material most likely form a gel-like structure containing embedded lignin aggregates with higher lignin concentrations than the original S2 cell wall.

ATR-FTIR spectroscopy of sound waterlogged xylem compared to reference xylem showed evidence for abiotic hydrolysis of acetyl groups in glucomannan and ester bonds in lignin-carbohydrate complexes but no evidence for degradation of the glucomannan backbone. In addition, confocal Raman imaging of sound cell wall compartments compared to the same cell wall compartments in reference material showed indications of possible minor abiotic hydrolysis and oxidation of the lignin polymer (PAPER III).

Dansk resumé

Vanddrukne anoxiske miljøer er ekstreme økosystemer, der drastisk nedsætter leve mulighederne for trænedbrydende organismer og reaktionshastighederne for abiotiske nedbrydningsveje. Specialiserede fakultative anaerobe erosionsbakterie konsortier har evnen til, at nedbryde en lang række træsorter i forskellige typer (nær)anoxiske økosystemer. Nedbrydningen er langsom og ukomplet, hvorfor arkæologisk træ kan bevares i disse miljøer i årtusinder. En stor mængde kulturelle informationer bevares i det vanddrukne træ på grund af det unikke nedbrydningsmønster, der bevarer originale dimensioner og overfladedetaljer. Veddet er dog ofte blødt, svampet og uden styrke, og en konserveringsbehandling er nødvendig. For at forstå den nedbrudte træstrukturs mekaniske egenskaber og potentielle imprægneringsmidlers interaktion med den, er det nødvendigt at karakterisere den kemiske struktur på det ultrastrukturelle niveau. Dette vil forbedre muligheden for at udvikle egnede og omkostningseffektive konserveringsmetoder til vanddrukkent arkæologisk træ. Derudover er vanddrukkent arkæologisk træ velegnet til at undersøge den langsomme og ukomplette anaerobe nedbrydning af plantemateriale, der kun sparsomt er undersøgt. Dette kan være med til at forbedre forståelsen af omfanget af kulstof udledningen fra vanddrukne anoxiske miljøer, der optræder som kulstof lagre i det globale kulstof kredsløb og måske bane vejen for nye enzymatiske reaktionsveje indenfor udvinding af brændstof og kemikalier fra biomasse (PAPER I).

Ultrastruktural morfologi og kemisk sammensætning blev undersøgt på det sub-cellulære niveau i vanddrukkent arkæologisk rødgran [*Picea abies* (L.) Karst] og skovfyr [*Pinus sylvestris* L.]. Materialet blev udgravet fra to anoxiske vanddrukne fundpladser og var udelukkende nedbrudt af erosions bakterier. Konfokal Raman mikrospektroskopi, UV-mikrospektrofotometri, lysmikroskopi, skanningelektronmikroskopi, transmissionelektronmikroskopi, kompositionsanalyser, ATR-FTIR spektroskopi og størrelseskromatografi blev anvendt for at forbedre forståelsen af den tilbageværende træstruktur efter nedbrydning via erosionsbakterier i vanddrukne anoxiske miljøer (PAPER II og PAPER III).

Morfologiske analyser viste et typisk nedbrydningsmønster fra erosion bakterier i den tilbageværende træstruktur. Trakeider blev nedbrudt til fordel for parenkymceller og epitelceller. Tværsnit af medium nedbrudt vanddrukkent træ viste en tilfældig fordeling af nedbrudte og intakte celler side om side. Dette kan meget let lede til den tolkning at træmaterialet indeholder en tilfældig fordeling af intakte og nedbrudte trakeider. Men i længderetningen af individuelle trakeider findes skiftende områder med nedbrudt og intakt cellevægsmateriale. I trakeiderne var sekundærcellevæggen nedbrudt til fordel for den sammensatte midtlamel og cellehjørner. S2 cellevægslaget var nedbrudt til fordel for S1 laget og S3 laget var ofte kun delvist nedbrudt selv i områder hvor hele S2 laget var nedbrudt. Det stærkt lignificerede ydre S2 cellevægslag i trykved var ikke nedbrudt af erosionsbakterier. Ringporer var generelt bedre bevaret end det omkringliggende S2 lag.

Denne forskel i nedbrydningsgrad af nogle celletyper og cellevægskomponenter skyldes højest sandsynligt ikke kun højere ligninkoncentration, men også forskelle i kemisk sammensætning og supramolekylær struktur af biopolymererne i cellevæggen (PAPER II).

Kompositionsanalyser og ATR-FTIR spektroskopi viste højere lignin og lavere kulhydrat indhold i det tilbageværende vanddrukne xylem sammenlignet med reference xylem. Derudover korrelerede den relative stigning i ligninindhold og det relative fald i kulhydratindhold med nedbrydningsgraden. Dette var forventet. Tilstedeværelsen af kulhydrater i totalt nedbrudt xylem, hvor S2 cellevægslaget var nedbrudt i alle trakeider stemmer overens med at parenkym og epithel celler, midtlamel og S1 laget er bevaret, samt at S3 laget er delvist bevaret (PAPER III).

Et amorft restmateriale lå tilbage efter nedbrydning af den sekundære cellevæg. Dette restmateriale varierede i udseende. To særskilte typer kunne observeres i lysmikroskop og tre i transmissionelektronmikroskop (PAPER II). Konfokal Raman mikrospektroskopi og UV-mikrospektrofotometri viste, at restmaterialet altid indeholdte en hvis mængde lignin eller lignin-lignende stoffer. Lignin koncentrationen varierede fra lavere til højere niveauer end intakt S2 cellevægslag; ofte indenfor tværsnittet af enkelte trakeider. Restmaterialet viste meget lave koncentrationer af kulhydrater og en brat overgang mellem intakt og nedbrudt cellevæg. Dette er en indikation på effektiv polysakkarid nedbrydning (PAPER II and III). De to typer restmateriale observeret i lysmikroskop viser ikke nogen forskelle i kemisk sammensætning af kulhydrater, men begge viste et meget lavt (ikke eksisterende) kulhydrat indhold.

Den kemiske sammensætning af lignin i restmaterialet svarede til den kemiske sammensætning af lignin i intakte vanddrukne S2 cellevægslag. Dog kan de-polymerisering ikke udelukkes i forbindelse med Raman og UV-spektroskopi (PAPER II and III). En førstehånds størrelseskromatografi analyse peger på delvis de-polymerisering af lignin i restmaterialet. Samlet set viste resultaterne en høj grad af lignin bevaring i den tilbageværende træstruktur. Resultaterne peger i retningen af, at det tilbageværende lignin og lignin-lignende stoffer i restmaterialet danner en gel-lignende struktur med indlejrede lignin aggregater med højere ligninindhold end det oprindelige S2 cellevægslag.

ATR-FTIR spektroskopi af intakt vanddrukkent xylem sammenlignet med reference xylem viste tegn på abiotisk hydrolyse af acetalgrupper på glykomannan og esterbindinger i lignin-kulhydrat komplekser, men ingen tegn på nedbrydning af glykomannan backbone. Yderligere viste Konfocal Raman microspektroskopi indikationer på en mulig mindre abiotisk hydrolyse og oxidation af lignin i intakte cellevægsdele sammenlignet med reference materiale (PAPER III).

List of publications

PAPER I

Pedersen, N.B., Björdal, C.G., Jensen, P., Felby, C. (2013): Bacterial Degradation of Archaeological Wood in Anoxic Waterlogged Environments. In: Stability of Complex Carbohydrate Structures. Biofuel, Foods, Vaccines and Shipwrecks. Harding, S.E. (ed.). The Royal Society of Chemistry. Special Publication No. 341. Pp 160-187.

PAPER II

Pedersen, N.B., Schmitt, U., Koch, G., Felby, C., Thygesen, L. G. (2014): Lignin distribution in waterlogged archaeological *Picea abies* (L.) Karst degraded by erosion bacteria. *Holzforschung*, Volume 68, Issue 7, pp 791-798.

PAPER III

Pedersen, N.B., Gierlinger, N., Thygesen, L. G. (2015): Bacterial and abiotic decay of waterlogged archaeological *Picea abies* (L.) Karst studied by confocal Raman imaging and ATR-FTIR spectroscopy. *Holzforschung*, Volume 69, Issue 1, pp 103–112.

Publications, not part of this thesis

Peer reviewed

Mortensen, M.N., Bojesen-Koefoed, I., Gregory, D., Jensen, P., Jensen, J.B., Moesgaard, A. le B., Pedersen, N.B., Pokupčić, N., Strætkvern, K. and Taube, M. (2014): Conservation and drying methods for archaeological materials modified for use in northern areas. In: Gulløv, H.C. (ed.): *Northern Worlds – landscapes, interactions and dynamics*. *Research at the National Museum of Denmark. Proceedings of the Northern Worlds Conference. Copenhagen 28-30 November 2012*, pp. 369-381.

Pedersen, N.B., Jensen, P., Botfeldt, K. (2013): A strategy for testing impregnation agents for waterlogged archaeological wood – examination of azelaic acid. In: Proceedings of the 11th ICOM Group on Wet Organic Archaeological Materials Conference. Greenville, NC 2010.

Wiinblad, T.M., Pedersen, N.B. (2011): Alkalisk Udvaskning af Arkæologiske Jernkompositter. Meddelelser om Konservering. 1-2011. Pp 14-20.

Non- peer reviewed

Jensen, P.; Pedersen, N.B.: Examination of D-mannitol as an impregnation agent for heavily degraded waterlogged archaeological wood. Proceeding of 12th ICOM Group on Wet Organic Archaeological Materials Conference. May 2013. Istanbul, Turkey. *In press*

List of conference contributions

2013

12th ICOM Group on Wet Organic Archaeological Materials Conference. May 2013. Istanbul, Turkey. *Oral presentation and poster presentation.*

2011

Final Conference of COST ACTION IE0601: Wood science for cultural heritage. 14th-15th November 2011. Paris, France. *Oral presentation.*

Waterlogged Materials working group meeting, Nordic Association of Conservators. The National Museum of Denmark, 11th of November, 2011. *Oral presentation.*

International Conference Shipwrecks 2011. Chemistry and Preservation of Waterlogged Wooden Shipswrecks. 18th-21st October 2011. Stockholm, Sweden. *Oral presentation.*

Royal Society of Chemistry Discussion Meeting: Stability and Degradation of Complex Carbohydrate Structures: Mechanisms and Measurement. Burlington House, London. 5th of September 2011. *Oral presentation.*

2010

Nordic Conservation PhD Student Colloquium, the School of Conservation, the Royal Danish Academy of Fine Arts. Copenhagen, Denmark, November 2010. *Oral presentation.*

Cost Action FP0802 workshop: Wood Structure/Function Relationships. Hamburg, Germany, October 2010. *Poster presentation (2nd prize).*

Waterlogged Materials working group meeting, Nordic Association of Conservators. Conservation Vest, Ølgod, Denmark, August 2010. *Oral presentation.*

11th ICOM Group on Wet Organic Archaeological Materials Conference. May 2010. Greenville, North Carolina, USA. *Oral presentation.*

"The important question is whether one can develop a picture of the ultrastructure of the wood from chemical analysis of it, because it is the ultrastructure that governs the behaviour of the wood on which the selection of a suitable conservation method depends." ***(Hoffmann 1981)***

1 Introduction

1.1 Background

Wood is a versatile raw material. It is strong, flexible, and workable and has been used for a variety of purposes throughout history such as large construction work for ships and bridges and small delicate objects such as tools and weapons. Wood is composed of the most abundant biopolymers polysaccharides and lignin, which are produced from CO_2 and water by photosynthesis. When trees die or wood is discarded it is returned as inorganic carbon by complex biotic and abiotic decay mechanisms (overview by Berg and McClaugherty 2014). The huge amounts of wooden artefacts that have been made throughout human history are almost all decayed or burned off, but a few pre-historical objects have been preserved in extreme ecosystems with very slow abiotic decay processes and little support for wood degrading organisms.

Waterlogged environments such as marine and freshwater sediments, bogs, wetlands, and waterlogged soils are such extreme ecosystems, which are identical in one major feature: They are anoxic or near anoxic. The decay processes are extremely slow and incomplete compared to decay mechanisms in most aerobic ecosystems. Decay rates are inhibited by low temperatures, the recalcitrant nature of the lignocellulose, and lack of mechanical damage and UV-light. Biotic processes are greatly restricted due to the lack of oxygen, which basically eliminates the function of all oxidative enzyme systems. This lack of complete and fast decay systems makes anoxic environments act as large sinks for carbon in relation to the global carbon cycle (Tate 2000; Young and Frazer 1987). It is also the basic reason why waterlogged wood can be preserved for centuries, millennia or in exceptional cases even millions of years in these environments (Obst et al. 1991; Thieme and Maier 1995).

However, archaeological wooden objects found in waterlogged anoxic or near anoxic environments are not free from decay. The wood material is often soft, spongy, low in density, and high in water content due to slow microbial degradation and possible minor effects by abiotic decay. Erosion bacteria are the main degraders in waterlogged wood, often combined with some soft rot fungi and tunnelling bacteria in the surface layers (Björdal et al. 1999; Blanchette et al. 1990; Huisman et al. 2008). The unique degradation pattern in wood from waterlogged anoxic environments preserves the original dimensions and surface details of the wood. This makes the precious waterlogged wooden objects rich in cultural information. However, the wood has most often lost mechanical strength and does not have physical and chemical properties comparable to native wood (Hedges

1990; Schniewind 1990). Air drying will lead to irreversible alterations such as collapse, shrinkage, warping and splitting. The degree of distortion upon drying varies from superficial to total disintegration depending on the level of degradation. The waterlogged wooden objects need to be dried to obtain a stable form suitable for dissemination and research. Conservation procedures aim at preserving the wood structure as closely as possible to its original appearance in relation to dimensions, surface details, colour, stability, and aesthetics (Pedersen 2013). Conservation of waterlogged archaeological wood has developed into a complex and more scientific based approach since the first practical trials with alum by Herbst (Herbst 1861). However, conservation treatments used in the past and present are mainly based on trial and error; and to a lesser extent on macroscopic and microscopic material properties. This has led to successful conservation strategies (Christensen 1970; Jensen et al. 1994; Jensen and Jensen 2006; Jespersen 1981; Wittköpper s.a.) but also to serious damage of important cultural heritage objects (Bojesen-Koefoed 2013; Braovac and Kutzke 2012). The mechanical behaviour of wood is a result of the structural arrangement of the wood polymers (Salmén 2004). The physical behaviour of decayed wood is likewise controlled by the structural arrangement of the biopolymers in the residual wood structure. This makes it crucial to understand the chemical composition of the wood cell wall at the ultrastructural level and to understand how introduced impregnation agents chemically and physically interact on the sub-cellular level in the residual wood structure.

It is a general belief that the higher the level of lignin the more recalcitrant the plant is. However, this is a simplification. Other factors such as particle and pore size, moisture content, chemical composition, and *in situ* distribution of the different cell types and major cell wall components also affect the turnover rate (Wei et al. 2009). Decay mechanisms of the highly complex plant cell walls in anoxic waterlogged ecosystems are not fully understood and have not been given as much attention as aerobic processes and mechanisms of decay. Lack of understanding concerns both species description of the microorganism communities acting on the material, the enzymatic pathways used, and the chemical structure of the residue material (Kubicek 2013; van der Lelie et al. 2012). Combined ultrastructural and chemical characterization of residual plant material is one of several approaches to strengthen the knowledge of the decay mechanisms acting in these extreme ecosystems. In addition, a greater understanding of the little known enzymatic mechanisms for lignin degradation without the presence of oxygen has a potential for commercial interest within the field of turning lignocellulosic biomass into fuels and raw materials (Kataeva et al. 2013). Waterlogged archaeological wood preserved in anoxic or near anoxic environments for hundreds or thousands of years is well suited for studying the slow and incomplete anaerobic microbiological degradation of lignocellulose. Developing the understanding of factors controlling anaerobic lignocellulosic decay also have a potential towards a greater understanding of the global carbon cycle and how climate changes may push the carbon release from the large sinks of biogenic carbon stored in waterlogged ecosystems worldwide (Benner et al. 1984; Ko et al. 2009; Young and Frazer 1987).

Earlier studies on the chemical composition of the residual wood structure of waterlogged archaeological wood have mostly been driven by the cultural significance of the find or a wish to know more about a specific find prior to a conservation treatment and not as often to understand the chemical composition of a specific decay type. This has led to numerous publications on the chemical composition of waterlogged wood that has been described as waterlogged and in terms of wood species but not in terms of decay type and degree of degradation. This makes it impossible to link the chemical analysis to the physical appearance and properties of the material. The chemical modifications of the wood cell wall depend upon type of microorganisms, wood species, and degree of degradation. It is of prime importance to determine these variables prior to chemical analysis. In addition, it is preferred to study the different decay types separately. Only by understanding the decay types separately it is possible to understand the interaction between several decay types. Selecting sample material with only one decay type is a great challenge as the waterlogged archaeological wood has been submerged uncontrolled for several hundred or thousands of years and care must be taken in the sample selection and collection. In addition compositional analysis and spectroscopic techniques are traditionally performed on average xylem samples and not on individual cells and cell wall layers. However, the anatomical and molecular structure of wood is complex and anisotropic and so is the bacterial decay pattern and the waterlogged submerging environment. The anisotropy on the biopolymeric level makes it necessary to obtain spatially resolved chemical information on the sub-cellular level in order to understand the decay and the residual material left after degradation.

1.2 Objective and hypothesis

The objective of this thesis is to study the morphological and chemical composition of waterlogged archaeological softwood at the sub-cellular level to improve our understanding of the residual structures following erosion bacteria decay in waterlogged anoxic environments. The goal is to improve the ability to develop suitable and cost effective conservation treatments for waterlogged archaeological wooden objects rich in cultural information. In addition it is the goal, to obtain more information of the decay mechanisms acting in the waterlogged environment, as it may strengthen the knowledge on anaerobic degradation of biomass and gain insight into the present only little known anaerobic enzyme systems able to deconstruct the plant cell wall.

The hypothesis for this thesis is that anaerobic decay mechanisms of lignocellulosic cell wall structures differ from aerobic decay mechanisms and that these cause a unique decay pattern and chemical composition of the biopolymers in the residual cell wall structure. It is already known that erosion bacteria are able to metabolise cellulose in the lignified cell wall and that lignin is conserved to a greater extent than the carbohydrates. But it is an open question how the chemical structure of the residual wood structure looks like when viewed with a high spatial resolution at the cell wall level and in three dimensions. It is also an open question if lignin is metabolised by the anaerobic bacteria or if the bacteria

solely deconstruct the lignocellulose to gain access to the carbohydrates. In both cases it is an open question which enzymatic processes are active under the given anaerobic conditions.

1.3 Outline of thesis

Wood is a highly complex composite material. Chapter 2 introduces the most important characteristics for softwood from xylem level to chemical composition and supramolecular structure of the biopolymers that build up the wood cell wall. Waterlogged anoxic environments and the decay mechanisms acting herein are also highly complex. Chapter 3 introduces decay mechanisms for plant material in natural waterlogged ecosystems, anaerobic decay of lignocellulose and bacterial decay of wood with special focus on erosion bacteria. Chapter 4 describes the consideration given to wood species, waterlogged environment, and retrieval conditions for the sample material used in the study. This is followed by a presentation of the Norway spruce [*Picea abies* (L.) Karst] poles and Scots pine [*Pinus sylvestris* L.] pole used as sample material in the present work. Excavation site, visual description, cutting of samples, and species determination are covered. The remaining chapters contain results from laboratory analyses performed on the selected sample material and discussion of those in relation to already published work. Chapter 5 presents the morphological decay pattern of erosion bacteria decay in waterlogged wood combined with light, transmission and scanning electron microscopy examinations of the sample material used in this study. Chapter 6 introduces results obtained from numerous studies on the chemical composition of waterlogged wood and presents results on compositional analysis and ATR-FTIR spectroscopy data obtained on the sample material used in this study. Chapter 7 presents results on spatially resolved information on the chemical composition of polysaccharides in individual cell wall layers and in residual material left after secondary cell wall decay obtained with confocal Raman imaging. Chapter 8 presents the results obtained with UV-microspectrophotometry, confocal Raman imaging, and transmission electron microscopy on the lignin distribution and composition of individual cell wall layers and in residual material left after secondary cell wall decay. The chapter do also present the results of a single size exclusion chromatography analysis of extracted residual material from heavily decayed archaeological Norway spruce wood.

2 Softwood ultrastructure and chemical composition

2.1 Xylem composition

Wood consists of a number of different cell types. Softwood has a relatively simple structure. 90-95 % of the cells are tracheids that conduct water and nutrient and give strength in the axial direction of the living tree. Parenchyma cells are mainly situated in the rays. Parenchyma cells both store nutrients and conduct water and nutrients in the radial direction of the living tree. Epithelia cells are situated around resin channels and produce and secrete resins (Figure 2.1). Each cell type may vary at the anatomical level in order to adapt to the physiological conditions within the tree. Latewood, earlywood, heartwood, sapwood, and reaction wood are examples of how tracheids in softwood adapt to different functions within the wood structure. The individual cells in the xylem are connected through three types of pits to create an axial and radial system of interconnected cells. Bordered pits are situated between tracheids, simple pits between parenchyma cells, and half-bordered pits between tracheids and parenchyma cells. The pits control the transport of sap and water in the living tree; and they are the most frequent points of entry for the wood degrading organisms in dead wood (Fengel and Wegener 2003; Fujita and Harada 2001; Harris and Stone 2008; Saka 2001).

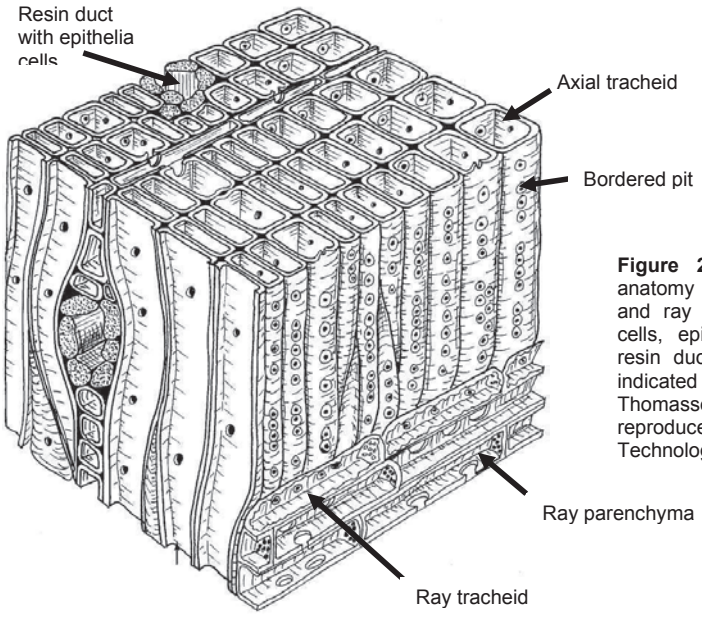

Figure 2.1: Sketch of the wood anatomy of a typical softwood. Axial and ray tracheids, ray parenchyma cells, epithelia cells surrounding a resin duct, and a bordered pit are indicated by arrows. From Thomassen (1977); the figure is reproduced with permission of Danish Technological Institute.

2.2 Chemical composition

The three main building blocks of wood cell walls are the structural polysaccharides cellulose and hemicelluloses, and the polyphenol lignin. In addition, the wood cell wall contains water, and small amounts of inorganic components, resins, proteins, and pectin. Wood cell walls consist of 65-75% polysaccharides and 25-35% lignin (dry weight) regardless of cell type (Fengel and Wegener 2003).

Cellulose is structured in long unbranched chains of β-D-glucopyranose (D-glucose) units joined by (1→4)-glucocidic linkages; which makes the smallest repeating unit the disaccharide cellobiose. The average degree of polymerization is about 6000-14,000 glucose units depending on the cell wall layer. The cellulose chains are arranged in microfibrils which are highly ordered bundles of parallel cellulose chains held together by hydrogen bonding and van de Walls forces. Due to the highly ordered structure of the cellulose chains the microfibrils have crystalline properties (Fengel and Wegener 2003; Harris and Stone 2008; Thygesen et al. 2005). The microfibrils provide the structural reinforcing network of the cell wall. The primary factor that determines mechanical properties of wood fibres is the arrangement of the cellulose microfibrils at different angles with respect to the longitudinal fibre axis with variations in different layers as well as arrangement into microfibrillar aggregates (Salmén and Burgert 2009).

Hemicelluloses are branched polysaccharides composed of several different sugar monomers with a much lower degree of polymerisation (500–3,000 sugar units) than cellulose. Glucomannan and xylan are the two most abundant hemicelluloses in softwood. The proportion of glucomannan in softwood is about 12-18 % (*Picea abies* 13.6 %; *Pinus Sylvestris* 12.4 %). Softwood glucomannan consists of a heteropolymer backbone composed of mannose and glucose units linked by β-(1→4)-glycosidic bonds. The mannose and glucose unit ratio is about 3:1 but the units are randomly distributed. Galactose residues are attached to the backbone by α-(1→6)-glycosidic linkages. Acetyl groups are distributed equally on the C2 and C3 of the mannose units. Glucomannan in softwood is more specifically named O-acetyl-galactoglucomannans (Figure 2.2a) (Fengel and Wegener 2003; Harris and Stone 2008; Scheller and Ulvskov 2010). The proportion of xylans is about 5-15 % in softwood (*Picea abies* 5.6 %; *Pinus sylvestris* 7.6%). Softwood xylans consists of a homopolymer backbone of xylose units linked by β-(1→4)-glycosidic bonds. Arabinofuranose units are linked to the xylan backbone by α-(1→3)-glycosidic bonds. In addition the xylan backbone has side groups of 4-O-methylglucuronic acid. The xylose units are not acetylated in softwood and are more specifically named arabino-4-O-methylglucuronoxylans (Figure 2.2b) (Fengel and Wegener 2003; Harris and Stone 2008; Scheller and Ulvskov 2010).

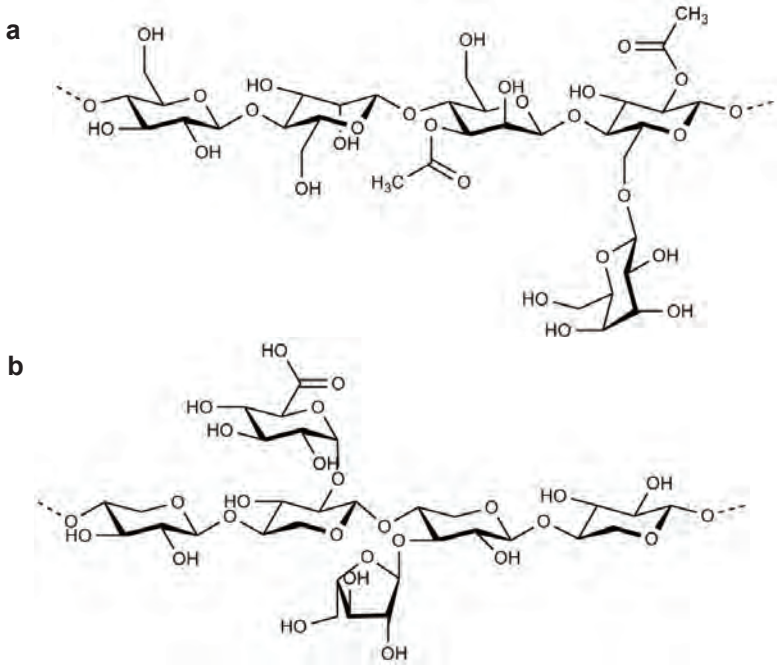

Figure 2.2: Chemical structure of the two most abundant hemicelluloses in softwood, O-acetyl-galactoglucomannan (a) and arabino-4-O-methylglucuronoxylan (b). Redrawn from Fengel and Wegener (2003).

Lignin is a complex cross-linked polymer that is built up by a combination of the three basic phenyl propane monomers: coniferyl alcohol, sinapyl alcohol, and p-coumaryl alcohol (Figure 2.3). The monomers are linked by ether and carbon-carbon bonds with no regular or ordered repeating units. The most abundant linkages in softwood lignin are β-O-4 (approx. 50 %), β-5 (approx. 12 %), 5-5 (approx. 10 %), and α-O-4 (approx. 7%) (See linkage positions in Figure 2.3).

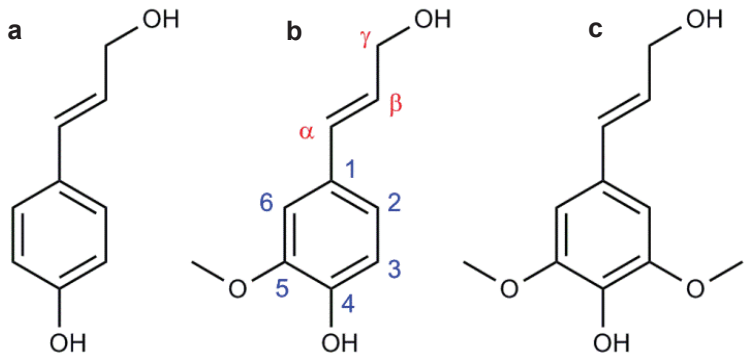

Figure 2.3: The three basic phenyl propane monomers: p-coumaryl alcohol (a), coniferyl alcohol (b), and sinapyl alcohol (c) in lignin. Coniferyl alcohol is the dominant monomer in softwood lignin. The monomers are linked by several different bonds; the most important being β-O-4, β-5, 5-5, and α-O-4. The nomenclature for the linkage positions are shown in (b). Redrawn from Dimmel 2010.

Lignin has no characteristic molecular weight and average values from 400 to more than one million Dalton have been reported. The principle function of lignin in plants is three-fold. Lignin supplies compression strength. Lignin forms a barrier for evaporation and, thus helps to channel water to critical areas of the plant. In addition, lignin has an important function in protecting the plant cell wall from microbiological attack of the more readily degradable carbohydrates. Lignin monomers with one aryl-OCH_3 group stem from coniferyl alcohol and are referred to as guaiacyl units, monomers that stem from sinapyl alcohol and p-coumaryl alcohol are referred to as syringyl units and p-hydroxyphenyl units, respectively. The term "condensed" lignin refers to carbon-carbon linkages at the C-5 position within the polymer. Condensed structures can both be native or formed during lignin reactions. More than 95 % of the monomers in softwood lignin are guaiacyl units with the remainder consisting mainly of p-hydroxyphenyl units and trace amounts of syringyl units. Hardwood lignin contains both coniferyl and sinapyl alcohol whereas p-coumaryl is more widespread in grasses and compression wood in softwoods. The lignin structure and content varies within the xylem and within the individual cell wall layers (Akin 2008; Dence and Lin 1992; Dimmel 2010).

2.3 Ultrastructure

The wood cell wall is organised in primary and secondary cell wall layers surrounded by a middle lamella holding the individual wood cells together. The primary wall is a thin cell wall located next to the middle lamella. It consists of cellulose microfibrils arranged in thin crossing layers with high amounts of embedded pectin. The transition from the middle lamella to the primary wall is diffuse and the two layers are termed compound middle lamella. The secondary wall is a thick cell wall with cellulose microfibrils arranged in highly organised parallel structure. The angel and the direction of spin (S-helix or Z-helix) in the microfibril structure vary within the secondary cell wall. This results in three distinctive layers in softwood tracheids termed S1, S2, and S3 from the primary wall and toward the lumen (Figure 2.4). Table 2.1 shows the thickness of the individual cell wall compartments in Norway spruce tracheids.

Table 2.1: Average thickness and average distribution of cellulose, hemicellulose, and lignin in the individual cell wall layer of Norway spruce tracheids. The number intervals reflect differences between earlywood and latewood. Data from Fengel and Wegener (2003).

	Thickness	**Cellulose**		**Hemicellulose**		**Lignin**	
	µm	% of the wall layer	% of total cellulose	% of the wall layer	% of total hemi-cellulose	% of the wall layer	% of total lignin
Compound middle lamella	0.09	14	3-4	27	15-21	59	18-27
S1 layer	0.26-0.38	35-36	5-9	35-36	16-23	27-31	8-10
S2 layer	1.66-3.69	58-59	87-92	14-15	56-69	27	63-74
S3 layer	0.09-0.14						

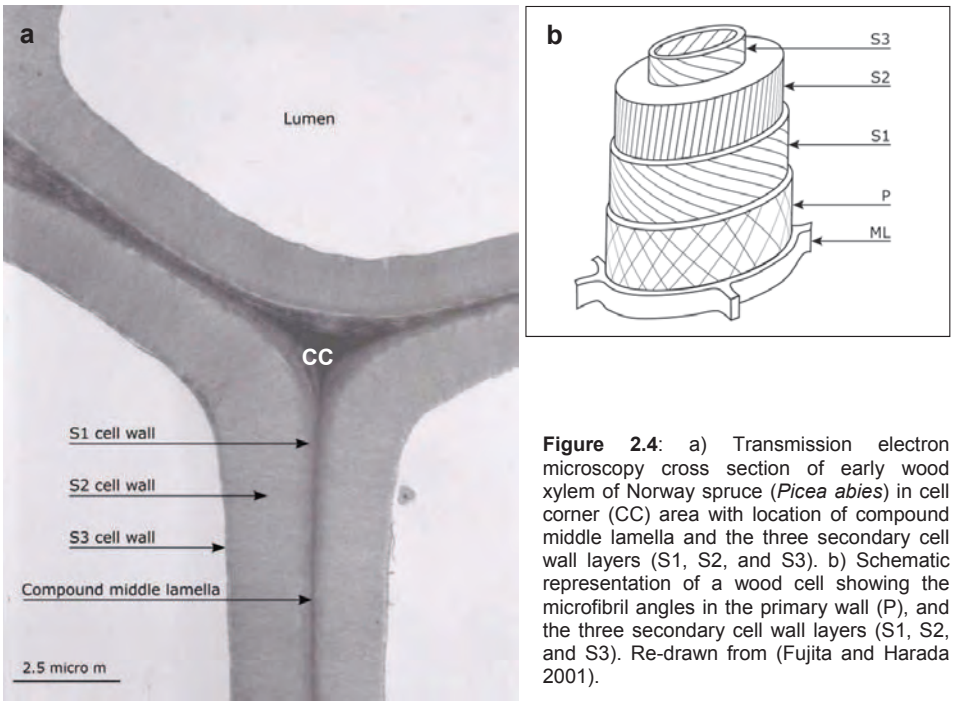

Figure 2.4: a) Transmission electron microscopy cross section of early wood xylem of Norway spruce (*Picea abies*) in cell corner (CC) area with location of compound middle lamella and the three secondary cell wall layers (S1, S2, and S3). b) Schematic representation of a wood cell showing the microfibril angles in the primary wall (P), and the three secondary cell wall layers (S1, S2, and S3). Re-drawn from (Fujita and Harada 2001).

The S1 layer in Norway spruce tracheids is composed of microfibrils orientated approx. 70-90 degrees to the tracheids axis and in S-spin direction. The microfibril orientation shifts gradually and in a clockwise direction from a S-helix to a Z-helix either within the S1 layer or in the inner part of the S2 layer. The microfibril orientation in the dominant S2 layer is a Z-helix but with a much steeper angle in the range 9-32 degrees parallel to the fibre axis for different softwood species. The S3 layer is very thin and located next to the cell lumen. The microfibril orientation is shifted from a steep Z-helix (40 degrees) in counter-clockwise direction to a S-helix (20 degrees) from the inner to the outer part of the layer (Figure 4.2b) (Abe and Funada 2005; Brändström et al. 2003).

Table 2.1 shows the lignin, cellulose, and hemicellulose distribution in the individual cell wall layers of Norway spruce. In addition to the difference in microfibril angel the chemical composition of the cell wall layers differ. The compound middle lamella contains a high proportion of lignin, relative high amounts of hemicellulose, and low amounts of cellulose. The S1 and S2 layers contain roughly the same amount of lignin but vary in carbohydrate composition. The S2 layer has a high amount of cellulose whereas the S1 layer contains equal amounts of cellulose and hemicellulose. The S3 layer is very thin which is why the chemical composition data is included in data for the S2 layer in Table 2.1. The S3 layer in softwood is reported to have irregular occurrence of lignin with values varying from concentrations as the S2 layer to higher levels (Donaldson 1987; Scott and Goring 1970). In addition it has been found that the S3 layer thickness varies

both within and between Monterey pine (*Pinus radiate* D. Don) tracheids (Singh et al. 2002a). Irregular lignin distribution in both secondary cell wall and cell corner middle lamella has been suggested but seems to be more pronounced in hardwoods than in softwoods (Agarwal 2006; Singh et al. 2002b; Singh and Daniel 2001; Tirumalai et al. 1996).

2.4 Organisation of the biopolymers

The structural organisation of the wood polymers in the cell wall is complex and not fully understood. Studies of the S2 layer in softwood tracheids and hardwood fibres has shown that parallel ordered cellulose microfibrils are assembled into aggregates (fibrils). The aggregates have a varying size from single microfibrils of 3.5 nm in width to aggregates as large as 30 nm with average sizes in the 16-20 nm range. The average size is the same across the S2 layer giving a uniform supramolecular structure of the cell wall layer. The cellulose aggregates are closely associated to hemicellulose; primarily glucomannan in softwood. The glucomannan is arranged in parallel with the aggregates and has a high degree of hydrogen bond coupling to them. The cellulose aggregates are ordered in a concentric lamella structure in the cell wall with different angles relative to the longitudinal axes of the wood cell as described above. In the longitudinal direction of the cell wall the cellulose aggregates are mildly undulating, which creates a small lens shaped spacing between the aggregates approximately 5-10 nm wide (Figure 2.5). Xylan is mainly found in these regions arranged parallel to the cellulose microfibrils. Within this xylan network lignin polymerises (Figure 2.5).

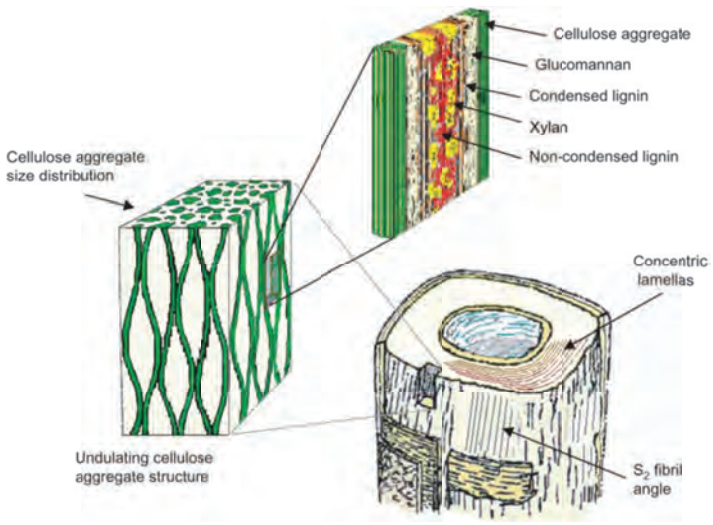

Figure 2.5: Sketch of the organisation of the biopolymers in the S2 cell wall layer. Cellulose aggregates with varying size are closely associated to glucomannan that is arranged in parallel with the cellulose. The cellulose microfibrils are mildly undulating in the longitudinal direction. This creates a small lens shaped spacing between the aggregates. Xylan is mainly found in these regions arranged parallel to the cellulose microfibrils. Lignin polymerises within this xylan network. From Salmén and Burgert (2009), De Gruyter Holzforschung, Walter De Gruyter GmbH Berlin Boston, 2009. Copyright and all rights reserved. Material from this publication has been used with the permission of Walter De Gruyter GmbH.

Due to the spatial limitations of the lens shaped spaces the lignin is to some extent structurally ordered in the longitudinal direction of the microfibrils. Strong attractive interactions between the phenyl ring in the lignin polymer and OH-groups of the carbohydrates may contribute to this orientation. Lignin is not bound directly to cellulose. The hemicellulose is situated between the two polymers with hydrogen bonding towards the cellulose microfibrils and covalent bonding towards the lignin, the latter called lignin carbohydrate complexes. In softwood the glucomannan within the cellulose aggregates are closely associated with a condensed lignin structure. This is followed outward by xylan associated to an un-condensed lignin structure (Bardage et al. 2004; Brunow and Lundquist 2010; Salmén 2004; Salmén and Burgert 2009; Salmén et al. 2012; Terashima et al. 2009).

The composition and supramolecular structure of the biopolymers in the compound middle lamella differs significantly from the secondary cell wall. The microfibrils are not highly ordered in concentric layers and are embedded in the polysaccharides pectin and xyloglucan. The lignin content is high (Table 2.1) with a high proportion of p-hydroxyphenyl units and condensed structures and higher molecular weight than in the secondary cell wall. In addition the lignin situated in the middle lamella is not constrained by the cellulose aggregates and do not possess any structured order of the polymer. The lignin in the secondary cell wall and in the middle lamella is therefore expected to be different in both mechanical and chemical properties (Salmén et al. 2012; Scheller and Ulvskov 2010; Terashima et al. 2012).

3 Wood decay under oxygen restricted conditions

3.1 Biotic versus abiotic decay

Wood is degraded both by biotic and abiotic mechanisms (Figure 3.1). The most important biotic mechanisms in natural environments are fungi, bacteria, insects, and marine crustaceans. Important abiotic mechanisms are mechanical and chemical weathering such as interactions with wind, current, precipitation, UV light, heat, hydrolysis and oxidation reactions (Appelqvist and Björdal 2011; Blanchette et al. 1990; Feist and Hon 1984; Goldstein 1984; Kirk and Cowling 1984).

Biotic decay is by far the most destructive decay type of wood. In water saturated soils and sediments oxygen is only available by diffusion. This restriction is enough to exclude all types of insects, marine crustacean, and the fast wood degrading Basidiomycetes such as white and brown rot fungi (Kim & Singh 2000). Soft rot fungi caused by Ascomycota are able to degrade the wood cell wall in the upper most layers of a waterlogged ecosystem where some oxygen is present (Björdal 2012; Capretti et al. 2008; Daniel and Nilsson 1998; Eriksson et al. 1990) (Figure 3.1).

Abiotic decay by slow hydrolysis was the predominant explanation for decay in relation to waterlogged archaeological wood in anoxic environments (Hoffmann and Jones 1990) until it was generally accepted in the 1990ties that bacteria are responsible for the main decay (Björdal et al. 1999; Blanchette 1995; Blanchette et al. 1990). However, possible decay by wood degrading bacteria was suggested already in the 1940ties and 1960ties with the aid of light microscopy studies (Boutelje and Bravery 1968; Harmsen and Nissen 1965; Liese 1950) and verified by studies using scanning and transmission electron microscopy in the 1980ties (Nilsson and Daniel 1986; Singh and Butcher 1991). Even though microbiological decay are now agreed to be the most important, abiotic decay may have some influence on the wood material during the long burial period in waterlogged environments. Waterlogged wood with intact micro-morphology has shown signs of holocellulose depolymerisation and chemical changes in the lignin-carbohydrate complex (Borgin et al. 1975b; Gelbrich et al. 2008). Shorter carbohydrate chains and detachment of the lignin polymer from the hemicellulose will result in more available hydrogen bonding sites. Compared to sound wood a slightly higher degree of shrinkage upon drying must be expected. But the abiotic decay caused is thought to be of minor importance compared to the extensive change in micro-morphology obtained by microorganisms.

The main mechanism for both abiotic and enzyme catalysed biotic degradation of carbohydrates is hydrolysis of acetal linkages in cellulose and hemicellulose. The carbohydrates are thereupon depolymerised and solubilised (Goldstein 1984). In anoxic waterlogged environments the abiotic acid hydrolysis of the carbohydrates is extremely slow due to the mildly acidic conditions, and the low temperature in the submerged environment, and the very slow reaction rate of auto-hydrolysis. The half-life of cellulose in neutral pH is estimated to about 100 million years (Wilson 2008). The aromatic

structure of lignin with delocalised electrons provides a range of possible redox reactions and radical reactions which break down the ether, ester and carbon linkages of the lignin molecular structure.

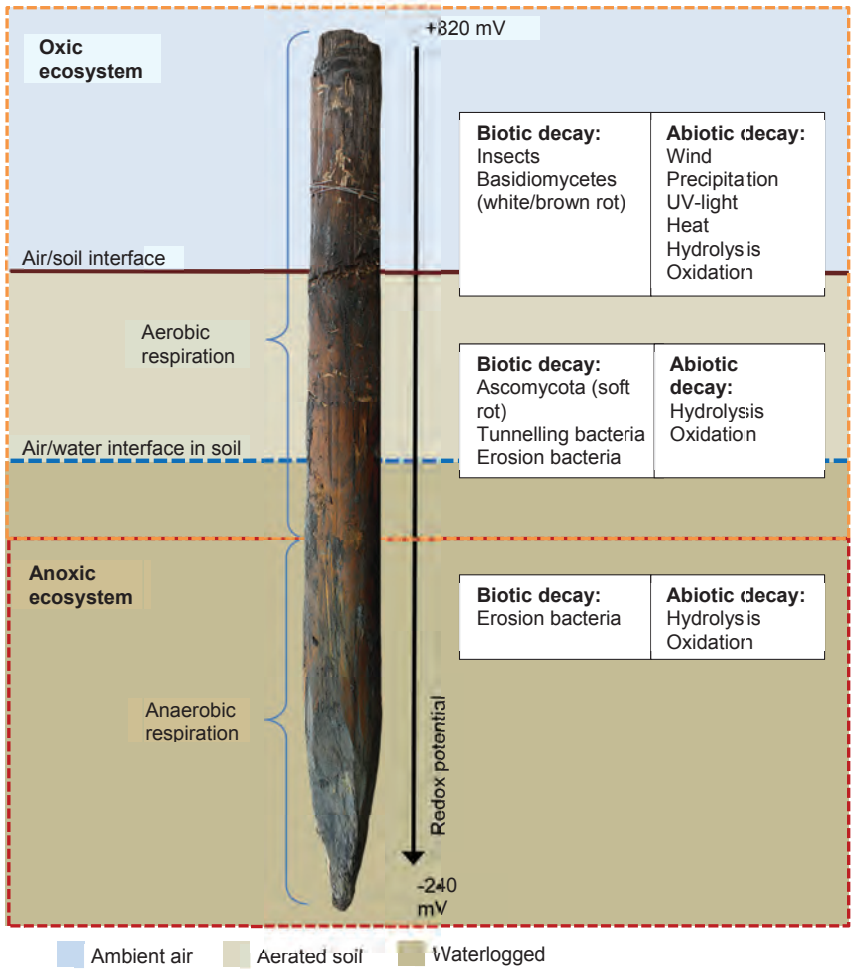

Figure 3.1: Sketch of correlation between environmental conditions and biotic (living organisms) and abiotic (non-living) wood decay for a wooden pole exposed to ambient air, an aerated soil and a waterlogged soil. In ambient air wood degrading organisms have free access to oxygen (oxic environment) and can thereby drive the needed aerobic respiration. The turnover rate of wood by wood degrading insects and fungi is fast. The oxygen concentration in the soil decreases with depth and amount of water. When the soil is completely waterlogged only small amounts of oxygen are available. This oxygen-poor environment provide basis for the growth of soft rot fungi and bacteria with less oxygen requirements but also slower decay rates. The oxygen concentration is further decreased with depth and turns completely anoxic (without oxygen). The waterlogged anoxic environment only provide basis for anaerobic respiration. The only known anaerobic biotic wood degraders are erosion bacteria.

3.2 Biotic decay mechanisms

Living organisms derive energy for cellular functions through oxidation of suitable energy sources. When plant material is used as an energy source the oxidation is facilitated via a respiratory electron transport chain. In aerobic metabolism oxygen is used as terminal electron acceptor, but when oxygen level drops drastically other terminal electron acceptors such as nitrate, sulphate, and carbon dioxide are used. However, the metabolic energy output is not as high for the anaerobic metabolism processes as for aerobic respiration. In water saturated soils and sediments, oxygen is only available by diffusion. Diffusion is slow and the oxygen concentration decreases with the depth of burial and the concentration of organic particulate material. This leads to aerobic respiration in the uppermost layer of a waterlogged ecosystem and sulphate reduction and/or methanogenesis in the lower most reduced layers of the soil/sediment (Killham 1994; Tate 2000).

A great variety of cellulolytic bacteria and fungi are able to convert insoluble cellulosic substrates to soluble sugars that can be used as an energy source by the bacteria and fungi. The conversion is catalysed by a variety of different enzymes; the cellulases. These enzymes hydrolyse the β-1,4-glucosidic bonds in cellulose. Due to the intermolecular bonding in the crystalline structure, multiple cellulase enzyme systems acting in synergy are needed to efficiently degrade cellulose. Fungi are not known to be able to perform anaerobic respiration. However, anaerobic bacteria have evolved highly effective systems for extracellular degradation of polymeric substances due to the low mass yield of anaerobic respiration per hydrolysed sugar unit. A strategy unique to anaerobic bacteria is the organisation of cellulases in multi-component complexes known as cellulosomes attached to the bacterial cell wall (Bayer et al. 1998; Bayer et al. 2008; Wei et al. 2009; Wilson 2008). Most hemicelluloses are amorphous due to their branched and substituted structure and the carbohydrates are more readily accessible to enzymes than the glucose molecules in cellulose. Hemicelluloses are therefore easier to hydrolyse but a wide range of different hemicellulases are needed to de-branch and depolymerise the complex structure of hemicelluloses (Decker et al. 2008).

A wide range of fungi and bacteria that are able to hydrolyse polysaccharides cannot degrade lignin. In these cases carbohydrates in the cell wall will not be accessible for degradation as the lignin physically blocks the polysaccharides. Degradation of lignocellulosic plant cell wall material is therefore restricted to highly specialised fungi and bacteria that are able to either assimilate lignin or at least deconstruct the plant cell wall enough to gain access to the polysaccharide fraction of the cell wall. Decay mechanisms for wood decaying aerobic fungi have been studied extensively (Kubicek 2013). Anaerobic lignocellulosic degradation has not been studied with as much attention but it is a general belief that lignins and lignocellulose are far more recalcitrant in anoxic environments as lignocellulosic biomass accumulates in natural anoxic submerging environments.

Lignin monomers, low-molecular weight oligomers, and chemically modified lignins are metabolised by anaerobic bacteria (Eriksson et al. 1990; Ko et al. 2009; Pareek et al. 2001; Vicuña 1988; Young and Frazer 1987; Zeikus et al. 1982; Zimmermann 1990). The pathways and transformation mechanisms for the bacterial decomposition is still uncertain (Young and Frazer 1987; van der Lelie 2012). In addition, the contribution of bacteria to degradation of native high molecular weight lignin directly from the plant cell wall in natural anoxic environments is not known (Vicuña 1988; Zimmermann 1990). A few studies show evidence for slow but incomplete anaerobic bacterial assimilation of high molecular weight lignin in radiolabeled native plant material (Benner et al. 1984), in newspaper (mechanical or semimechanical pulp) (Pareek et al. 2001), and in organosolve lignin (Ko et al. 2009) incubated with bacteria consortia collected directly from natural anoxic environments. However, experiments with newspaper and organosolve lignin do not give a solid proof for the ability of anaerobic microbial consortia to metabolise native lignin as it is situated in the native plant cell wall. A single solid evidence for the ability of anaerobic bacteria consortia to deconstruct wood cell walls has been found (van der Lelie et al. 2012). The morphological decay pattern is in agreement with erosion bacteria decay observations on waterlogged archaeological wood found in anoxic or near anoxic environments. The same study did also find evidence for the existence of DNA within the anaerobic bacterial consortium that codes for enzymes homologues to fungal lignin oxidation enzymes.

It is generally believed that the anaerobic degradation of lignocellulose consists of bacteria consortia acting together to deconstruct the plant cell wall (Vicuña 1988; Zimmermann 1990). This is deduced from two facts: Secondary degraders have been observed in relation to erosion bacteria and cross-feeding is a well-known strategy in natural ecosystems. In addition is was found that isolated pure bacteria stains from natural habitats do not maintain their ability to degrade plant cell walls (Beguin and Aubert 1994; Björdal et al. 2000; Nilsson and Björdal 2008b; Singh et al. 1990; Wei et al. 2009). However, one study has shown that a single anaerobic thermophilic bacteria strain (*Caldicellulosiruptor bescii*) is able to metabolise native switchgrass (*Panicum virgatum* L.) by solubilising the lignin and assimilate the polysaccharides (Kataeva et al. 2013). The bacteria strain is able to degrade the switchgrass at 78 °C. This high temperature alone will perform a mild pre-treatment of the lignocellulose that will influence the supramolecular structure and thereby render the accessibility of target sites of enzymatic conversion. This “pre-treatment” is only likely to occur in natural environments as an extremely slow abiotic effect.

3.3 Wood decay under oxygen restricted conditions

Bacterial degradation of wood

Wood is quickly colonized by bacteria under waterlogged conditions. These bacteria can either be wood-inhabiting or true wood degrading bacteria. True wood degrading bacteria are able to degrade the lignocellulosic cell wall. Wood-inhabiting bacteria can either feed

on the pectin rich pit membrane and thereby improve the permeability of the wood, feed on non-structural carbohydrates, feed on residual material from the primary breakdown of the cell wall (secondary degraders), or be more passive colonizers (Greaves 1971). The true wood degrading bacteria are named after the unique micro-morphological decay pattern they produce in the cell wall. Tunnelling and erosion bacteria are the two most commonly reported bacteria types in waterlogged wood. But erosion bacteria are the main degraders in waterlogged anoxic or near anoxic environments where aerobe wood decaying organisms are suppressed (Björdal and Nilsson 2008; Björdal et al. 1999; Huisman et al. 2008; Kim and Singh 2000; Singh et al. 1990; Zabel and Morrell 1992) (Figure 3.1). Aerobic microbial decay patterns are, however, not uncommon in waterlogged wood from oxygen restricted environments especially in the surface layer of the wood. This can both be due to a long service life before waterlogging or waterlogging with enough available oxygen to support growth of soft rot fungi and tunnelling bacteria (Björdal et al. 1999; Blanchette and Hoffmann 1994; Kim et al. 1996; Singh et al. 2003).

Erosion bacteria

It is still discussed if erosion bacteria can thrive under completely anoxic conditions. Even though waterlogged archaeological wood is found in anoxic environments this environment may not have been present in the whole submerging history of the artefact. However, various studies point toward the ability for erosion bacteria to metabolise lignocellulose without the presence of oxygen. Cellulosomes have been observed in the contact zone between erosion bacteria and the cell wall in several studies (Björdal et al. 2000; Holt 1983; Singh and Butcher 1991; Singh et al. 1990; van der Lelie et al. 2012). This is a common energy saving strategy of anaerobic bacteria (Bayer et al. 2008). In addition, laboratory experiments conducted by Kretschmar et al. (2008) and Nilsson and Björdal (2008b) suggest that erosion bacteria are facultative anaerobes and even tolerate presence of hydrogen sulphide. This is supported by the recent finding by van der Lelie et al. (2012) that a free-living microbial consortium was capable of degrading poplar biomass under anoxic conditions with ultrastructural decay patterns resembling erosion bacteria decay.

The decay rate of erosion bacteria is very slow. Active erosion bacteria decay has been reported in the inner portions of a 1200 years old Viking age pine pole (Björdal et al. 2000). However, the submerging period is not the primary decay factor (Giachi and Pizzo 2007; Huisman et al. 2008; Schniewind 1990). Factors such as wood species and quality, wood permeability in relation to soil hydrology, soil/sediment composition, and soil texture determine the decay rate (Klaassen and van Overeem 2012). Erosion bacteria are active within a great span of wood species and waterlogged ecosystems (Björdal et al. 1999; Blanchette et al. 1990; Holt and Jones 1983; Huisman et al. 2008; Kim et al. 1996; Klaassen 2008a; Singh et al. 1990) but it is not known if different species are responsible for the same ultrastructural decay pattern in for instance both aquatic and terrestrial ecosystems.

Observations at the ultrastructural level with electron microscope show that erosion bacteria are short rod-shaped (3-5 µm long) and Gram negative. They are firmly attached to the cell wall and move by gliding. Bacteria with morphology different from erosion bacteria have been observed on close association to the erosion bacteria. These bacteria are believed to be secondary degraders that are part of a consor**ti**um that act together to degrade the cell wall (Björdal et al. 2000; Kim and Singh 1994; Singh et al. 1990). The identity of erosion bacteria has not yet been established. Attempts to isolate and grow monocultures with traditional microbiological methods have failed (Nilsson and Björdal 2008a; Nilsson and Björdal 2008b; Nilsson et al. 2008; Schmidt et al. 1995; Schmidt et al. 1987). From DNA analysis on sub-cultured bacterial isolates and DNA extracted directly from wood it was concluded that erosion bacteria most likely fall within the *Cytophaga-Flavobacterium-Bacteroides* sub group. However, the *Pseudomonas*, *Cellvibrio*, and *Brevundimonas* groups were also commonly found in waterlogged wood (Landy et al. 2008). Another attempt to identify erosion bacteria with molecular biological techniques concluded that many bacteria from heavily decayed waterlogged wood belonged to families which have lignocellulolytic capacity, but also that a major part of the bacteria found are unclassified and therefore unknown (Helms 2008; Helms et al. 2004). Van der Lelie et al. (2012) have used the approach of metagenomics to study the total genetic material recovered from a free-living microbial consortium capable of degrading poplar biomass under anoxic conditions. This approach helps survey the 95-99.9% of microorganisms that are not readily cultured by traditional microbiological methods. It was found that the community performed a typical erosion bacteria attack on the cell wall. It was dominated by *Magnetospirillum*, *Bacteroidetes*, *Clostridiales*, *Cyanobacteria*, and *Methanomicrobia*; fungi were absent. The largest number of glycoside hydrolases was found to be associated with the *Bacteroidetes* which indicates that members of this class are key biomass degraders in the analysed community. This is consistent with the finding of Landy et al. (2008).

4 Sample material

4.1 Criteria for selection of sample material

Wood is a complex composite material both at molecular, macromolecular, supramolecular, cell wall, and xylem level (Chapter 2). In addition the submerging environments contain numerous factors that affect the preservation state of the wood (Chapter 3). This stresses that many considerations must be addressed when choosing waterlogged material for a research study.

Softwood was chosen in preference to hardwood due to the more simple anatomical features of softwood compared to hardwood. Softwood consists of two or three different cell types with tracheids accounting for 90-95% of the xylem structure. In addition, softwood tracheids have been studied extensively especially in connection with the pulp and paper industry, and several studies have been performed on softwood in relation to waterlogged archaeological wood decay. This yields a good basis for interpretation and understanding of obtained results.

It was of prime importance to retrieve sample material from an anoxic waterlogged environment to be able to study the decay patterns of erosion bacteria without contamination from other wood degraders, such as soft rot fungi and tunnelling bacteria. It is impossible to be certain that the wood has been under complete anoxic conditions from waterlogging until excavation when working with timespans of several hundred or even thousands of years. However, information on the burial environment from archaeological stratigraphic investigations and lack of fungal decay and tunnelling bacteria in the wood structure are good indicators for lack of oxygen in the submerging environment. Wood material with a gradient of decay from surface to core was prioritised to be able to analyse differences in decay stages.

Freshly excavated material was of great importance. Post-excavation degradation will otherwise be hard to control. It is important to secure the sample material in low oxygen conditions right after retrieval and until sample preparation to avoid abiotic oxygen driven post-excavation reactions and contamination of e.g. tunnelling bacteria and soft rot fungi that most likely are present in the waterlogged environment or in the surrounding air as spores waiting for more favourable conditions. In addition the wood must be kept waterlogged at all times and cannot be frozen. This is necessary to avoid physical changes/destruction of the ultrastructure of the material that can obscure results when spatial distribution of the wood polymers in the cell walls is to be investigated.

It turned out to be troublesome to obtain suitable sample material. Most archaeological excavations in Denmark are conducted when developers need to go below ground and the excavations are often carried out under massive time pressure. It is often unpredictable what is found during excavations and the state of preservation of the archaeological objects. In addition, the archaeologists have to document the object before retrieval and

then decide if the object should be classified as a museum object and thereby preserved in the museum collection or if the object should be discarded and thereby available as sample material for research. To avoid post-excavation storage problems already described above it is by far the best to be present at the excavation and have a clear agreement with the archaeologist about which objects can be used for research purposes.

4.2 Norway spruce poles from Kongens Nytorv

Excavation site

Museum of Copenhagen has conducted large excavations in the city centre of Copenhagen due to construction of the metro city ring. At an excavation at Kongens Nytorv, Copenhagen (Denmark) from January 2010 until September 2011 several rows of softwood poles were found situated in the moat that surrounded medieval Copenhagen (Figure 4.1). The poles were debarked Norway spruce stems with sharpened ends most likely felled in the same year (Anon 2012). The construction is interpreted as a temporary bridge built to allow entrance to the eastern part of Copenhagen (Lille Kongensgade) as a new entrance/gate (Østerport) and a moat were constructed nearby. It was not possible to dendrochronologicially date the poles but a pine plank included in the construction was dated to 1614 ± 15A.D (Anon 2012). The moat was backfilled as soon as the construction of Østerport was completed (approximately 1620). From written sources and the dating it is believed that the bridge was in service for approximately five years. The moat was in service from the end of the 16th century and has been water filled in the whole period to act as a defence construction. It has been cleaned for waste and natural sedimentation relatively often (personal comment: Excavation leader Morten Steineke, Museum of Copenhagen).

The placement of the poles in a moat offers very good conditions for an anoxic waterlogged environment. Stagnant waters and high levels of organic material provide anoxic conditions at the bottom of the moat. The short service life of the poles followed by backfilling probably led to an undisturbed waterlogged site. Even a brick wall that was part of the fortification excavated just 60 cm below modern ground level was surprisingly well preserved (Figure 4.1). Figure 4.2 shows the different preservation states of the poles under anoxic conditions in the moat and of a pole situated outside the moat. The pole situated outside the moat was above groundwater level. In addition the burial environment was disturbed in modern times resulting in oxygenated conditions and thereby fungal attack of the wood.

Retrieval

The upper part of the softwood poles were unearthed in the middle of February 2011 and finally excavated the 1st of March 2011. The upper 30-50 cm of the poles was exposed to the surrounding air from the date of discovery until excavation. This part of the poles had dried out and severe splits and fissures had developed. The day before retrieval of the poles (28th of February 2011) the ground water table was lowered by pumping water out of the excavation site and the soil was removed around the poles. At least two thirds of

the poles were exposed to the surrounding air for 24 hours before the poles were finally retrieved.

Figure 4.1: Overview of excavation site (KBM 3829 Kongens Nytorv) with several rows of softwood poles situated in the former moat (grey clay). A more than 600 years old brick wall is seen in the back ground. Part of a wooden palisade dated to the 13th century was found underneath the stone/brick wall. Picture © Museum of Copenhagen.

Figure 4.2: a) The excavation site at Kongens Nytorv showing the waterlogged nature of the moat just before retrieavel of the poles. The bucket contained a pump that ran constantly to lower the ground water level. Picture © Museum of Copenhagen. b) Pole situated outside the moat close to a concrete cable station placed under ground in modern times. The pole was clearly in a bad condition compared to the poles within the moat and is most likely attacked by brown rot fungi due to aeration of the site.

Cutting and storage of pole discs

Immediately after retrieval from the site the poles were photographically documented by the museum, the sharpened end was cut off, and the pole sawn into several discs (cross sections) with a chain saw (Figure 4.3). A disc with a thickness of about 6 cm was cut off for dendrochronology analysis. This was followed by cutting a second disc. In some cases a third disc was cut off about 30 cm from the first disc, and in one case a forth disc was cut off 30 cm above the third disc. In this manner up to three discs with a thickness of 12-26 cm were collected from the poles in the whole length of the pole. Only the samples from the bottom have been waterlogged until excavation whereas the top and middle discs were waterlogged until 24 hours before excavation. The very upper part of the poles exposed to ambient air for two to three weeks were discarded (Figure 4.3). The discs were placed in plastic bags and filled with tap water over night. Less than 24 hours later the discs were placed in a plastic bucket each with tap water. The water was purged with nitrogen gas and the buckets were sealed with an airtight lid. All samples were stored cold (5 °C).

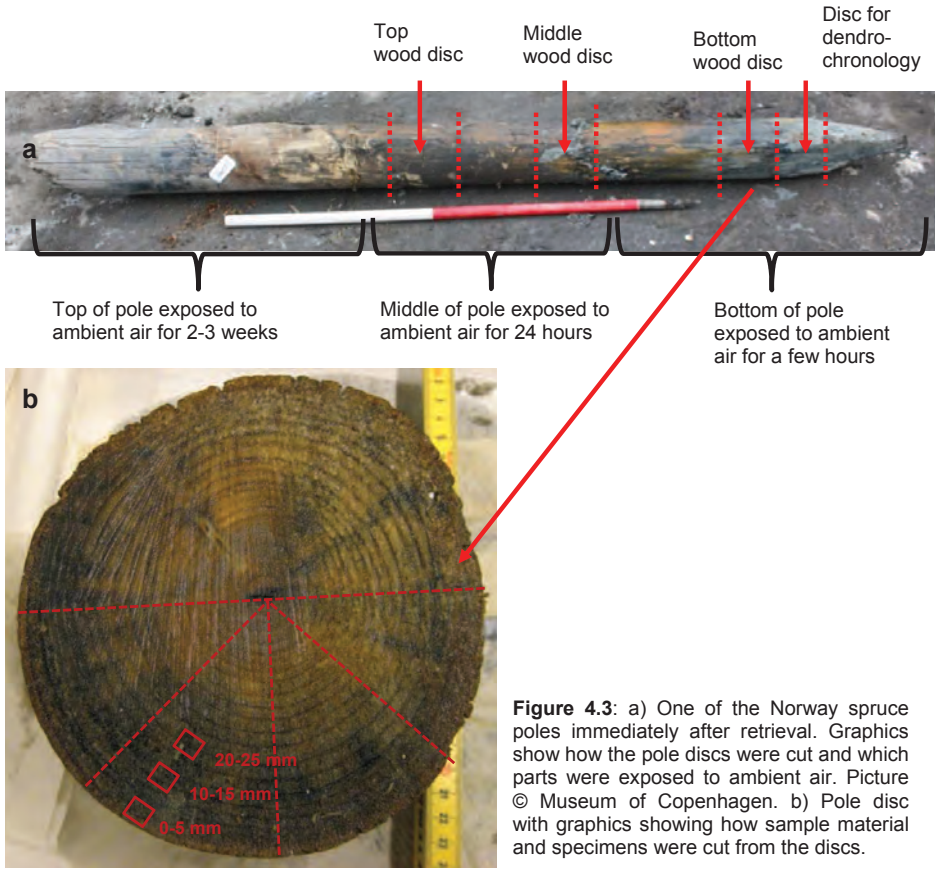

Figure 4.3: a) One of the Norway spruce poles immediately after retrieval. Graphics show how the pole discs were cut and which parts were exposed to ambient air. Picture © Museum of Copenhagen. b) Pole disc with graphics showing how sample material and specimens were cut from the discs.

Selection

Three poles (65498, 64921, and 65087) were selected as sample material. Figure 4.4 shows a plan of the excavation site with the three selected poles encircled with green. Figure 4.5 shows the poles still situated in the moat. The criteria for selection were that the poles contained an outer soft layer of decayed xylem and that the xylem contained larger regions free from compression wood. Apart from some initial light microscopy examinations all analyses were performed on the wood discs from the lowest part of the poles where the wood had been kept waterlogged at all times until retrieval.

Visual description of sample material

The three poles were all debarked and only contained tool marks in the lower sharpened end. None of the poles showed visible dehydration damage such as collapse of the surface layer. The poles did not have a visible border between sap- and heartwood. All three poles contained a hard inner part indicating sound xylem and a soft and spongy outer layer indicating some degradation. Black precipitations were observed on the surface of all three pole samples. This is most likely sulphur compounds formed in the anoxic environment.

The bottom-disc from pole 65498 was approximately 14 cm in diameter and 13 cm in the longitudinal direction. The pole contained 20 broad growth rings between 1-2 mm and 5 mm. The xylem was yellow brown but darker in the surface area up to 4-5 cm from the surface towards the pith.

The bottom-disc from pole 64921 was approximately 15 cm in diameter and 18 cm in the longitudinal direction. The pole contained numerous narrow growth rings only 1 mm thick or thinner. The xylem was dark grey from surface to pith.

The bottom-disc from pole 65087 was approximately 16 cm in diameter and 18 cm in the longitudinal direction. The pole contained 24 broad growth rings between 2 and 5 mm. The xylem was darker in the surface area 2-3 cm from the surface towards the pith.

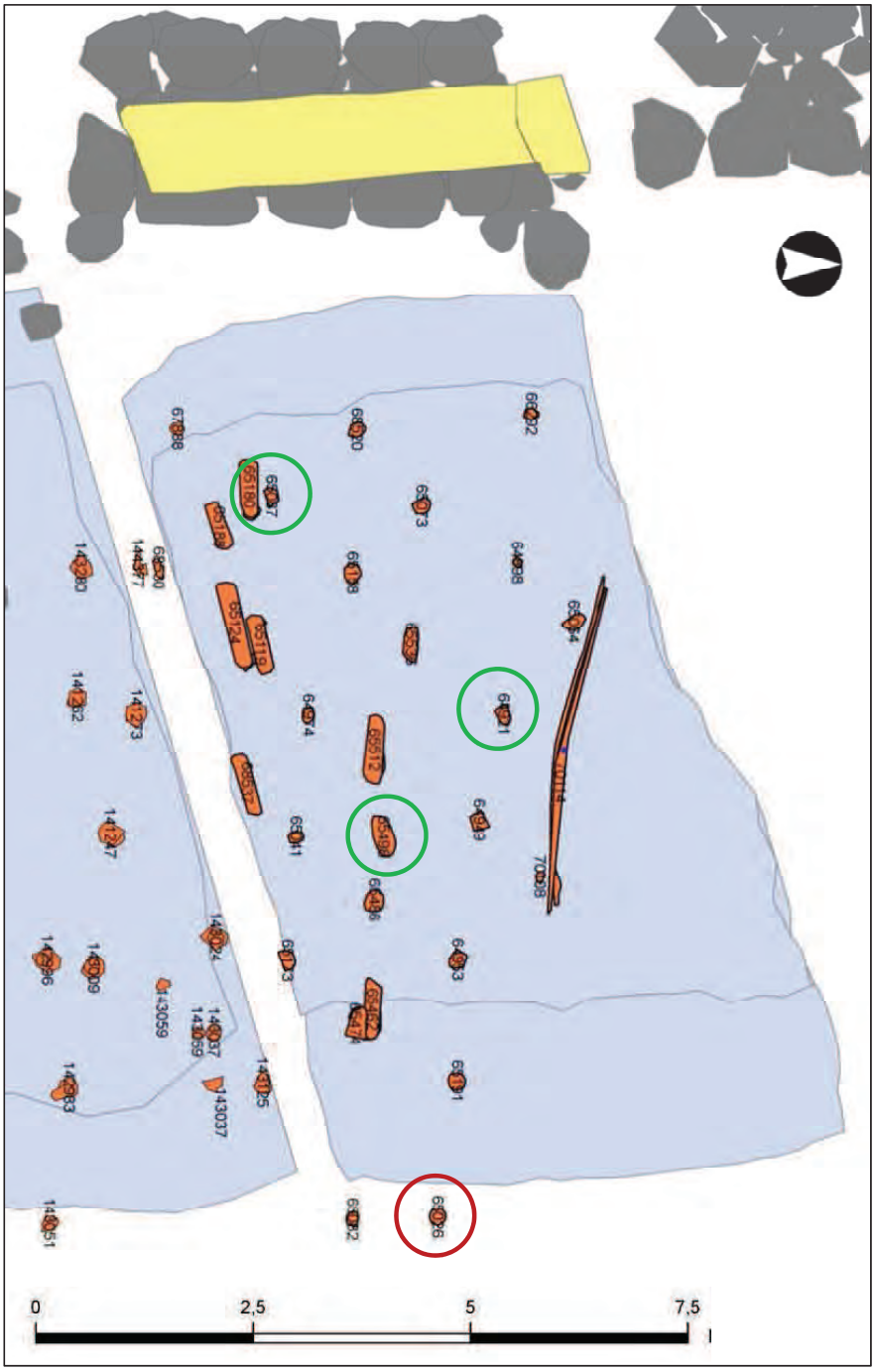

Figure 4.4: A plan of the excavation site showing the boundary of the moat (blue), the wooden piles (orange), stones (grey), and the brick wall (yellow). The wood piles encircled with green are the three poles used as sample material. The wood pole encircled with red is the pole placed outside the moat shown in Figure 4.2b. Scale 7.5 meter, 1:60. Shown with permission from Museum of Copenhagen.

Figure 4.5: Overview of poles on excavation site (KBM 3829 Kongens Nytorv). The arrows show the three poles selected for sample material. Picture © Museum of Copenhagen.

Cutting of samples from the pole discs

A disc about 4 cm in the longitudinal direction was cut off from each pole disc. This disc was cut in half. One half was kept frozen (-20 °C) the other half was cut in four equal sized pieces (Figure 4.3b). The four pieces were kept waterlogged in cold storage (5 °C) in separate polyethylene bags with tap water where all air bubbles were excluded. One of the four pieces was used for compositional analysis (acid insoluble lignin, carbohydrates, ash, and extractive content). A xylem sample covering the surface and 25 mm inward was dried and ball milled. This gave average compositional values for xylem from the heavily decayed surface layer to intact xylem. Another piece was used for density measurements. Two pieces were used for light microscopy, scanning electron microscopy, transmission electron microscopy, ATR-FTIR spectroscopy, UV-microspectrophotometry, and confocal Raman imaging (Table 4.1). Specimens for density and microscopic and micro-spectroscopic examinations were taken 0-5 mm, 10-15 mm, and 20-25 mm from the surface in a straight line from surface to core to cover xylem with heavy, intermediate, and low decay, respectively (Figure 4.3b). All specimens were taken from normal grown xylem and contained at least one growth ring to represent both early and late wood.

Table 4.1: Overview of specimens extracted from three waterlogged Norway spruce poles (KBM), one waterlogged archaeological Scots pine pole (ÅHM), recent Norway spruce (reference) and Scots pine (reference) and the analytical methods performed om the specimens: Light microscopy (LM), scanning electron microscopy (SEM), transmission electron microscopy (TEM), Infrared spectroscopy (ATR-FTIR), UV-microspectrophotometry (UMSP), UV-absorbance line spectra (UMSP, line), confocal Raman imaging (Raman), and size exclusion chromatography (SEC).

Sample	length from surface	LM	SEM	TEM	ATR FT-IR	UMSP	UV-line	Raman	SEC
Picea abies, sapwood	-	x		x	x	x	x	x	
Picea abies, heartwood	-				x				
KBM 65498-A	0-5 mm	x	x	x	x	x		x	
KBM 65498-A	10-15 mm	x	x	x	x	x	x	x	
KBM 65498-A	20-25 mm	x	x	x	x	x			
KBM 65498-A	sound xylem	x			x				
KBM 65498-B	0-5 mm	x		x	x	x			
KBM 65498-B	10-15 mm	x		x	x	x	x	x	
KBM 65498-B	20-25 mm	x		x	x	x			
KBM 65498-B	sound xylem	x			x				
KBM 64921-A	0-5 mm	x			x			x	
KBM 64921-A	10-15 mm	x		x	x	x	x		
KBM 64921-A	10-15 mm	x		x		x			
KBM 64921-A	20-25 mm	x			x				
KBM 64921-A	sound xylem	x			x				
KBM 64921-B	0-5 mm	x			x	x	x	x	
KBM 64921-B	10-15 mm	x		x	x	x	x		
KBM 64921-B	20-25 mm	x			x				
KBM 64921-B	sound xylem	x			x				
KBM 65087-A	0-5 mm	x			x	x			x
KBM 65087-A	10-15 mm	x			x			x	
KBM 65087-A	20-25 mm	x			x				
KBM 65087-A	sound xylem	x			x				
KBM 65087-B	0-5 mm	x			x	x			
KBM 65087-B	10-15 mm	x			x			x	
KBM 65087-B	20-25 mm	x			x				
KBM 65087-B	sound xylem	x			x				
Pinus sylvestris, sapwood	-	x			x	x			
Pinus sylvestris, heartwood	-				x				
ÅHM, NIBE	0-5 mm	x	x		x				
ÅHM, NIBE	10-15 mm	x			x	x			
ÅHM, NIBE	20-25 mm	x			x				

Determination of wood species

Light microscope examination (Appendix A) showed uniform almost squared cells (tracheids) only interrupted by rays and resin ducts which confirmed that the poles were coniferous. Ray tracheids were present whereas spiral thickening was absent. The cross field contained piceoid, cupressoid, or taxodioide pits but lacked fenestriform and pinoid pits. Epithel cells were thick walled. This determines that the poles are either *Larix* or *Picea*. Lack of colour difference between sap- and heartwood, gradual transition from early to late wood and few (approximately 6-9) epithel cells around horizontal resin ducts showed that the poles are *Picea* (Jane 1970; Wilson and White 1986). Norway spruce (*Picea abies*) is the only native species of Northern Europe within the genus *Picea* (Hather 2000). Denmark is not a natural habitat for *Picea abies*. It is likely that it has been planted already in medieval times but reliable evidence is not given until the end of the 18th century. The poles could very likely be imported from Norway, Sweden or south of Bremen in Germany (Lange 1999; Ødum 1968).

4.3 Scots pine pole from Nibe

Excavation site

The Historical Museum of Northern Jutland (Nordjyllands Historiske Museum) excavated softwood material from a well, dated to the 17-18th century in Mellemgade 21 (land register 136a), Nibe (Denmark) in summer 2010. The well construction consisted of four poles placed vertically creating a square and three planks placed horizontally to scaffold the vertical poles. The poles were kept waterlogged and oxygen free by wrapping with several layers of plastic. The poles were stored cold from retrieval until sample preparation. The placement of the poles in a demolished well offers good condition for an anoxic waterlogged environment since the ground water level very likely is high in an area chosen for construction of a well.

Visual description and cutting of pole discs

One pole was selected as sample material. The pole was sharpened at one end and roughly chopped with an axe in the longitudinal direction to give an almost pentagonal cross section (Figure 4.6). The pole was 138 cm long and approximately 11 cm in diameter in the widest area of the pole. The upper part of the pole suffered from surface destruction most likely due to fungal decay. The lower part of the pole was in a very good state of preservation without any visible dehydration damage such as collapse of the surface layer. The wood was soft and spongy.

Two pole discs 40 mm in the longitudinal direction were cut 50 cm and 110 cm from the tip of the pole. The cutting of the pole discs revealed intact heartwood with a diameter of approximately 45 mm. The heartwood was not located in the centre of the pole but close to the surface on one side of the pole (Figure 4.6). The pole contained 27 narrow growth rings (1-2 mm) 50 cm from the tip of the pole. The xylem was light yellow brown with slightly lighter heartwood. The discs were placed in individual polyethylene bags filled with tap water. The bags were placed in an airtight plastic bucket and stored cold (5 °C).

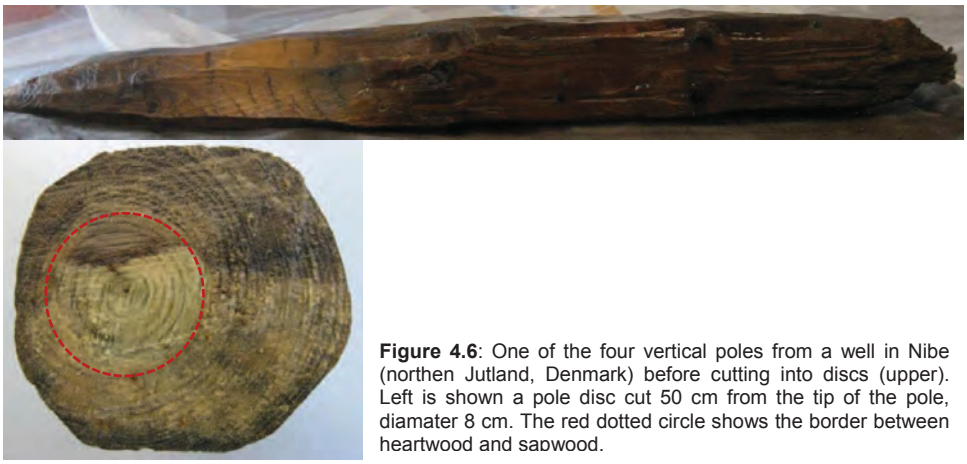

Figure 4.6: One of the four vertical poles from a well in Nibe (northen Jutland, Denmark) before cutting into discs (upper). Left is shown a pole disc cut 50 cm from the tip of the pole, diamater 8 cm. The red dotted circle shows the border between heartwood and sapwood.

Cutting of samples from the discs

The disc taken 110 cm from the tip of the pole was only used for light microscope examinations. The disc taken 50 cm form the tip of the pole was used for light microscope examinations, scanning electron microscopy, composition analysis, density measurements, ATR-FTIR spectroscopy, and UV-microspectrophotometry (Table 4.1). This disc was cut in half. One half was used for compositional analysis. The heartwood was included and gave thereby average values for the composition of the whole pole. The other half was cut in two equal sized pieces. One piece was used for microscopy and micro-spectroscopy, and one piece was used for density measurements. Like the Norway spruce poles from Kongens Nytorv samples were taken 0-5 mm, 10-15 mm, and 20-25 mm from the surface (Table 4.1).

Light microscope examination (Appendix A) showed uniform almost squared tracheids only interrupted by rays and resin ducts in cross section. This confirmed that the pole was coniferous. Presence of dentate walls in ray tracheids and large fenestriform ray pits demonstrated that the pole was *Pinus sylvestris* (Scots pine) (Hather 2000; Wilson and White 1986).

5 Morphological decay pattern

5.1 Macroscopic appearance

Erosion bacteria decay begins at the wood surface where the bacteria access the xylem through rays. The bacteria gain access to the cell lumen of individual tracheids through pits, and the attack on the lignocellulosic cell wall starts from the lumen side of the cell wall. The decay progresses from the surface and inwards in the wood xylem. The decay is slow and the wood is often heterogeneously decayed in a gradient from surface to core. The decayed surface is soft and spongy while the sound core is as hard as normal wood; only totally degraded material has a homogeneous soft structure from surface to core (Björdal 2000; Christensen 1970; Florian Mary-Lou 1981).

5.2 Microscopic decay pattern in cross section

The morphological decay pattern of erosion bacteria decay viewed in cross section is well documented in the literature (PAPER I). This knowledge is presented here along with examples from the sample material used in the present study.

Typical erosion bacteria decay pattern

A typical erosion decay pattern is observed as a heterogeneous decay with sound tracheids adjacent to heavily degraded tracheids (Figure 5.1 and 5.2). Only totally disintegrated xylem contains entirely decayed tracheids. Sound tracheids are morphologically identical to reference material even when viewed with electron microscopy (Figure 5.2a, b). Erosion bacteria degrade the secondary cell wall whereas the compound middle lamella and the cell corners are left intact (Figure 5.1c, Figure 5.2 b, c, Figure 5.3). However, the bacteria do not utilize the secondary cell wall completely but leave behind an amorphous residual material that reduce the cell lumen region or in some instances even fills up the whole cell lumen (Figure 5.1, 5.2d, 5.3). Totally disintegrated wood consists of a fragile skeleton of the compound middle lamella filled up by residual material (Figure 5.1c and h). As the lignin-rich compound middle lamella is not degraded, the morphology of the wood is preserved and it is possible to distinguish different cell types even in heavily decayed wood (PAPER II, Björdal 2000; Björdal et al. 2000; Björdal et al. 1999; Blanchette et al. 1990; Holt and Jones 1983; Kim and Singh 1994; Kim and Singh 2000; Kim et al. 1996; Klaassen 2008a; Schmidt and Liese 1994; Singh and Butcher 1991).

The waterlogged Norway spruce poles

Light microscopy examinations (Appendix A, Figure 5.1) of the bottom discs of the three Norway spruce poles from Kongens Nytorv showed typical erosion bacteria decay as described above. No typical decay patterns of tunnelling bacteria or soft rot fungi (PAPER I) were found in any of the disc samples (PAPER II). One Norway spruce pole was examined in the top, middle and bottom region. Examinations showed that not even the upper part of the submerging environment contained enough oxygen to support the

growth of tunnelling bacteria or soft rot fungi. This further supports that the lower part of the poles have been submerged in a waterlogged anoxic environment from positioning in the moat until excavation.

The waterlogged Scots pine pole

Light microscope examinations (Appendix A) of the Scots pine pole from Nibe showed a mixture of soft rot (PAPER I) and erosion bacteria decay pattern in the upper part of the pole whereas the bottom part only showed typical erosion bacteria decay pattern (Figure 5.4). This indicates that the bottom part of the pole has been situated in an anoxic or near anoxic environment throughout the submerging period whereas oxygen has been available in at least a time interval in the environment surrounding the upper part of the pole.

Degree of degradation

The degree of degradation is proportional to the number of decayed wood cells randomly distributed among sound cells. By microscopic examination of a given region in the sample the degree of degradation can be classified by evaluating the relative proportion of sound to decayed cells (Björdal et al. 1999; Klaassen 2008a; Kretschmar et al. 2008; Macchioni et al. 2013). Figure 5.1c shows heavily decayed latewood tracheids with only few sound tracheids left whereas Figure 5.1d shows less severe decay with many intact tracheids and two tracheids with partly decayed secondary cell wall. The same erosion bacteria decay pattern is seen in early- and latewood and there seems to be no preference for either early- nor latewood (PAPER II). However, it was found that the residual material in earlywood was less dense than residual material from latewood tracheids (Figure 5.1e and f). Earlywood contains less cell wall material in proportion to the cell area and this is most likely the reason why the residual material appears less dense.

The waterlogged Norway spruce poles

Light microscopy examinations (Appendix A, Figure 5.1) of the bottom disc of the three Norway spruce poles from Kongens Nytorv showed heavy decay of the surface layer; at minimum the outermost two or three growth rings contained very few if any sound tracheids. The xylem was intact two to four centimetres from the surface and appeared similar to the reference material (recent Norway spruce) in the light microscope. One centimetre below the surface between one half and two thirds of the tracheids were degraded.

The waterlogged Scots pine pole

Light microscope examinations (Appendix A, Figure 5.4) of the Scots pine pole from Nibe showed that the sapwood was totally disintegrated at the surface; no sound tracheids were present. The inner part of the sapwood was also heavily degraded however with a few sound tracheids present. The heartwood was sound.

Secondary cell wall decay

Observations at the ultrastructural level with electron microscope show that the erosion bacteria attack is initiated from the cell lumen and progress towards the compound middle lamella. The bacteria attach themselves to the S3 layer and the S3 layer is penetrated locally. The attack then progresses into the S2 cell wall layer. The S3 layer can often be seen overlaying the residual material even in heavily decayed tracheids (Figure 5.2d). The bacteria align their main axis parallel to the cellulose microfibrils. In this way each bacterium produces a narrow erosion groove as they move along the fibre. Clusters of bacteria produce a ribbed cell wall surface (Figure 5.5) (Björdal et al. 2000; Holt 1983; Nilsson and Björdal 2008b; Singh and Butcher 1991; Singh et al. 1990). The bacteria terminate the decay when either the S1 layer or the compound middle lamella is reached (Figure 5.2c) (Björdal et al. 2000; Kim and Singh 2000; Singh et al. 1990; PAPER II). In the present study transmission electron microscopy examinations of the boundary between sound cell wall material and decayed cell wall did not show a zone of intermediate decay (Figure 5.2e). The same is observed in transmission electron studies of material with active erosion bacteria; the bacteria are aligned on the border between intact cell wall and the residual material (Björdal et al. 2000). This indicates that erosion bacteria utilize the cell wall effectively and most likely in a single step.

Residual material

The residual material left after erosion bacteria decay of the secondary cell wall is believed to consist of residual products from cell wall decay, such as lignin or lignin degradation products, mixed with bacterial slime and secondary degraders (Kim et al. 1996; Singh and Butcher 1991; Singh et al. 1990) but the chemical composition has not been studied until now (PAPER II and PAPER III; Chapter 7 and 8).

In the present study light microscopy examinations show (Appendix A) that the residual material has an amorphous structure and differs in colour (PAPER II). Two types of residual material were defined on this background (PAPER II). Type I is light in colour and appears smooth in structure. Type II is more dense and darker in colour (Figure 5.1 c and f and Figure 5.4). This was further examined with Toluidine Blue. Toluidine blue is a polychromatic stain useful for plant cell walls. It stains non-lignified tissue and pectin containing middle lamella reddish purple whereas lignified tissue is stained blue-green (Kutscha and Gray 1972). The specificity of the stain has shown to be questionable as it seems to be the case for many light microscopy stains (O'Brien et al. 1964). But among several tested for softwood xylem, toluidine blue was superior to other lignin specific stains (Kutscha and Gray 1972). It is highly usable for staining waterlogged wood decayed by erosion bacteria. It stains sound secondary cell wall light green-blue as reference xylem, the compound middle lamella a slight darker green-blue and the residual material in different shades of blue (Figure 5.1g and h). The structural heterogeneity of the residual material is clearly seen in earlywood stained with toluidine blue (Figure 5.1

h). Furthermore toluidine blue staining clearly shows colour differences in the residual material between adjacent tracheids (Figure 5.1 g).

In light microscope it was observed that a higher portion of the residual material with a lighter and smoother appearance was present close to the wood surface whereas a higher portion of the darker and more granular residual material was observed closer to the un-decayed core; this was observed in both the waterlogged Norway spruce and Scots pine. The two observed types of residual material could give the impression that the cell wall is decayed in two stages. But this is most likely not the case as discussed in Chapter 7 and 8. Scanning electron microscopy analysis of both the waterlogged Norway spruce and Scots pine material (Appendix A) clearly showed the heterogeneous nature of the residual material but did not show the two types of residual material distinguishable with light microscope (Figure 5.3).

Transmission electron microscopy analysis of the waterlogged Norway spruce stained with $KMnO_4$ revealed three different types of residual material (PAPER II). $KMnO_4$ stain is oxidising the lignin polymer within the cell wall. This results in precipitation of the dark and water insoluble reaction product MnO_2 at the reaction site. The higher the lignin content in a given region of the cell wall the darker this area is when viewed in the transmission electron microscopy (Schmitt and Melcher 2004). Type 1 was light grey and mottled (Figure 5.2d). Type 2 was also light grey and mottled but had in addition darker grey or even black areas and areas with circular transparent perforations (Figure 5.2b, c). Type 3 was black with circular transparent perforations (Figure 5.2f). The three types were not observed within the same tracheid but in adjacent tracheids.
Observations of a granular and in some cases heterogeneous residual material from erosion bacteria decay have been reported earlier (Björdal et al. 2000; Kim and Singh 1994; Kim et al. 1996; Singh et al. 1990). Björdal et al. (2000) found two types of granular residual material in waterlogged spruce and pine. Newly produced residual material had a homogeneous appearance whereas residual material in heavily decayed tracheids close to the pole surface had a more heterogeneous appearance. The two types were also observed within single tracheids as two distinct concentric regions. This description is not consistent with the present study. The creation of a heterogeneous residual material is explained by the presence of secondary degraders that have been observed to utilise the residual material for their nutrition thereby changing the density of the residual material (Björdal et al. 2000; Kim and Singh 1994; Singh et al. 1990). This study presents the hypothesis that the difference in structural and visual appearance of the residual material is due to physical movement and aggregation of the residual lignin within the residual wood structure (Chapter 8).

Figure 5.1 a: Cross section of Norway spruce (*Picea abies*) latewood reference material viewed in light microscope. Scale bar = 50 µm.

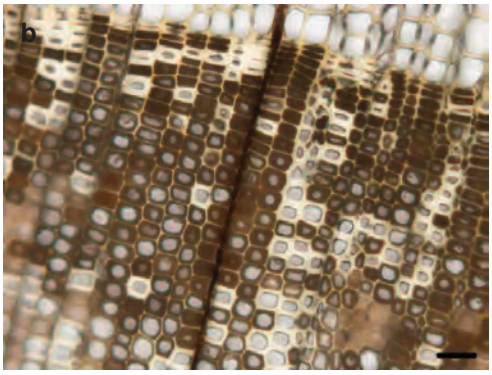

Figure 5.1 b: Cross section of waterlogged archaeological Norway spruce decayed by erosion bacteria viewed in light microscope. The typical pattern of sound tracheids (white) adjacent to decayed tracheids (brown to dark brown) is easily recognised when compared to sound Norway spruce xylem (Figure 5.1 a). Scale bar = 50 µm.

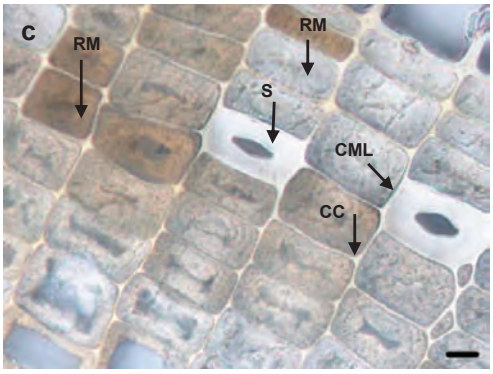

Figure 5.1 c: Cross section of waterlogged archaeological Norway spruce decayed by erosion bacteria viewed in light microscope. Heavily decayed surface layer of pole. Only few sound tracheids are left in the xylem (S). Compound middle lamella (CML) and cell corners (CC) are preserved in decayed tracheids. Decayed tracheids contain a heterogeneous residual material (RM) both with regard to structure and colour. Light and dark coloured residual material is shown with arrows. Scale bar = 10 µm.

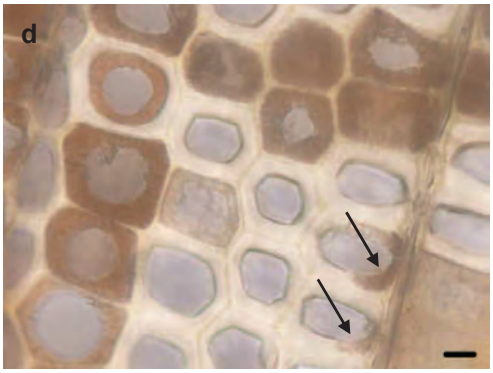

Figure 5.1 d: Cross section of waterlogged archaeological Norway spruce decayed by erosion bacteria viewed in light microscope. Intermediate decay stage with many sound tracheids (light coloured). Two tracheids have partly decayed cell wall (arrows). Scale bar = 10 µm.

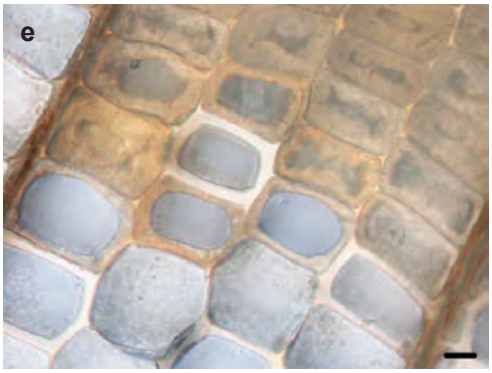

Figure 5.1 e: Cross section of waterlogged archaeological Norway spruce decayed by erosion bacteria viewed in light microscope. Transitional zone between earlywood and latewood show same erosion bacteria decay pattern as latewood. Scale bar = 10 µm.

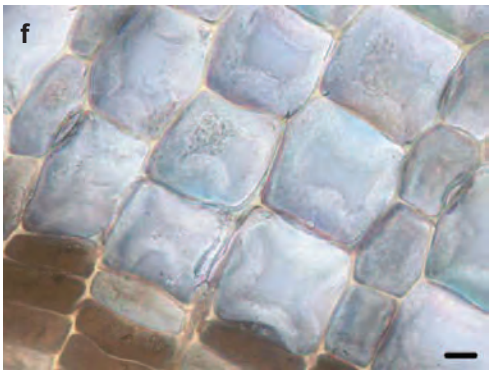

Figure 5.1 f: Cross section of waterlogged archaeological Norway spruce decayed by erosion bacteria viewed in light microscope. Earlywood show same erosion bacteria decay pattern as latewood. However, the residual material is less dense. Scale bar = 10 µm.

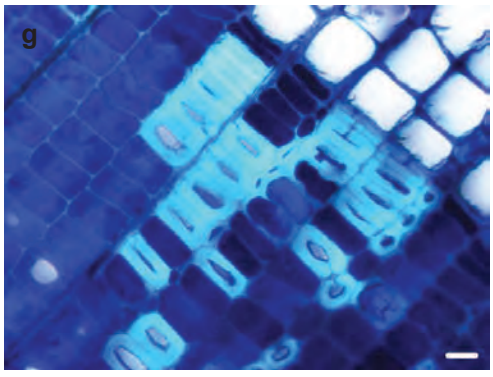

Figure 5.1 g: Cross section of waterlogged archaeological Norway spruce decayed by erosion bacteria viewed in light microscope. Intermediate decayed latewood stained with toluidine blue. Sound cells are light green-blue, compound middle lamella a slightly darker green-blue, whereas the residual material has different shades of blue. Scale bar = 20 µm.

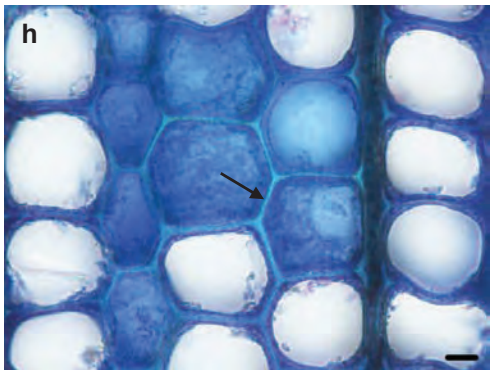

Figure 5.1 h: Cross section of waterlogged archaeological Norway spruce decayed by erosion bacteria viewed in light microscope. Heavily decayed earlywood stained with toluidine blue. All tracheids are decayed. The compound middle lamella is morphologically intact (arrow) and much lighter in colour than the residual material. The heterogeneous nature of the residual material is clearly seen. Scale bar = 10 µm.

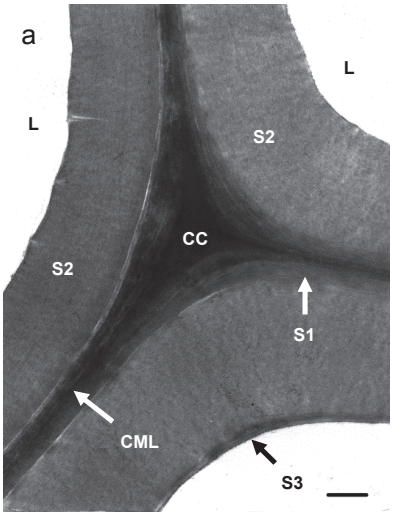

Figure 5.2 a: Transmission electron microscopy cross section of Norway spruce (*Picea abies*) latewood reference material in cell corner area. CC = cell corner, CML = compound middle lamella, S1 = S1 layer, S2 = S2 layer, S3 = S3 layer, L = lumen. Scale bar = 0.75 µm.

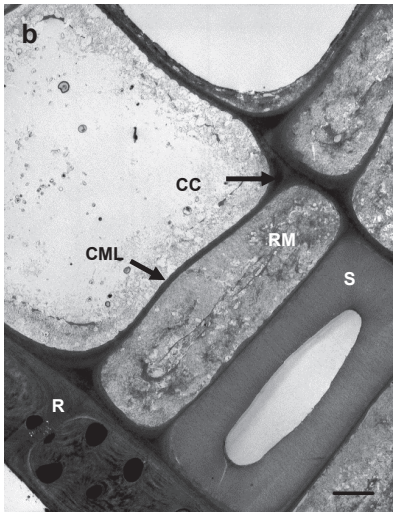

Figure 5.2 b: Transmission electron microscopy cross section of waterlogged archaeological Norway spruce decayed by erosion bacteria. A sound tracheid (S) and a sound ray parenchyma cell (R) are seen next to decayed tracheids. Decayed tracheids have intact cell corners (CC) and compound middle lamella (CML) and hold an amorphous residual material (RM). Decayed latewood tracheids contain Type 2 residual material. Scale bar = 3.3 µm.

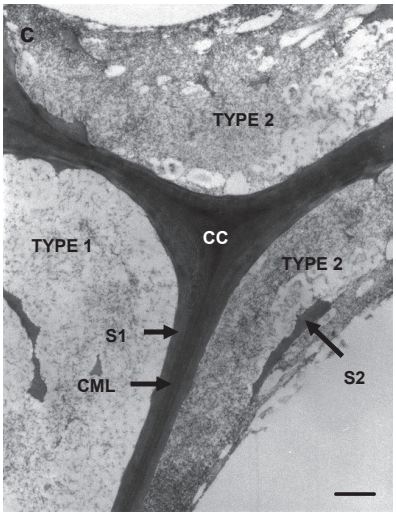

Figure 5.2 c: Transmission electron microscopy cross section of waterlogged archaeological Norway spruce decayed by erosion bacteria; cell corner area with three adjacent heavily decayed tracheids. Cell corner (CC), compound middle lamella (CML), S1 layer, and small S2 layer regions are intact. Type 1 residual material (RM) is present in one tracheid and Type 2 in two tracheids. Scale bar = 0.75 µm.

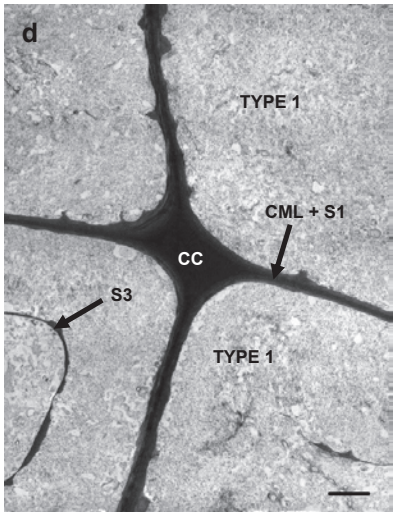

Figure 5.2 d: Transmission electron microscopy cross section of waterlogged archaeological Norway spruce decayed by erosion bacteria; cell corner (CC) area with four adjacent heavily decayed tracheids. All four tracheids contain Type 1 residual material that fills up the lumen. Intact S1 layer and fragments of intact S3 layer are seen. Scale bar = 2 µm.

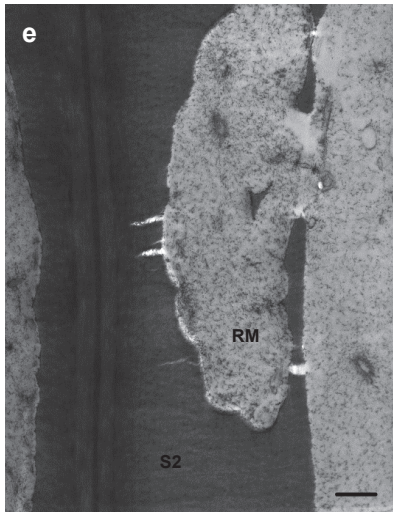

Figure 5.2 e: Transmission electron microscopy cross section of waterlogged archaeological Norway spruce decayed by erosion bacteria; two adjacent tracheid walls with partial decay. No intermediate decay stage is seen at the boundary between sound S2 layer and residual material (RM). Scale bar = 0.75 µm.

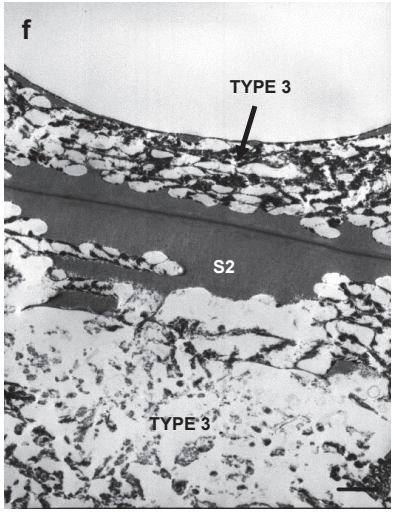

Figure 5.2 f: Transmission electron microscopy cross section of waterlogged archaeological Norway spruce decayed by erosion bacteria; two adjacent tracheid walls both containing Type 3 residual material. Some intact S2 layer regions are still present. Scale bar = 2 µm.

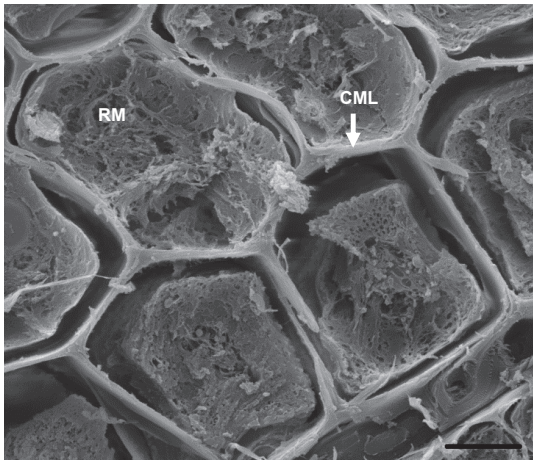

Figure 5.3 Cross sectional view in scanning electron microscopy of waterlogged archaeological Scots pine heavily decayed by erosion bacteria. All tracheids are decayed; the compound middle lamella (CML) is intact and a heterogeneous residual material (RM) fills up the whole tracheid. Scale bar = 10 µm.

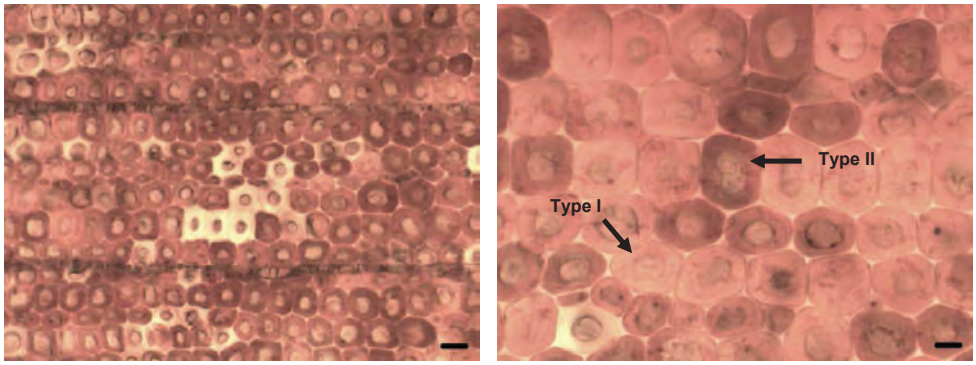

Figure 5.4: Light microscope cross section of waterlogged archaeological Scots pine decayed by erosion bacteria. The sections are taken 10 mm from the surface. The xylem is heavily decayed since only few sound tracheids are left (white cells). The decayed tracheids contain an amorphous residual material that is either light and smooth (Type I) or darker and more granular (Type II). The sections are stained with Safranine O in ethanol. Scale bar = 20 µm (left) and 10 µm (right).

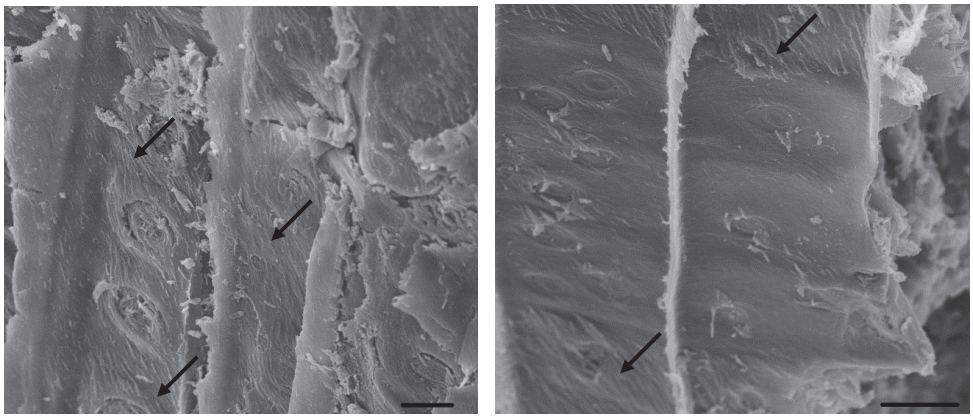

Figure 5.5: Longitudinal view of waterlogged archaeological Norway spruce wood decayed by erosion bacteria viewed in scanning electron microscopy. The decayed tracheids show the characteristic stripy appearance of the eroded cell wall (arrows). Scale bars = 10 µm.

Summary of observations in cross section

Table 5.1 summarises the observed morphological features of the waterlogged Norway spruce xylem when viewed in cross section with light and transmission electron microscopy.

Table 5.1: Light (LM), scanning (SEM) and transmission electron microscopy (TEM) observation on cross section of 400 years old waterlogged Norway spruce poles decayed by erosion bacteria.

Microscopic observation		Figure
Gradient of decay from surface to core: Heavily decayed surface layer with very few sound tracheids left; between half and two thirds of the tracheids decayed 10 mm from the surface; majority of tracheids sound 20-40 mm from the surface		-
Mixture of decayed and intact tracheids for both early and late wood; No special preference for early or late wood.		5.1b, e
Ray parenchyma cells and epithelia cells remained sound even in heavily decayed xylem		5.7
Sound tracheids did not show any sign of decay when compared to reference material		5.1, 5.2
Tracheids with partly intact S2 cell wall showed no intermediate decay stage between sound S2 cell wall and the eroded cell wall		5.2e
Preferential decay of the S2 cell wall; compound middle lamella and cell corners were not decayed		5.1, 5.2, 5.3
S1 cell wall was most often intact; a thin layer of the S1 cell wall was decayed in a few cases		5.2
Parts of the S3 cell wall were often preserved even in heavily eroded tracheids		5.2
Residual material in tracheids after decomposition of the S2 cell wall most often filled up the lumina		5.1, 5.2, 5.3
Two types of residual material were observed in LM (Type I and II) and three types in TEM (Type, 1, 2 and 3):		
Type 1/I:	LM: Light in colour, smooth, both secondary cell wall area and lumen area filled up	5.1c, 5.4
	TEM: Light grey and mottled	5.2d
Type 2/II:	LM: Denser and granular, sometimes restricted to the secondary cell wall area	5.1c, 5.4
	TEM: Light grey and mottled, in addition darker grey or even black areas + areas with circular transparent perforations	5.2c
Type 3:	TEM: Black with circular transparent perforations	5.2f
Type 1/I and type 2/II present in all samples; Type I more frequently observed than Type II; Type 3 only present in two samples from the same pole; not observed in earlywood tracheids;		-
Type 1, 2 and 3 not observed within the same tracheid but often in adjacent tracheids		5.1, 5.4, 5.2c
Bordered pits often well preserved even when the S2 cell wall was heavily decayed; torus, initial pit border, and a thin extractive layer were always preserved		5.9

5.3 Decay viewed in longitudinal direction

The heterogeneous decay pattern of adjacent sound and decayed tracheids observed in cross section suggest that sound and decayed tracheids are distributed between each other. However, cross sections only provide information in one plane of the whole cell length. Björdal et al. (2005) have examined a series of 2D cross sections along 340 µm of the same cluster of pine tracheids. This showed that an apparently sound tracheid is not

necessarily sound in the whole length of the cell. In addition it was observed that moderately degraded tracheids consist of both degraded and sound regions. This shows that tracheids in most cases are heterogeneously decayed in the longitudinal direction unless complete degradation has taken place. In longitudinal direction erosion bacteria decay has either been reported as a stripy appearance of the wood cell wall (Kretschmar et al. 2008; Singh and Butcher 1991) or as a diamond- or V-shaped pattern (Björdal 2000; Björdal et al. 1999; Boutelje and Bravery 1968; Klaassen 2008a; Singh and Butcher 1991). Differences between the stripy- and the diamond-shaped decay pattern have been suggested to depend on oxygen limiting conditions resulting in a more incomplete utilisation of the wood substrate (Singh et al. 1990).

However, light microscopy examinations (Appendix A) in the tangential longitudinal direction of the waterlogged Norway spruce wood study showed regions with a stripy appearance and regions with characteristic diamond- and V-shaped notches within the same specimens (Figure 5.6). In addition, it was found that it is not easy to interpret longitudinal sections of erosion bacteria decay. A cut through tracheids in the longitudinal direction is not necessary placed in the centre of the tracheid but often through an arbitrary part of the cell wall. This makes it hard to interpret which part of the cell is actually examined. This could be partly overcome by limiting the examination to tracheids that were cut through the centre and thereby showed secondary wall on both sides of the lumen. Intermediate decayed latewood was most simple to interpret as the thick secondary cell wall in latewood was easily recognised in un-degraded regions. This gave a good starting point to determine what was present in the cell wall and what was present in the lumen of the tracheids.

Examination of tangential longitudinal sections indicated that the diamond- and V-shaped notches are alternating sound and decayed cell wall regions. Figure 5.6 shows that the notches are situated within the cell wall and not in the lumen. The stripy pattern follows the microfibril direction in the S2 layer of normal tracheids just as erosion bacteria have been shown to align themselves along the microfibrils during decay (Holt 1983). Furthermore the residual material has a relatively even staining with toluidine blue in these regions (Figure 5.6). This lead to the hypothesis that the stripy appearance are regions with a high degree of order in the residual cell wall material; meaning that no physical disturbance of the residual material had occurred after erosion bacteria decay in these regions. The stripes are ‘footprints’ after erosion bacteria. Individual erosion troughs cannot be viewed in light microscopy but repeated decay solely in the microfibril direction will most likely give a stripy appearance if residual cell wall material is left undisturbed.

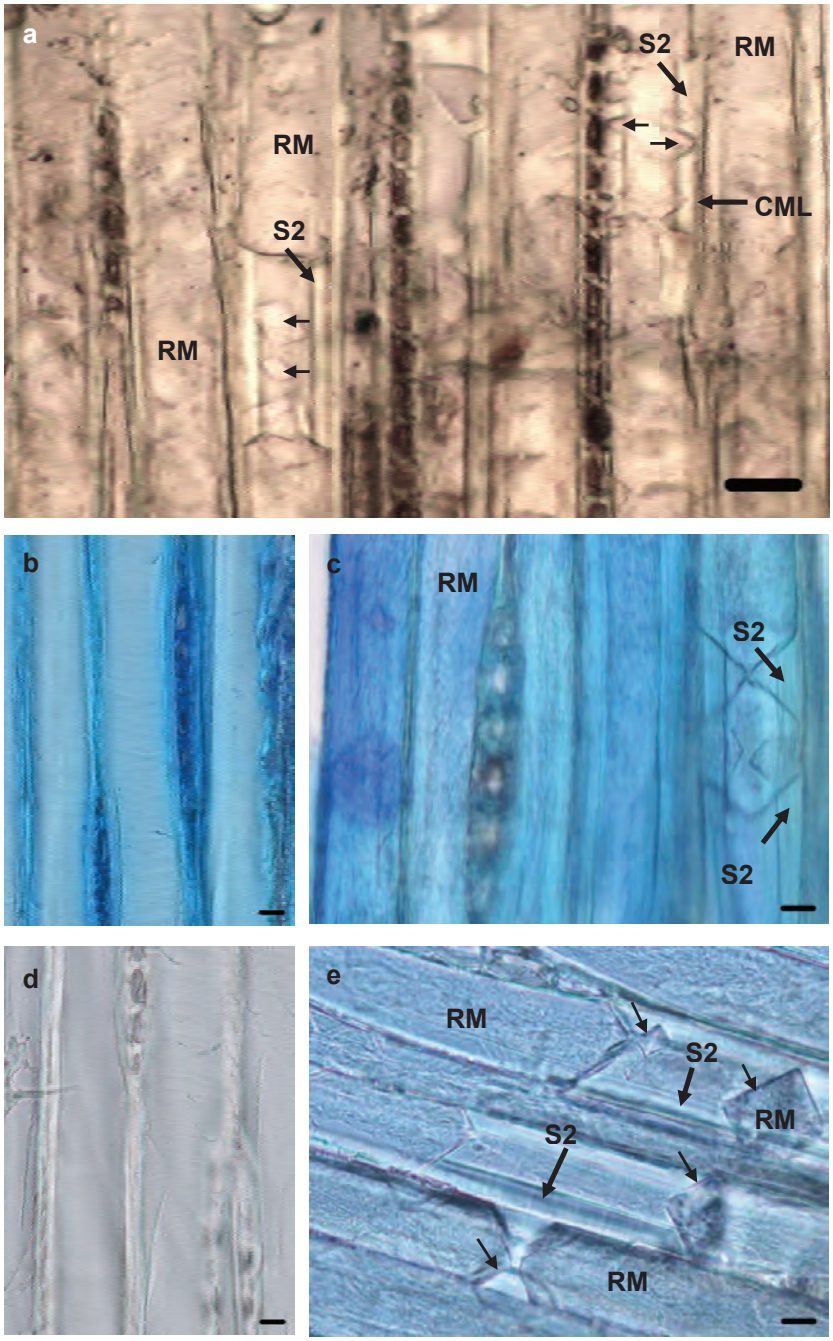

Figure 5.6: Light microscope images in tangential longitudinal direction of: a), c), e) waterlogged archaeological Norway spruce wood decayed by erosion bacteria; b) and d) reference material. a), d), e) are unstained; b) and c) are stained with toluidine blue. a) and e) Tracheids with alternating decayed and sound cell wall areas; diamond and V-shaped notches are indicated by small arrows. c) Left side of image show residual material (RM) with a stripy appearance. Right side show one tracheid with partly preserved S2 seen as a V-shape and a diamond shape containing RM. Scale bars = 25 µm for (a) and 10 µm for all others.

5.4 Decay resistance

It has been observed that heartwood is much more resistant to erosion bacteria decay than sapwood in some species (e.g. pine and oak) (Klaassen and van Overeem 2012). This is most likely due to pit closure, and formation of tyloses and toxic substances (e.g. tannins, lignans, terpenes, and stilbenoids). Differences in decay resistance have also been observed in different cell types in the wood xylem. Ray tracheids and ray parenchyma cells are generally well preserved in pine and spruce compared to axial tracheids (Björdal et al. 2000; Singh et al. 2006). Differences in decay have been found to correlate with lignin composition and concentration (Barbour and Leney 1986). In the present study the waterlogged Norway spruce poles from Kgs Nytorv showed a high degree of preservation of ray parenchyma cells and epithelial cells in resin ducts (Figure 5.7) (PAPER II). This could be explained by protection of the ray cells by phenolic resins. It could also be associated with the degree of lignification, since heavy lignification has been found in ray parenchyma cells of black spruce (Fergus et al. 1969; Westermark et al. 1988). Decay resistance of cell corners and compound middle lamella, the outer layer of S2 in mild compression wood (Kim and Singh 1999; Singh 1997b; PAPER II) (Figure 5.8), and the observed partial decay of the S3 layer support the hypothesis that erosion bacteria decay correlates with lignin composition and concentration (Barbour and Leney 1984).

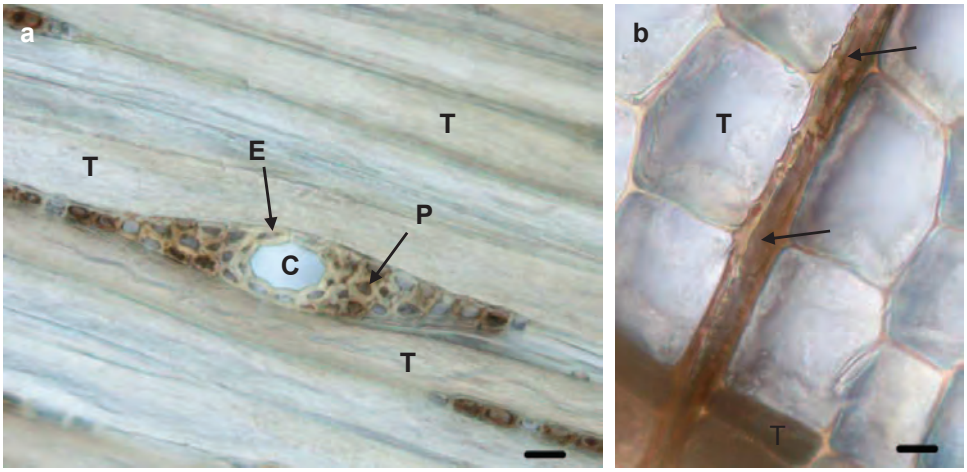

Figure 5.7: Waterlogged archaeological Norway spruce wood heavily decayed by erosion bacteria viewed in light microscope. a) Tangential longitudinal section showing preserved ray parenchyma cells (P) and epithelial cells (E) surrounding a radial resin canal (C). All surrounding axial tracheids (T) are decayed. Scale bar = 20 µm. b) Cross section in growth ring boundary showing decayed tracheids (T) but intact ray cells (arrows). Scale = 10 µm.

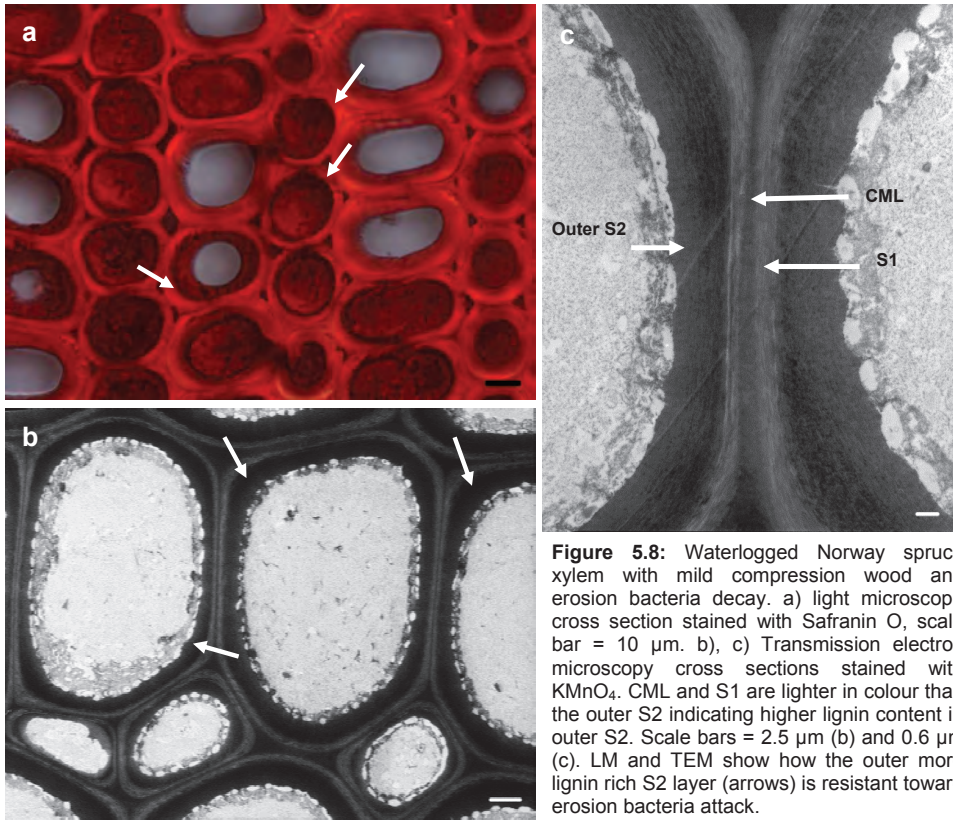

Figure 5.8: Waterlogged Norway spruce xylem with mild compression wood and erosion bacteria decay. a) light microscope cross section stained with Safranin O, scale bar = 10 µm. b), c) Transmission electron microscopy cross sections stained with $KMnO_4$. CML and S1 are lighter in colour than the outer S2 indicating higher lignin content in outer S2. Scale bars = 2.5 µm (b) and 0.6 µm (c). LM and TEM show how the outer more lignin rich S2 layer (arrows) is resistant toward erosion bacteria attack.

The S1 layer has been reported as more decay resistant than the S2 layer (Björdal et al. 2000; Kim and Singh 2000; Singh et al. 1990). Electron microscopy examination in the present study of the waterlogged Norway spruce material showed a high degree of S1 layer preservation both in the heavily decayed surface layer and the inner less decayed xylem of the poles (PAPER II). This confirms a more recalcitrant nature of the S1 cell wall layer compared to the S2 cell wall layer. The lignin content of S1 is reported as both slightly higher (Fengel 1969) and lower (Fromm et al. 2003) than the S2 cell wall layer in spruce tracheids. This suggests that the lignin concentration is not the reason for the more recalcitrant nature of the S1 layer. The chemical composition of the biopolymers, or the angle and direction of the cellulose micro fibrils may have an influence on decay resistance. The S2 layer is a thick layer with a constant microfibril angel which makes this layer homogeneous in terms of supramolecular structure. The S1 and S3 layer on the contrary have changing microfibril angles within a thin cell wall layer (Chapter 2). Erosion bacteria align themselves along the microfibrils (Holt 1983), and it seems reasonable that the microfibril angle or a change in microfibril angle has an influence on the recalcitrance of the S1 and S3 layers. Furthermore the lignin and hemicellulose composition in the outer layer of compression wood differs from the chemical composition of normal xylem (Chapter 2). This indicates that chemical composition of

the biopolymers may also be a factor controlling the recalcitrance nature of compression wood and not only the higher lignin concentration.

High lignin content is also reported in torus and initial pit borders of bordered pits in spruce (*Picea abies* and *Picea mariana* Mill.) and beech (*Fagus sylvatica* L.) latewood (Fergus et al. 1969; Fromm et al. 2003; PAPER II). This is believed to be part of the reason for the observed decay resistance toward erosion bacteria of especially torus and initial pit border in bordered pits (Figure 5.9) (Singh 1997a PAPER II). The bordered pits might be an impediment to the spread of erosion bacteria between tracheids. It has been reported that wood-inhabiting bacteria can degrade the pectin rich pit membrane and thereby improve the permeability of the wood (Greaves 1971). This would provide free access for erosion bacteria. But if the bordered pits are aspirated, the pit membrane will be overlaid with the lignin rich torus and the pits will be more resistant to bacterial decay.

The chemical composition and the supramolecular structure of the cell wall seem to be the controlling factors for erosion bacteria decay. The bacterial affinity to the microfibrils and the bacterial enzymatic tool box are optimised to the S2 cell wall layer. However, inter-cell transport by means of simple physical accessibility is important for the possibility of the bacteria to reach the individual cells and cell wall layers. Initial decay is often observed in close association with easily accessible transport routes as vessel elements in hardwood and large cross-field pits in pine whereas this is not necessarily observed close to rays in spruce and fir with small bordered cross-field pits (Björdal 2000; Klaassen 2008a). This is further supported by Klaassen (2008b) who has reported that wood species with high pit permability (eg. *Pinus sylvestris* sapwood) had a higher susceptibility to decay by erosion bacteria than species with low pit permability (eg. *Picea abies*).

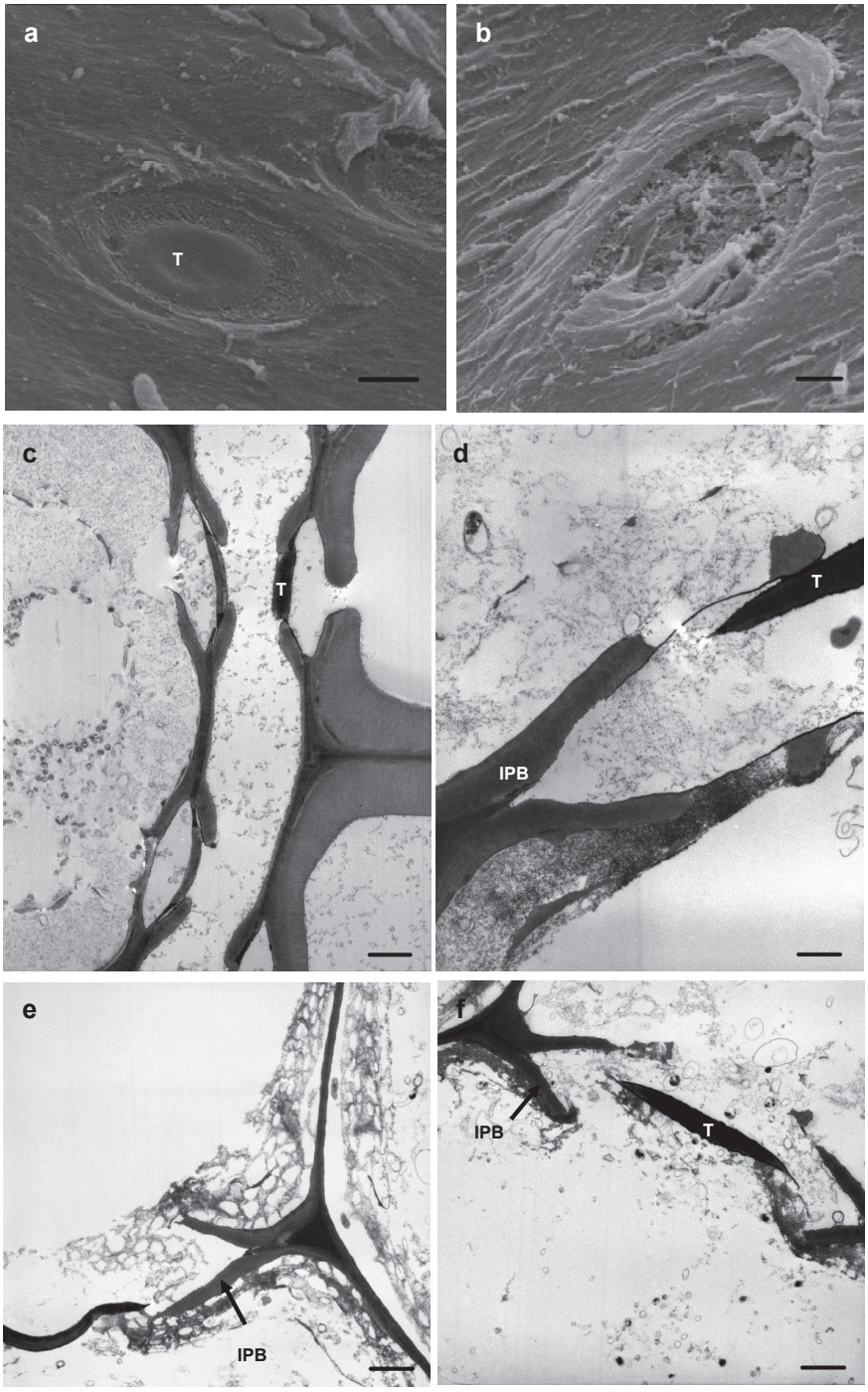

Figure 5.9: Bordered pits in Norway spruce decayed by erosion bacteria. Torus = T, initial pit border = IPB. Scanning electron microscopy image of intact pit (a) and decayed pit (b). c) Transmission electron microscopy image of intact pits in connection to ray tracheid. d) Transmission electron microscopy image of partly decayed bordered pit; torus and initial pit border are preserved; almost all S2 cell wall material is degraded. e) and f) Transmission electron microscopy images of heavily decayed tracheids with preserved initial pit border and torus. Scale bars = 2 µm (a, b, c, e, and f), scale bars = 0.75 µm (d).

6 Chemical analysis of waterlogged wood

6.1 Chemical composition

The chemical composition of waterlogged archaeological wood has been studied in a relatively wide range of publications (PAPER I). The results are unfortunately obscured by the fact that with the exception of a few cases the decay type has not been determined before analysis (Capretti et al. 2008; Gelbrich et al. 2008; Giachi and Pizzo 2009; Hedges et al. 1985; Obst et al. 1991; PAPER II; PAPER III). The wood is most often defined by wood species and as waterlogged and/or archaeological but not in terms of the morphological decay type (i.e. erosion bacteria, tunnel bacteria, soft rot). Since different decay organisms facilitate different ultrastructural pattern of decay it must be expected that the chemical composition is different in wood decayed by different microorganisms (PAPER I). In addition the picture is complicated given that slow abiotic decay may have some influence on the chemical composition (Borgin et al. 1975a; Pan et al. 1990; PAPER III). It is therefore crucial to determine potential decay type(s) and degree of degradation before chemical analyses.

6.2 Traditional analytical methods

The most widely used methods for chemical characterisation of waterlogged archaeological wood are traditional wet chemical and spectroscopic methods. Wet chemical methods are based on standards developed by the Technical Association of the Pulp and Paper Industry (TAPPI) to separate and determine the chemical constituents of wood quantitatively. The most widely used spectroscopic methods are Fourier Transform Infra-Red spectroscopy (FT-IR), Nuclear Magnetic Resonance spectroscopy (NMR), and analytical pyrolysis coupled to Gas Chromatographic and/or Mass spectroscopy (Py-GC/MS). Despite the general lack of determination of decay type all chemical compositional studies show a general trend of a preferential loss in carbohydrates as compared to the lignin fraction of the wood (PAPER I). This correlates well with the preferential decay of the cellulose rich secondary cell wall and the preservation of the lignin rich cell corners and middle lamella observed with microscopic techniques in wood degraded by erosion bacteria (Chapter 5).

Wet chemical analyses

Traditional compositional analyses were performed on the waterlogged archaeological Norway spruce and Scots pine and the reference materials used in the present study (Appendix A). The results are presented in Table 6.1 and 6.2. The results showed the expected general trend of elevated lignin content in proportion to the carbohydrate content for all four waterlogged poles compared to reference material (Table 6.1). The ash content is approximately ten times larger in the waterlogged wood compared to the reference material. Elevated inorganic content is a general trend observed in waterlogged archaeological wood (PAPER I). However, it cannot be directly associated with the degree of degradation (Gelbrich et al. 2008). The high inorganic level is most likely caused by a combination of the permeability of the wood structure (wood species, growth

conditions, degree of degradation, cracks and fissures), the level of inorganic components in the submerging environment, and the water flow at the burial site. This theory is supported by the fact that in cases where corroded metals are found in close contact with waterlogged wood the inorganic levels are many times greater than the levels found in reference material (Fors et al. 2011; Fors et al. 2014; Kim 1990; MacLeod and Richards 1996a).

***Table 6.1**: Average values obtain on compositional analysis (water-ethanol extractives, acid insoluble lignin (Klason), ash, and carbohydrate content) of waterlogged archaeological Norway spruce and Scots pine and reference material hereof. Carbohydrate content is the sum of the values presented in Table 6.2.*

	Extractives	**Klason lignin**		**Ash content**		**Carbohydrates**		**Mass balance**	
	%	%	SD	%	SD	%	SD	%	SD
Picea abies, ref	0.95	28	0.70	0.22	0.012	89	11	117	12
KBM 64921	0.63	35	0.60	1.8	0.52	56	3.0	92	2.2
KBM 65087	0.80	39	3.5	1.6	0.026	57	5.9	97	4.3
KBM 65498	0.46	41	0.087	2.1	0.11	64	4.4	106	3.3
Pinus Sylvestris, ref.	7.3	27	0.32	0.35	0.0048	70	2.3	100	1.9
ÅHM, pole	1.5	45	0.32	3.5	0.013	44	2. 1	91	2.5

***Table 6.2**: Average values of detected sugar monomers resulting from strong acid hydrolysis of the structural carbohydrates in waterlogged archaeological Norway spruce and Scots pine and reference material hereof.*

	Arabinan		**Galactan**		**Glucan**		**Xylan**		**Mannan**	
	%	SD	%	SD	%	SD	%	SD	%	SD
Picea abies, ref	0.66	0.20	0.41	0.18	64	8.3	8.7	1.17	15	1.5
KBM 64921	1.1	0.11	1.3	0.089	39	2.2	4.4	0.29	10	0.37
KBM 65087	0.31	0.15	0.5	0.12	41	4.0	4.4	1.24	11	1.2
KBM 65498	0.63	0.095	1.1	0.29	43	3.6	5.7	0.58	14	2.2
Pinus Sylvestris, ref.	1.8	0.075	1.9	0.067	46	1.8	8.0	0.15	12	0.52
ÅHM pole	1.8	0.10	2.5	0.13	27	1.4	5.7	0.49	7.0	0.064

Water soluble and organic extractives were contrary to the inorganic content lower in all four waterlogged poles compared to the reference material (Table 6.1). This is also a general trend observed in waterlogged archaeological wood (PAPER I). However, the reduction cannot be correlated to the degree of degradation (Gelbrich et al. 2008). It has been suggested that water flow and not microbial degradation is the major cause of depletion of organic extractives (Pan et al. 1990). Water soluble extractives are for a large part non-structural carbohydrates that are readily metabolised by bacteria in the initial stage of colonization (Blanchette et al. 1990; Greaves 1971; Wei et al. 2009). It is therefore not surprising that the content of water soluble carbohydrates was low when high performance liquid chromatography analysis was performed on the liquid collected after Soxleth extraction (Appendix A). Very low amounts of glucose and arabinose (approximately 10-20 µg monosaccharides per g wood meal) and undetectable amounts

of galactose, xylose, and mannose were found. This applied to all four poles. A theory might be that the erosion bacteria consortium acting on the lignocellulosic cell wall exhausts the carbohydrates liberated from the cell wall very effectively. This is supported by the observed cellulosomes in close association to active erosion bacteria indicating a highly efficient system for extracellular degradation of polymeric substances (Chapter 3.3). The theory is further supported by morphological observations of the residual material in the present study. In partly decayed tracheids residual material adjacent to intact cell wall material is not morphologically different from residual material elsewhere in the cell lumen (Figure 5.2e). This indicates that all degradable cell wall components are removed in close association with the actual deconstruction of the cell wall polymers. It seems plausible as anaerobic metabolism offers lower energy output than aerobic metabolism and high efficiency is needed. However, differences in the residual material within the same tracheids have been observed in association with secondary degraders (Chapter 5). It is not known which metabolic waste products these secondary degraders feed on and how fast they utilise the waste products after release from the primary degraders.

Table 6.2 shows the chemical composition of the structural carbohydrate fraction in the residual structure of the waterlogged Norway spruce and Scots pine material. The glucan and mannan content is reduced by approximately a third. The xylan content is approximately halved. The arabinan and galactan contents are halved, equal or in some instances increased. It is not surprising that all the major monosaccharides are present in the analysed wood material since the material used is a mixture of the heavily decayed surface layer, an intermediate zone of decay, and sound xylem in the inner part of the poles. This means that the material contains a relative big portion of morphological intact cell wall material.

Decay of hemicelluloses in preference to cellulose has been reported several times in waterlogged wood samples (Bardet et al. 2009; Hedges et al. 1985; Kim 1990; Obst et al. 1991; Pan et al. 1990; Wilson et al. 1993). This is a common explanation since hemicelluloses are more readily accessible for hydrolysis due to the branched and substituted structure compared to the crystalline structure of cellulose (Decker et al. 2008). However, this is a simplification. The microbiological decay of polysaccharides is not random in the exposed xylem but follows the bacterial frontier in the wood xylem from the initial attack at the surface towards the core. Furthermore it is not possible to establish a general trend regarding the decay resistance of some carbohydrates compared to others when the literature is reviewed (PAPER I). This could be because there are too many variables interfering with the results. Three important variables that should have an influence on the final chemical composition are wood species, decay type, and degree of degradation. Different wood species have different chemical composition and concentration of hemicelluloses and the results will vary alone because of the differences in the native material. Different decay types result in different ultrastructure and thereby different chemical composition of the residual structure. Some cell types and cell wall

compartments are more recalcitrant than others. This is further complicated by the random mixture of sound and decayed cell wall regions and the possibility of interference from abiotic decay mechanisms. Therefore, it is not easy to interpret the cause of observed differences in polysaccharide composition from analysis on average xylem samples. In this study (Table 6.2) and by Iiyama et al. (1988) and Hedges et al. (1985) it has been shown that xylan is decayed in preference to mannan. The glucomannan backbone in softwood contains mannose and glucose in the ratio 3:1 whereas the xylan backbone is a homopolymer. This means that the two polymer backbones roughly are degraded to the same degree in the material studied here.

ATR-FTIR analyses

In the present study ATR-FTIR analyses were performed on the waterlogged archaeological Norway spruce and Scots pine and the reference materials (Appendix A). The results are presented and discussed below. Figure 6.1 shows ATR-FTIR spectra of waterlogged archaeological Norway spruce and Scots pine and Norway spruce and Scots pine reference material in the fingerprint region from 1800-600 cm^{-1}. The samples were taken in the heavily decayed surface layer (0-5 mm from surface) of the poles, in the intermediate decay zone (10-15 mm from surface), and in the inner zone with primarily intact xylem (20-25 mm from surface) (Appendix A). Table 6.3 shows assignment of FT-IR bands for Norway spruce wood, spruce lignin, spruce milled wood lignin, spruce holocellulose, and oligosaccharides according to the literature (Fackler et al. 2010; Faix 1991; Marchessault 1962; Schwanninger et al. 2004). The table also lists the FT-IR bands observed in FT-IR spectra of Norway spruce reference material, waterlogged Norway spruce in intact xylem, and waterlogged Norway spruce in the heavily decayed outer surface layer from FT-IR spectra obtained in this study and presented in PAPER III. Figure 6.1a shows how the relative lignin content is increased and the relative carbohydrate content is decreased in the waterlogged Norway spruce compared to reference material. Bands assigned to lignin (1600 cm^{-1}, 1508 cm^{-1}, 1263 cm^{-1}, 1215 cm^{-1}, 1140 cm^{-1}, and 856 cm^{-1}) increases and band assigned to carbohydrates (1732 cm^{-1}, 1307 cm^{-1}, 1155 cm^{-1}, 1100 cm^{-1}, 1050 cm^{-1}, 1024 cm^{-1}, and 895 cm^{-1}) decreases (Table 6.3; Figure 6.1a). This is expected and is in agreement with previous spectroscopy studies of waterlogged archaeological wood (Gelbrich et al. 2008; Giachi and Pizzo 2009; MacLeod and Richards 1997; Pavlikova et al. 1993; Petrou et al. 2009; Pizzo et al. 2013). Furthermore Figure 6.1a shows how the intensity of bands assigned to lignin and carbohydrate correlates with the gradient of decay from pole surface to core. The spectrum of the heavily decayed surface layer (red line) has a marked increase in band heights assigned to lignin whereas the spectrum of xylem taken 20-25 mm from the surface (green line) has close resemblance to the spectrum of the reference material. The intermediate decayed xylem (blue line, 10-15 mm from surface) shows a spectrum in between these two spectra. This correlation has been shown previously in spectroscopic studies of chemical composition combined with determination of degree of degradation with light microscopy, density, or maximal water content measurements (Blanchette and Hoffmann 1994; Gelbrich et al. 2008; Pizzo et al. 2013; Wilson et al. 1993). Several spectroscopic methods are well suited for determining the degree of degradation.

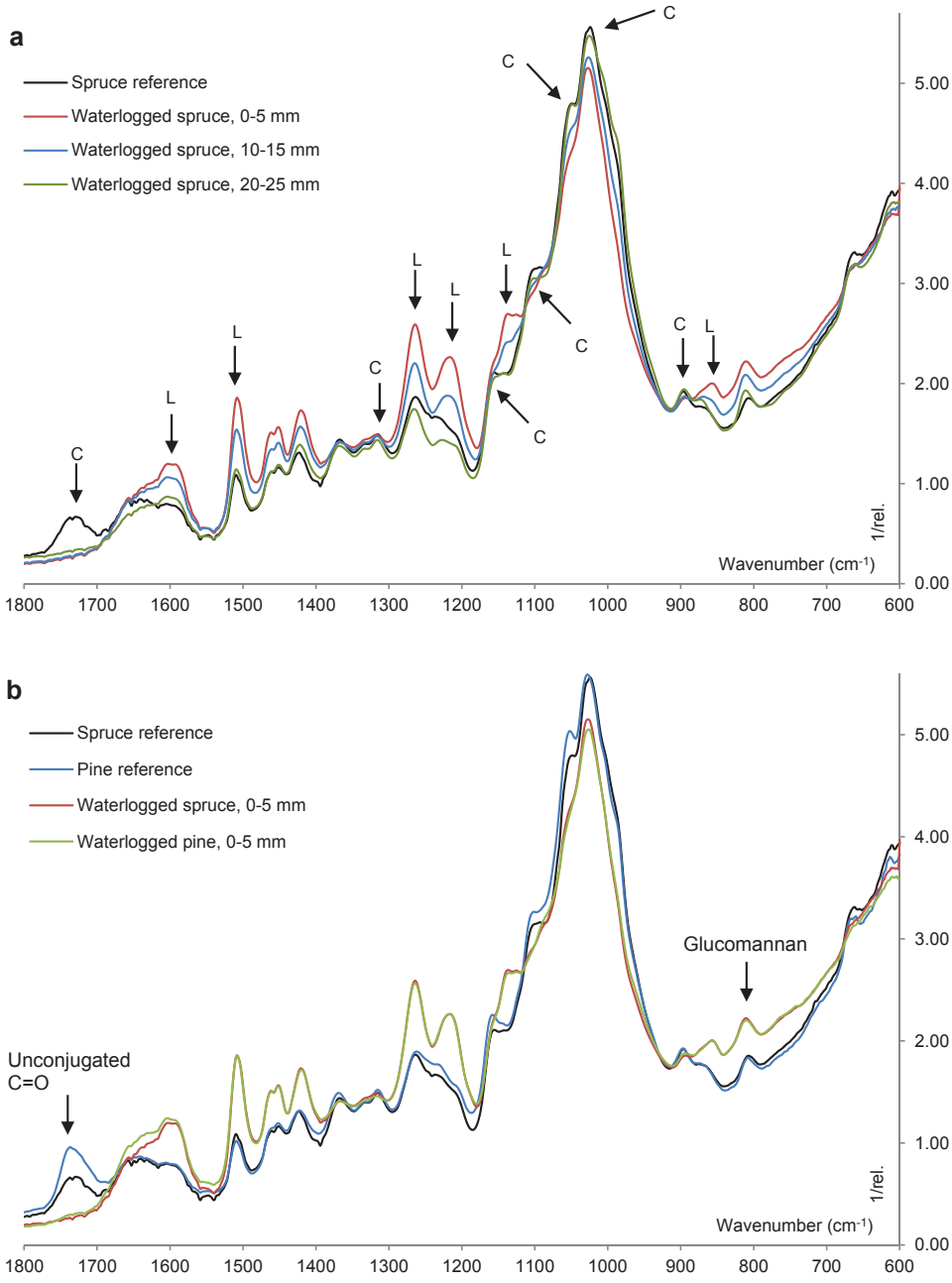

Figure 6.1: Average ATR-FTIR spectra of Norway spruce and Scots pine in the finger print region from 1800-600 cm^{-1}; normalized by standard normal variate (SNV) transformation. a) Spectra of waterlogged archaeological Norway spruce taken 0-5 mm, 10-15 mm, and 20-25 mm from the surface of the poles (gradient of decay). The relative lignin contribution in the spectra grows as the degradation increases. C = band mainly assigned to carbohydrate contributions, L = band mainly assigned to lignin contributions b) Spectrum of heavily decayed surface layer of both Norway spruce and Scots pine compared to reference wood. The band assigned to unconjugated carbonyl groups is completely lost (arrow). The band assigned to glucomannan (arrow) is strong in the heavily decayed waterlogged wood.

Table 6.3: FTIR assignment of bands from the literature of spectra of sound and heavily decayed waterlogged archaeological Norway spruce and reference material hereof.

Wavenumber (cm^{-1})	Band assignment for spruce milled wood lignin (MWL), cellulose, spruce wood, holocellulose, and/or oligosaccharides from [a], [b], [c], and [d].	Wavenumber (cm^{-1})	Reference *Picea abies*	Waterlogged Norway spruce, sound	Waterlogged Norway spruce, surface
1738-1709	C=O stretch in unconjugated ketons, carbonyls and ester groups, frequently of carbohydrate origin (cellulose, wood, holocellulose), conjugated aldehydes and carboxylic acids absorbs around and below 1700 [a]; C=O stretch in acetyl groups and/or carboxylic acid (1730-1725 cm^{-1})[d]; spruce MWL (1722 cm^{-1}) [c]	1732	m	-	-
1675-1655	C=O stretch in conjugated p-substituted aryl ketones (MWL) [a]; spruce lignin (1663 cm^{-1})[c]	1650-1630	m	m	m
1635	-OH bending vibration of adsorbed water (cellulose, wood, holocellulose) [a, d]				
1605-1593	Aromatic skeletal vibrations and C=O stretch (MWL, wood) [a]; spruce lignin (1596 cm^{-1})[c]	1605-1592	m	m	s
1515-1505	Aromatic skeletal vibrations (MWL, wood) [a]; spruce lignin (1510 cm^{-1})[c]	1508	m	m	s
1470-1455	CH_2 of pyran ring symmetric scissoring; OH plane deformation vibration (cellulose, wood, holocellulose)[a, d]	1452, 1460	m, m	m, m	s, s
1470-1460	C-H deformations; asymmetric in $–CH_3$ and $–CH_2$- (MWL, wood) [a]; spruce lignin (1464 cm^{-1})[c]				
1460	Asymmetric C-H bending (wood) [a]				
1430-1422	Aromatic skeletal vibrations combined with C-H in plane deformation CH_2 scissoring (cellulose, wood, holocellulose; MWL) [a]; O-H in plane bending in alcohol groups, carbohydrates (1430 cm^{-1}) [b]; aromatic skeletal vibrations with C-H plane deformation, spruce lignin (1423 cm^{-1})[c]; CH_2 symmetrical bending mode of hydroxymethyl (1430 cm^{-1})[d]; carboxylic acid and COO^- vibrations (1425 cm^{-1})[d]	1420	m	m	s
1370-1365	Aliphatic C-H stretch in CH_3, not in O-Me (MWL, wood), Symmetric C-H bending from methoxyl group[a]; C-H deformation vibrations, cellulose (1372 cm^{-1})[b]; spruce lignin (1367 cm^{-1})[c]	1365	m	m	v
1365-1335	OH plane deformation vibration (cellulose, wood, holocellulose)[a]	1327	v	v	w
1330-1325	Phenolic OH, S ring plus G ring condensed (i.e., G ring substituted in pos. 5), spruce lignin (1326 cm^{-1})[c]				
1317-1315	CH_2 rocking vibration (cellulose, holocellulose, wood)[a]; cellulose[b]; O-H in plane bending of alcohol groups /carbohydrates[b]	1307	v	v	w
1270-1266	G ring stretch, C=O stretch (MWL, wood)[a]; spruce lignin (1269 cm^{-1})[c]	1263	m	m	s

[a]Schwanninger et al. 2004, [b]Fackler et al. 2010, [c]Faix 1991, [d]Marchessault 1962; s = strong, m = medium, w = weak, vw = very weak, and ws = very strong intensity; sh = shoulder.

Table 6.3, continued: FTIR assignment of bands from the literature of spectra of sound and heavily decayed waterlogged archaeological Norway spruce and reference material hereof.

Wavenumber (cm^{-1})	Band assignment for spruce milled wood lignin (MWL), cellulose, spruce wood, holocellulose, and/or oligosaccharides from [a], [b], [c], and [d].	Wavenumber (cm^{-1})	Reference *Picea abies*	Waterlogged Norway spruce, sound	Waterlogged Norway spruce, surface
1235-1225	OH plane deformation, also COOH (cellulose, wood)[a]; C-O of acetyl in hemicellulose (1240 cm^{-1})[d]	1232	m	m	(overlapped)
1230-1221	C-C stretch, C-O stretch, C=O stretch (MWL)[a]; lignin, G condensed > G etherified, spruce lignin (1221 cm^{-1})[c]	1215	-	-	s
1205-1200	OH plane deformation (cellulose, wood, holocellulose)[a]	1207	v	v	(overlapped)
1162-1125	C-O-C asymmetric valence vibration (cellulose, wood, holocellulose)[a]; polysaccharides[b, d]	1155	m	m	weak sh
1140	Aromatic C-H in plane deformation, typical for G units[a]; G lignin in spruce lignin (1140 cm^{-1})[c]	1138-1143	-	m	s
1120-1115	Asymmetric in-phase ring stretching, C-C and C-O stretching (wood, holocellulose)[a]	1126	-	-	s
1110-1107	Ring asymmetric valence vibration (wood)[a], (polysaccharide)[b]	1105	s	s	w
1086	C-O deformation in secondary alcohols and aliphatic ethers (MWL)[a]; spruce lignin (1086 cm^{-1})[c]	1086	-	-	sh
1060-1015	C-O valence vibration mainly from C3-O3H (cellulose, wood, holocellulose)[a]; polysaccharide (1060 cm^{-1})[b]	1050	s	s	w
1047-1004	C_{alky}-O ether vibrations, methoxyl and b-O-4 (holocellulose)[a]	1024	vs	vs	vs
1035-1030	Aromatic C-H in-plane deformation, spruce lignin (1031 cm^{-1})[c]	-	(overlapped)	(overlapped)	(overlapped)
996-985	C-O valence vibration (cellulose, wood, holocellulose)[a]	990	s	m	-
895-892	Anomere C-groups, C1-H deformation, ring valence vibration (cellulose, wood, holocellulose)[a]; polysaccharide (897 cm^{-1})[b]; β-linkage in hemicellulose[d]	895	w	w	vw
875	Glucomannan[d]	867	vw	w	-
858-853	C-H out-of-plane in position 2, 5, and 6 of G units[a]; spruce lignin (858 cm^{-1})[c]	856	-	-	w
800	Glucomannan (810 cm^{-1})[d]	808	w	(m)	(m)
670	C-OH out-of-plane bending mode (wood, holocellulose)[a, d]	665	w	w	vw

[a]Schwanninger et al. 2004, [b]Fackler et al. 2010, [c]Faix 1991, [d]Marchessault 1962; s = strong, m = medium, w = weak, vw = very weak, and ws = very strong intensity; sh = shoulder.

Especially FT-IR analysis and Direct Exposure Mass Spectroscopy (DE-MS) are rapid, non-destructive, and accurate methods for measuring the extent of degradation (Colombini et al. 2007; Gelbrich et al. 2009; Lucejko 2010; MacLeod and Richards 1996b; Modugno et al. 2009; Sandak et al. 2010). However, care must be taken to measure representative sample areas to identify the different degrees of degradation within the material.

The present study shows that waterlogged Norway spruce and Scots pine xylem heavily degraded by erosion bacteria (0-5 mm from surface) produce very similar FT-IR spectra (Figure 6.1b). It is striking that the spectra of the waterlogged wood samples are almost identical whereas the two reference materials (Norway spruce and Scots pine) show minor differences.

The spectra of heavily decayed surface xylem (Figure 6.1 and PAPER III) show lower band intensities for bands assigned mainly to carbohydrates, as already mentioned above. However, taking into account that the cellulose rich S2 layer has been degraded, most of the bands assigned to carbohydrates (1307 cm^{-1}, 1155 cm^{-1}, 1100 cm^{-1}, 1050 cm^{-1}, 1024 cm^{-1}, 895 cm^{-1}, and 808 cm^{-1}) are fairly intensive. Compared to spectra of milled wood lignin from spruce (Faix 1991) it is evident that heavily decayed waterlogged wood decayed by erosion bacteria cannot be regarded as pure lignin. This is consistent with the fact that the compound middle lamella, the S1 layer and part of the S3 layer are morphologically intact and contain carbohydrates. It is also consistent with the fact that even millions of years old and heavily decayed waterlogged wood contains some carbohydrates (Obst et al. 1991).

The present study shows that the band at 1732 cm^{-1} is completely lost in all decay stages of the waterlogged wood (Figure 6.1). The band is assigned to C=O stretch in unconjugated carbonyls (Schwanninger et al. 2004) or more limited to C=O stretching of acetyl or carboxylic acid in hemicelluloses (Marchessault 1962). Complete loss of the band at 1735 cm^{-1} has been observed earlier in waterlogged wood, and has in some cases been assigned to degradation of hemicellulose (Giachi and Pizzo 2007; Kim 1990; MacLeod and Richards 1997; Sandak et al. 2010; Wilson et al. 1993). Complete loss of the 1732 cm^{-1} band was also observed in morphologically intact waterlogged Norway spruce and the depletion of unconjugated carbonyl groups must therefore be associated with abiotic decay during waterlogging (PAPER III). Band positions for unconjugated carbonyl groups are in the range from 1810-1690 cm^{-1} with esters giving the best match (Pavia et al. 2009). In softwood un-conjugated carbonyl groups are not present in significant amounts in lignin, but in the hemicellulose fraction as O-acetyl groups in galactoglucomannans (Figure 6.2a). In addition, unconjugated esters are present in lignin-carbohydrate complexes between the carboxylic acid groups in glucopyranosyluronic acid side chains of heteroxylans and OH groups of lignin (Figure 6.2b) (Balakshin et al. 2011; Balakshin et al. 2007; Brunow and Lundquist 2010; Harris and Stone 2008). A ^{13}C NMR study on milled wood lignin from 6,600 years old waterlogged intact hardwood

(*Bischofia polycarpa*) did also show lack of O-acetyl groups in the hemicellulose fraction. This was interpreted as slow in situ hydrolysis of the acetyl groups (Pan et al. 1990). Hydrolysis of acetyl groups and ester linkages in lignin-carbohydrate complexes are believed to cause changes in the supramolecular structure of the wood polymers and thereby change the mechanical properties of the wood. This is consistent with Borgin et al. (1975b) who found that morphological intact waterlogged wood had reduced strength properties of the middle lamella and inter fibrillar matrix but remarkbly stable microfibrils.

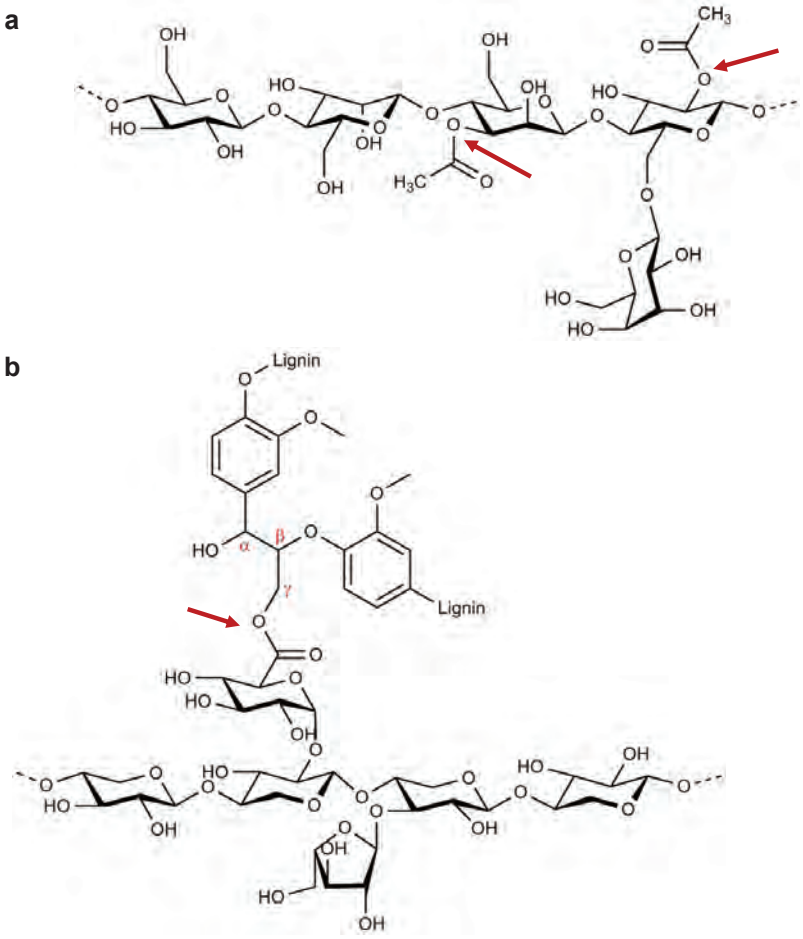

Figure 6.2: a) Structural representation of O-acetylated galactoglucomannan. The red arrows indicate the formed ester linkage between the acetyl group and the glucomannan backbone. Redrawn from Fengel and Wegener (2003). b) Structural representation of a direct ester linkage between uronic acid carboxylic acid on a glucuronarabinoxylan and the γ-hydroxyl on the side chain of a lignin monomer unit. The red arrow indicates the ester linkage. Redrawn from Harris and Stone (2008).

In conclusion the FT-IR analyses show that the glucomannan is de-acetylated and ester linkage in lignin-carbohydrate complexes are hydrolysed due to abiotic chemical processes in the waterlogged environment; but the analyses do not unveil if the hemicellulose backbones are degraded. The enhanced acidity from *in situ* hydrolysis of acetyl groups to acetic acid has a potential to catalyse hydrolysis of glycosidic bonds in polysaccharides and ether bonds in lignin and this way depolymerise the biopolymers. Due to low temperature, low concentration of acetic acid, relative high pK_a of acetic acid, and steric hindrance in the solid lignocellulosic material the process is believed to be very slow. Indeed the wet chemical compositional analyses show that xylan and mannan backbone monosaccharides are still present in the material (Table 6.2). This is further supported by the band at 808 cm^{-1} assigned to glucomannan (Marchessault 1962). This band opposes the general trend for depletion of carbohydrates in waterlogged wood compared to reference wood (Figure 6.1, Figure 3 in PAPER III). This suggests that the glucomannan backbone is preserved in the waterlogged wood structure. Depolymerisation of both lignin and polysaccharides is hard to detect in the FTIR spectra of lignocellulose as this will only result in a higher number of alcohol groups and lower number of ether functional groups.

Apart from the total loss of the unconjugated carbonyl stretch at 1732 cm^{-1} and the intensity increase in the band assigned to glucomannan at 808 cm^{-1} (and 865 cm^{-1}) only a minor difference is seen between the FT-IR spectra of intact waterlogged Norway spruce and reference material (Figure 3, PAPER III). It is therefore not possible to conclude from the FT-IR spectra whether the xylan backbone is partly hydrolysed or not. However, the compositional analyses indicate that the glucomannan and xylan backbone is depleted to the same extent. This suggests that the two hemicelluloses are removed together with the cellulose during erosion bacteria decay but that abiotic decay of the hemicellulose backbones is negligible.

6.3 Chemical imaging

The traditional analytical methods presented above provide results for the chemical composition of larger sample regions of the studied material. The methods are all based on milled wood or otherwise larger areas of the xylem. In the case of erosion bacteria decay the observed chemical composition will thus arise from an average of the residual material left after the secondary cell wall, sound cell wall regions, cell corners, compound middle lamella, and the partly decayed S1 and S3 layers. In cases where the material is totally degraded the average chemical composition will not include contributions from sound S2 layers but still an average of contributions from residual material, cell corners, compound middle lamella, sound S1 and S3 layers. Traditional analytical methods will not provide insight into the chemical composition of the residual material and sound cell wall compartments individually.

Chemical imaging where high resolution imaging and spectroscopic techniques are combined is a suitable approach to gain spatial resolved information on the chemical composition of wood with a resolution as high as 0.25 µm (Fackler and Schwanninger 2012; Fackler and Thygesen 2013; Gierlinger et al. 2012; Gierlinger and Schwanninger 2007; Koch and Kleist 2001; Pelletier and Pelletier 2010; Salmén et al. 2012). Such methods makes it possible not only to distinguish between individual cells but also between individual cell wall compartments; and thereby to obtain chemical composition of residual material and sound cell compartments separately. This approach has so far been conducted on waterlogged wood with high resolution UV-microspectrophotometry (Cufar et al. 2008; Rehbein et al. 2013; PAPER II), confocal Raman imaging (PAPER III), and coherent Raman scattering (van der Lelie et al. 2012). Results hereof are presented in Chapter 7 and 8.

7 Carbohydrate distribution and decay

7.1 Determination of polysaccharide degradation

The structural carbohydrates are decayed in preference to lignin in microbial decayed waterlogged wood, but even in heavily decayed wood submerged for thousands or millions of years some carbohydrates are still preserved (Hatcher et al. 1981; Obst et al. 1991). In case of erosion bacteria decay morphological studies show a preferential decay of the carbohydrate rich secondary cell wall (PAPER 1, Chapter 5) with the loss of birefringence in polarised light. This is evidence for a breakdown of the crystalline cellulose microfibrils in the secondary cell wall (Björdal 2000; Singh and Butcher 1991; Singh et al. 1990). However, the content of amorphous carbohydrates in the residual material has not been studied up until now, and neither has the chemical composition of sound cell wall compartments in the residual wood structure (PAPER III).

Confocal Raman imaging is a suitable approach to gain spatial resolved information on the chemical composition of individual cell wall layers *in situ* (Agarwal 2006; Gierlinger et al. 2012; Gierlinger and Schwanninger 2007; Richter et al. 2011; Sun et al. 2011). The technique has been used in this study to analyse the carbohydrate distribution, content, and composition of the residual wood structure left after erosion bacteria decay in five waterlogged archaeological Norway spruce specimens (Table 4.1). The technique used involves sequential measurements of spectra of adjacent sample positions for every 0.33 µm. From the obtained Raman spectra, images can be constructed based on integrated intensities of band positions characteristic for a chemical bond of interest. Each spectrum corresponds to one pixel in the constructed Raman image. Every Raman image is thus based on thousands of spectra, each being a spatially resolved molecular 'fingerprint' of the cell wall (PAPER III). Assignment of characteristic Raman band positions for softwood is listed in Table 7.1.

7.2 Sound cell wall compartments

Overall the sound tracheids in waterlogged archaeological wood decayed by erosion bacteria had the same carbohydrate distribution and content as reference material (compare Figure 7.1b and 7.2b) (PAPER III). The tracheids had high levels of carbohydrates in the secondary cell wall and low levels in cell corners and compound middle lamella. The similarity between reference material and sound cell wall areas was expected as intact cell wall material is identical to reference material when viewed in light, scanning and transmission electron microscopy (Björdal et al. 2000; Blanchette et al. 1990; PAPER II)(Chapter 5). However, the chemical structure was not identical. Average Raman spectra extracted from Raman images of sound S1 and S2 layers of waterlogged wood compared to S1 and S2 layers in reference material show minor spectral differences in the CC and CO stretching vibrations around 1095 cm^{-1} (Figure 7.3 and 7.4; Table 7.1). This indicates minor changes in the chemical composition of the carbohydrate fraction of morphologically sound wood cell walls. This change must be

attributed to abiotic decay after 400 years of waterlogging as detected with ATR-FTIR analysis (Chapter 6).

Table 7.1: Band assignment for Raman spectra of cellulose, lignocellulose, lignin, and softwood from the literature.

Band (cm^{-1})	Assigned to	Material
250-750	Skeletal bending modes in CCC, COC, and OCC; methine bending (CCH and OCH); skeletal stretching CC and CO; OH out op plan bending[1]	Cellulose fibres extracted from alga and ramie
380	Cellulose, no contributions from other carbohydrates[2,5]	Black spruce; Plant cell wall/lignocellulose
900	HCC and HCO bending localized at the C-6 atoms[1,2]	Cellulose fibres extracted from alga and ramie; Black spruce
950-1180	CC and CO stretching motions; 997, 1034, 1057, 1095, 1118 and 1123 cm^{-1} CC and CO stretching motion parallel to the chain axis[1]	Cellulose fibres extracted from alga and ramie
1095-1097	Carbohydrate (cellulose, xylan, glucomannan)[1,5]	Black spruce; Plant cell wall/lignocellulose
1123	Carbohydrate (cellulose, xylan, glucomannan)[1]	Black spruce
1134-1136	Coniferaldehyde structures, lignin (no other contributions)[3,6]	Black spruce
1246-1255	Xylan (deconvoluted spectrum) [7]	Pine (*Pinus radiate*)
1267-1274	Aromatic ether (aryl-O of aryl-OH and aryl-O-CH_3) in G unit in lignin[3,4,7]	Black spruce; Pine (*Pinus sylvestris*); Pine (*Pinus radiate*)
1294-1296	Cellulose[7]	Pine (*Pinus radiate*)
1307-1315	Xylan (deconvoluted spectrum) [7]	Pine (*Pinus radiate*)
1318-1330	S unit, lignin[7]	Pine (*Pinus radiate*)
1333	Aliphatic O-H bend in lignin[3]	Black spruce lignin
1337-1343	Cellulose[2,7]	Black spruce, Pine (*Pinus radiate*)
1377	Cellulose[2]	Black spruce
1454	O-CH_3 deformation; CH_2 scissoring[3]	Black spruce lignin
1456	Cellulose[2]	Black spruce
1540-1760	Lignin[5]; Aromatic ring stretching at 1601 (s) and 1658 (m)[2]	Plant cell wall/lignocellulose; Black spruce
1623	Coniferaldehyde structures, lignin (also contribution from other chromophore structures in lignin)[6]	Black spruce
1660	Aromatic ring-conjugated ethylenic and carbonyl structures (also contribution from other chromophore structures in lignin)[6]	Black spruce
2800-3000	CH and CH_2 stretching vibrations[1]	Cellulose fibres extracted from alga and ramie
2843	C-H stretch in O-CH_3, symmetric[3]	Black spruce lignin
2895-98	CH and CH_2 stretching in cellulose[1,3]; CH and CH_2 stretching in carbohydrates[5]	Cellulose fibres extracted from alga and ramie; softwood cellulose; Plant cell wall/lignocellulose
2938, 3065	C-H stretch in O-CH_3, asymmetric[3]	Black spruce lignin
3200-3500	OH stretching vibrations predominantly oriented parallel to the chain axis[1]	Cellulose fibres extracted from alga and ramie

[1]Wiley and Atalla (1987), [2]Agarwal and Ralph (1997), [3]Agarwal (1999), [4]Saariaho et al. (2003), [5]Gierlinger and Schwanninger (2007), [6]Agarwal and Ralph (2008), [7]Sun et al. (2012).

Unfortunately the confocal Raman imaging technique does not offer the possibility to directly distinguish cellulose, xylan, and glucomannan from each other. The amorphous structure of hemicellulose results in broader bands and lower signal intensity at the same spectral positions as cellulose due to many identical chemical bonds (Agarwal and Ralph 1997). However, Sun et al. (2012) have found that it is possible to obtain xylan specific bands at 1246-1255 cm^{-1} and 1307-1315 cm^{-1} with deconvoluted spectra. This was not done in the present study but could be a possible solution to further investigate the chemical changes due to abiotic decay with the confocal Raman technique.

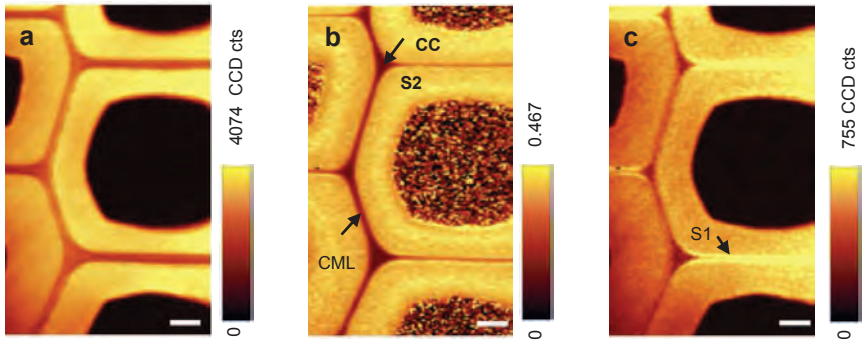

Figure 7.1: Confocal Raman images of cross sections of recent Norway spruce (*Picea abies*) reference material. Image a) is generated as a sum filter from 2840-3000 cm^{-1} (CH and CH_2 stretching vibrations). The image is a good indicator for the quality of the section. In this case it can be seen that the intensity increases from left to right which indicates a slightly uneven surface. Image b) is generated as ratios of sum filters from 1080-1190 cm^{-1} (CC and CO stretching vibrations, carbohydrates) and from 1540-1720 cm^{-1} (aromatic ring stretching, lignin). Image c) is generated as a sum filter from 1080-1190 cm^{-1}. Carbohydrate content is large in the S2 layer (S2) and minor in cell corners (CC) and compound middle lamella (CML). The S1 layer is visible in the tangential direction of the wood (image c) due to an increase in peak intensity related to orientation of the microfibrils in the S1 layer relative to the laser polarisation (arrow). Scale bars = 5 µm.

7.3 Erosion bacteria decay

Confocal Raman images constructed from the integrated intensity of the 2900 cm^{-1} band showed generally a good quality of specimens cut from waterlogged wood (Figure 7.2 a, d, g). This shows that with some practical training it is possible to hand cut planar wood sections from the soft material usable for high quality image analyses.

Confocal Raman images of waterlogged wood showed a strong depletion of carbohydrates in the residual material from the degraded S2 layers of all analysed tracheids decayed by erosion bacteria (PAPER III). The Raman images also showed a higher amount of carbohydrates in the compound middle lamella than in the residual material of decayed tracheids; the carbohydrate content in the residual material was as low as in cell corners (Figure 7.2 b, c, e, f, h, i). Average Raman spectra extracted from residual material in five specimens (Table 4.1) confirmed that the lack of carbohydrates in the Raman images did not originate from artefacts in the imaging process (Figure 7.3). The band at 1095 cm^{-1} characteristic for CC and CO stretching vibrations mainly in

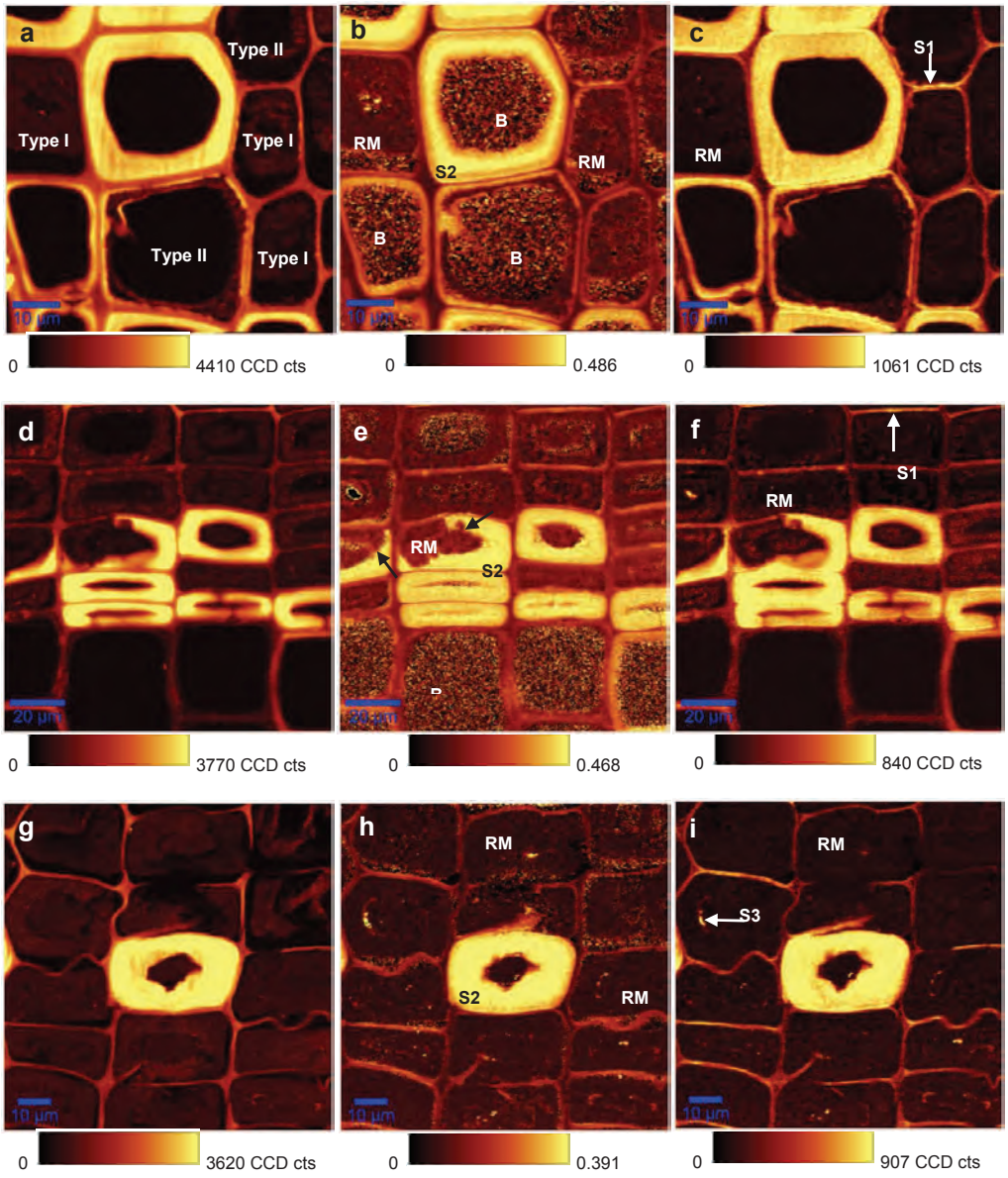

Figure 7.2: Confocal Raman images of three cross sections from two waterlogged Norway spruce poles decayed by erosion bacteria. Image a), d), and g) are generated as a sum filter from 2840-3000 cm^{-1} (CH and CH_2 stretching vibrations) to evaluate the quality of the sections, which in general is high. Image b), e), and h) are generated as ratios of sum filters from 1080-1190 cm^{-1} (CC and CO stretching vibrations, carbohydrates) and from 1540-1720 cm^{-1} (aromatic ring stretching, lignin). The background (B) is mottled which makes it difficult to distinguish small areas with high carbohydrate content within the residual material. Image c), f), and i) are generated as a sum filter from 1080-1190 cm^{-1}. In these images it is possible to detect sound S1 layers in the tangential direction of the wood sections, and minor areas of sound S3 layer in otherwise degraded tracheids.
The images show in general that sound S2 layers have carbohydrate contribution comparable to reference material (Figure 7.1). The carbohydrate content in the residual material of decayed S2 layers is very low; as low as in cell corners and lower than in compound middle lamella areas. Image d), e), and f) contains two tracheids with partly preserved S2 layer. The border between sound S2 and residual material (RM) is abrupt (arrows in image e). Image a) contains two types of residual material when observed in light microscopy prior to analysis. The two types are shown on the image.

carbohydrates was completely missing. The band at 2900 cm^{-1} characteristic for CH and CH_2 stretching vibrations was heavily reduced in intensity due to the low amounts of carbohydrates in the residual material. However, increased fluorescence signifies that caution should be used when interpreting the low polysaccharide fraction in the residual material. The Raman spectra obtained from the waterlogged wood samples showed spectra with more noise than the reference spectrum (Figure 7.3). This is most likely due to an increased fluorescence caused by the higher relative lignin content and/or chromophores formed in the waterlogged material. The high fluorescence means that the carbohydrate fraction could be less well resolved. However, this seems not to be the case for two reasons. The background fluorescence in the residual material is comparable to the background fluorescence in sound S2 layers and not drastically higher compared to S2 layers in reference material (Figure 7.3). In addition, sound S2 layers in waterlogged wood have carbohydrate band intensities (1095 cm^{-1} and 2900 cm^{-1}) comparable to the band intensity in reference material (Figure 7.3). It can therefore be concluded that the carbohydrate depletion in the residual material of decayed tracheids is due to erosion bacteria decay and not a band intensity decrease as a result of high fluorescence (PAPER III).

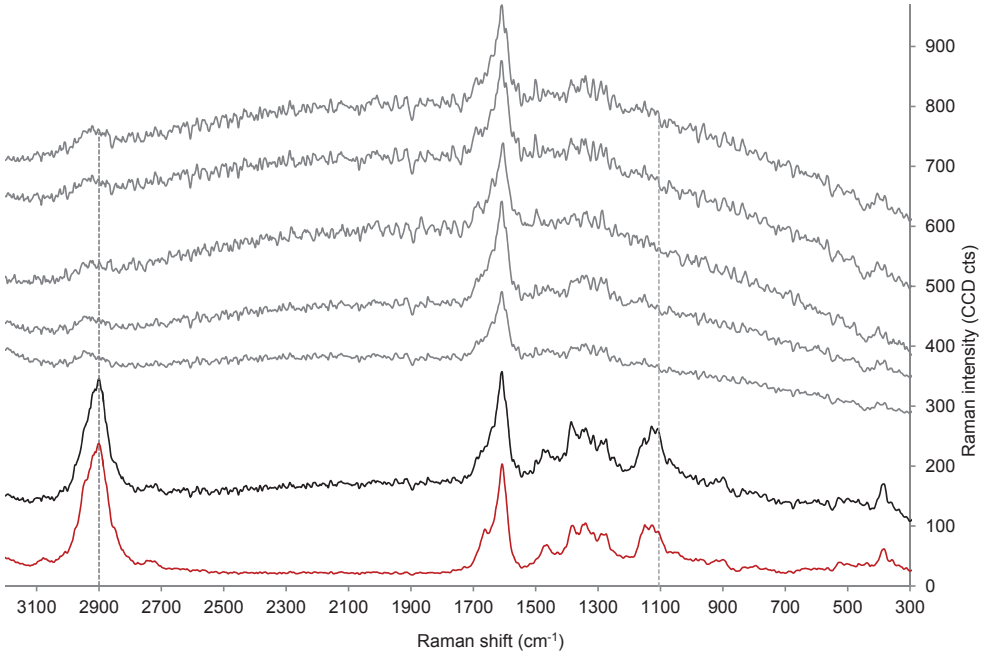

Figure 7.3: Average Raman spectra of residual material in five different waterlogged archaeological specimens (grey lines), sound S2 layer in one analysed specimen of waterlogged archaeological wood (black line), and the S2 layer in reference material (red line). Average spectra of residual material show total lack of CC and CO stretching vibrations (1095 cm^{-1}) mainly from carbohydrates and severe depletion of CH and CH_2 stretching vibrations (2900 cm^{-1}) which contains a large contribution from carbohydrates. The fluorescence background is not markedly higher in spectra from the residual material compared to the spectrum of sound S2 layer and the S2 layer in reference material. The spectrum of sound S2 layers in waterlogged wood shows same intensity level for the carbohydrate specific bands as the reference material. The reason for the very low carbohydrate contribution in residual material is not due to fluorescence interference but can be ascribed to erosion bacteria decay.

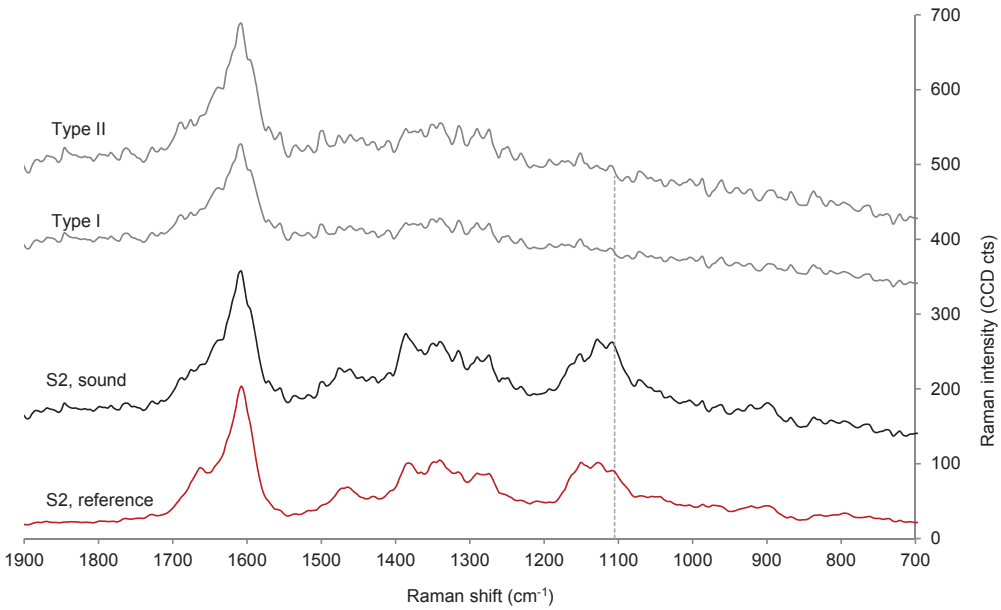

Figure 7.4: Average Raman spectra of two types of residual material (Type I and II) in waterlogged archaeological wood decayed by erosion bacteria (grey lines), the S2 layer in the reference material (red line), and the sound S2 layer in the same waterlogged archaeological wood specimen (black line). Both types of residual material show total lack of CC and CO stretching vibrations (1095 cm^{-1}) mainly assigned to carbohydrates. The visual difference between the two types of residual material in light microscopy cannot be assigned to differences in the carbohydrate content. The intensity of the aromatic ring stretching band at 1600 cm^{-1} assigned to lignin show an intensity difference between the two types of residual material but not a chemical difference. It is therefore more likely that the visual difference observed in light microscopy is due to difference in lignin distribution.

It was expected that the carbohydrate content in the secondary cell wall was decreased in the decayed areas of the tracheids. Ultrastructural studies show that erosion bacteria preferentially decay the S2 layer (Chapter 5). Polarised light studies show breakdown of crystalline cellulose and chemical analysis show carbohydrate depletion proportional to degree of degradation (Chapter 6). However, the degree of carbohydrate depletion was previously not known. The confocal Raman imaging analyses indicate that the carbohydrate fraction, both the cellulose and the hemicellulose are effectively metabolised from the wood cell wall (PAPER III).

Light microscopy investigations of the waterlogged material showed two types of residual material in tracheids decayed by erosion bacteria; a light grey amorphous material (Type I) and a denser and darker amorphous material (Type II) (PAPER II, Chapter 5). The confocal Raman imaging technique was used to determine if the two types of residual material showed any differences in chemical composition. The distribution of the two types of residual material as seen with light microscopy prior to analysis is shown in Figure 7.2a for the investigated specimen. The Raman images of this specimen did not show any differences between the carbohydrate distribution and content in the two types of residual material (Figure 7.2 b and c). Average Raman spectra of the two types of

residual material confirmed a band intensity lower than the signal to noise limit for the carbohydrate band at 1095 cm^{-1} for both types of residual material (Figure 7.4). The visual difference between the two types of residual material can therefore not be related to differences in the carbohydrate content.

The erosion bacteria are firmly attached to the cell wall where they move along the microfibrils and slowly deconstruct the cell wall. The observed presence of secondary degraders in close association to erosion bacteria (Björdal et al. 2000; Kim and Singh 1994; Singh et al. 1990) suggests that it is not a single bacteria strain but a bacteria consortium acting on the lignocellulosic cell wall material (Chapter 5). The bacteria consortium effectively metabolises the carbohydrates released from the wooden cell wall. This leads to the hypothesis that the enzymatic deconstruction of the lignocellulosic cell wall material to gain access to the polysaccharides is the rate limiting step in the decay process as the carbohydrates are consumed as soon as they are released. This is supported by transmission electron microscopy examinations (Chapter 5, Figure 5.2e) and confocal Raman images (Figure 7.2 d, e, and f) that show an abrupt border between sound S2 layers and residual material. The cell wall is either sound or converted to an amorphous residual material without any carbohydrates present. It is also supported by the finding that both type I and II residual material (in light microscopy, Chapter 5) did not contain any carbohydrates. The hypothesis is further supported by results obtained by traditional analytical methods performed on waterlogged archaeological wood that show intact crystallinity of cellulose microfibrils, only minor changes in the degree of polymerization of the cellulose, and no line broadening of carbohydrate signals (high resolution solid-state nuclear magnetic resonance spectroscopy). These analysis strongly indicates that chemical rearrangement of carbohydrates inside the morphological sound cell wall do not take place (Bardet et al. 2004; Bardet et al. 2009; Gelbrich et al. 2008; Sandak et al. 2009; Sandak et al. 2010). The hypothesis is further supported by the low amount of water soluble carbohydrates present in the wood material (Chapter 6). Ineffective consumption of released carbohydrates by the erosion bacteria consortia would result in higher amounts of extractible water soluble carbohydrates. It is not surprising that the consumption of carbohydrates is highly efficient when considering the very slow decay rates under the extreme conditions given in the waterlogged and oxygen free ecosystems.

Raman images constructed solely from the band at 1095 cm^{-1} (Figure 7.2 c, f, i) reveal small areas of high carbohydrate content (PAPER III). This is interpreted as un-decayed fractions of S3 layers due to the spatial position and the fact that un-decayed fractions of S3 layers have been observed with transmission electron microscopy (PAPER II, Chapter 5). In addition, Figure 7.2 c, f, and i provides better information on the preservation state of the S1 layer. The S1 layer can be detected in the tangential direction of the wood section in this study due to different orientations of the tangential and radial cell walls of the microfibrils in the S1 layer relative to the laser polarisation. Changing the laser polarization from parallel (0°) to perpendicular (90°) in cross sections leads to very large changes in the Raman intensity of almost all characteristic bands (Agarwal and Atalla

1986; Gierlinger et al. 2010; Thygesen and Gierlinger 2013). This means that it is possible to detect the S1 layers in the tangential direction of cross sections even though the S1 layer is not more than approximately 0.38 µm thick in Norway spruce latewood (Table 2.1). In the tangential direction of decayed tracheids it is clearly seen that the carbohydrate fraction of the S1 layers is preserved (PAPER III). This is in agreement with a high degree of morphological intact S1 layers observed in transmission electron microscopy on the same sample material (PAPER II, Chapter 5). The results establish that carbohydrates detected with traditional analytical methods in waterlogged wood decayed by erosion bacteria stem from un-decayed S2 layers, unaltered compound middle lamella, and remnants of the S1 and S3 layers, as well as abiotic changes in the polysaccharide composition (Chapter 6).

From this and earlier studies the general picture of carbohydrate decay by erosion bacteria under anoxic conditions is a preferential decay of the S2 cell wall layer and partial decay of the S3 layer. Within single tracheids alternate regions of intact and decayed S2 cell wall layers are present in the longitudinal direction unless the tracheids are totally disintegrated; a cell wall region is either decayed or intact. The carbohydrate fraction of the cell wall is effectively utilised; no carbohydrates or only trace amounts are present in the residual material. Intact cell wall regions have the same carbohydrate content and distribution as reference tracheids. However, ester bonds in lignin-carbohydrate complexes and acetyl groups attached to glucomannan are abiotically hydrolysed (Chapter 6). This has implications for the supramolecular structure of the biopolymers and therefore the mechanical behaviour of the residual cell wall regions.

8 Lignin distribution and decay

8.1 Determination of lignin degradation

Lignin degradation in waterlogged anoxic environments can be approached both quantitatively and qualitatively. The quantitative approach determines the lignin mass loss from the wood structure due to either microbial metabolism or physical removal of lignin detached from the cell wall. The qualitative approach determines the chemical modification of the lignin structure due to degradation. Quantitative studies on the mass loss of lignin from waterlogged archaeological wood have only been conducted in a few cases with varying results (Hedges et al. 1985; Sandak et al. 2010). Numerous qualitative studies on waterlogged archaeological wood generally show that the chemical structure of lignin is conserved to a high degree (PAPER I). However, the reported minor alterations of the lignin structure are not consistent. The difference in the reported quantitative and qualitative lignin degradation in waterlogged wood could possibly be explained by differences in decay type and degree of degradation. This is often not reported in the studies and hinders comparison of results. In addition differences in wood species and burial environment, and different sensitivity of the applied analytical methods may have a substantial influence on the outcome of such analyses (PAPER I).

Except for a few contributions (Cufar et al. 2008; Rehbein et al. 2013) (PAPER II, PAPER III), studies of lignin in waterlogged wood have been conducted on either whole xylem samples or lignin extracted from the wood (PAPER I). In these cases the chemical composition of the lignin is measured as an average of the residual wood structure. In cases of erosion bacteria decay the lignin composition will feature a mixture of lignin from cell corners, compound middle lamella, sound secondary cell wall (S1, S2, and S3 layers) and residual material left after secondary cell wall decay. In cases where the composition is conducted on lignin isolated from the xylem the lignin fraction is still a mixture of different cell wall compartments. Furthermore minor chemical modifications of the lignin are expected dependent on method of isolation (Lundquist 1992).

Semi-quantitative spatial resolved information on the lignin distribution and chemical composition of individual cell wall layers in plant material *in situ* can among others be obtained with confocal Raman imaging and high resolution UV-microspectrophotometry (Fackler and Thygesen 2013; Fukazawa 1992; Gierlinger et al. 2012; Gierlinger and Schwanninger 2007; Koch and Kleist 2001 and Chapter 6). In addition, transmission electron studies combined with $KMnO_4$ staining is a suitable method to gain knowledge of the lignin distribution in individual cell wall layers (Schmitt and Melcher 2004). In this study the three methods were used to study distribution and chemical compositional of individual cell wall layers and residual material in waterlogged archaeological wood decayed by erosion bacteria (PAPER II and PAPER III). UV-microspectrophotometry was performed as two dimensional UV-absorbance scanning profiles (mapping) of cross sections across the cell wall at constant wavelength (280 nm) with a resolution of 0.25 µm x 0.25 µm. In addition, photometric point analysis between 240 and 400 nm with a

spot size of 1 μm^2 was performed. The method is semi-quantitative if the same embedding media, section thickness, and wavelength are used for the analysed specimens (PAPER II). The confocal Raman imaging technique involves sequential measurements of spectra of adjacent sample positions for every 0.33 µm in cross section as described in Chapter 7 and PAPER III. Assignment of characteristic Raman band positions for softwood is listed in Table 7.1.

8.2 Sound cell wall compartments

In the present study sound tracheids in the waterlogged archaeological wood showed the same lignin distribution and content as reference material with all three applied techniques. This can be seen by comparing Figure 5.2a with Figure 5.2b (transmission electron microscopy), by comparing Figure 8.1a and b with Figure 8.1c and d (UV microspectrophotometric scanning profiles), and by comparing Figure 8.4a and b with Figure 8.4c (confocal Raman images). Tracheids with partly preserved S2 layer showed the same lignin distribution and content as sound tracheids and as reference material (Figure 8.1e and Figure 8.4d) (PAPER II, PAPER III). This demonstrates that S2 layers in tracheids of waterlogged archaeological wood with sound morphological appearance had unaltered lignin content and distribution. The result is consistent with the typical erosion bacteria decay pattern of random distribution of morphological sound cells and decayed cells (Chapter 5).

The observation of high lignin content in corners and compound middle lamella and lower lignin content in the secondary cell wall was expected from earlier studies on softwood (Fengel 1969; Fergus et al. 1969). More recent studies have shown that lignin in secondary cell walls, compound middle lamella and cell corners might be more heterogeneously distributed than suggested by UV studies (Agarwal 2006; Daniel et al. 1991; Singh et al. 2002b; Tirumalai et al. 1996). In the present study none of the three methods showed lignin depleted cell corner or compound middle lamella regions. But minor variations in lignin distribution were observed in the secondary cell wall of Norway spruce tracheids (Figure 8.4a and b; Figure 8.1a).

Despite the identical lignin distribution and content in sound waterlogged tracheids and reference tracheids minor chemical differences were observed with the confocal Raman imaging technique in the present study. All spectra of morphologically intact cell wall compartments (cell corners, compound middle lamella, S1 layers, and S2 layers) in waterlogged wood possessed several shoulders in the spectral region from 1540-1720 cm^{-1} characteristic for aromatic ring stretching in lignin that were not observed in spectra of reference material (PAPER III). In addition the band at 1660 cm^{-1} characteristic for aromatic ring conjugated ethylene and carbonyl structures is less pronounced in the waterlogged samples compared to reference material. This could indicate abiotic decay of the wood structure due to waterlogging for 400 years since the studied cell wall compartments were free from microbial decay. ATR-FTIR spectra of sound waterlogged wood compared to reference xylem did not show any clear evidence for chemical changes

in the lignin fraction of the wood material due to waterlogging (Figure 3 in PAPER III). This together with lack of band broadening in the Raman spectra indicates that the chemical changes are minor. The observe reduction in the band at 1660 cm^{-1} could indicate incomplete abiotic hydrolysis of aromatic ring conjugated ethylene and carbonyl structures in the lignin fraction of the cell wall. Band positions for the observed shoulders are consistent with band positions in photo and enzymatic oxidised and heat treated wood and thermo mechanical pulps (PAPER III). This suggests that abiotic chemical changes in the waterlogged wood could also stem from structures such as conifer aldehyde, conjugated C=C, conjugated C=O, o-quinone, and p-quinone due to minor oxidation of the lignin fraction (PAPER III). A single study has identified oxidative changes in lignin isolated from 900-2200 years old morphologically intact waterlogged *Quercus robur*. It was concluded that the lignin is slowly affected by the waterlogged environment (Borgin et al. 1975a). Evidence for oxidised lignin in waterlogged archaeological wood has been found in previous studies (PAPER I). However, it was not established if this oxidation was due to biotic or abiotic decay as a consequence of the design of the conducted studies.

8.3 Erosion bacteria decay

Lignin distribution in residual material

In the present study transmission electron microscopy examinations of waterlogged Norway spruce showed three types of residual material (Type 1-3) with varying amounts and distribution of lignin (Chapter 5 and PAPER II). UV-absorbance profiles of the residual material from both waterlogged Norway spruce and Scots pine confirmed a great variety of lignin distribution (Figure 8.2 and 8.3). Based on scanning profiles from 165 analysed Norway spruce latewood tracheids it was possible to divide the lignin distribution of the residual material into five types (Type A-E) (Figure 8.3; Figure 3 and Table 1 in PAPER II). The UV-scanning profiles showed a more complex lignin distribution than found by transmission electron microscopy, but the results are still in agreement with each other. Type A (Figure 8.3a and b) corresponds well with Type 1 (Figure 5.2d). Comparison of UV-absorbance values for Type A residual material with sound S2 layers in waterlogged wood and in reference material showed that the absorbance values were significantly lower in Type A residual material (PAPER II). This indicated that the UV-absorbance was not just lower because of a uniform redistribution of the S2 lignin but was either metabolically decayed or physically removed in the longitudinal direction of the tracheid. Type B was only observed in a few tracheids and was not found by transmission electron microscopy. Type C and D (Figure 8.3d, e, f, g, h, and i) correspond well with Type 2 (Figure 5.2b and c). Type E (Figure 8.3j, k, and l) corresponds well with Type 3 (Figure 5.2f). The lignin content in Type E residual material was often very high in a large proportion of the cross sectional area of the tracheid. This clearly shows that some residual material regions have higher lignin levels than intact secondary cell wall (Figure 8.3j and k). Type E and A was mainly seen in the heavily decayed surface layers of the Norway spruce poles, and UV-absorbance profiles

reveal that tracheids with Type E residual material in some cases were situated next to tracheids with low UV-absorbance (Type A/C) (Figure 8.3k). The waterlogged Scots pine latewood tracheids showed the same tendency of UV-absorbance distributions as observed in waterlogged Norway spruce (Figure 8.3). The most frequently observed types were Type C and D, as in Norway spruce specimens, whereas the two homogeneous types (Type A and B) were not observed in the Scots pine material. This could be due to the fact that only 30 tracheids in one specimen 10 mm from the surface was analysed.

The confocal Raman imaging technique confirmed the observed heterogeneous distribution of lignin in the residual material of decayed tracheids (PAPER III). Images constructed as sum filters from 1540-1720 cm^{-1} representing aromatic ring stretching in lignin (Agarwal and Ralph 1997) showed that all decayed tracheids contained residual material with high, intermediate, and low levels of aromatic compounds within the same tracheid (Figure 8.4c, d, and e). This corresponds to levels seen in compound middle lamella, levels seen in sound S2 layers, and lower levels than seen in sound S2 layers, respectively. The Raman data demonstrates that the uneven lignin distribution in the residual material did not stem from sample modification as a side effect of Spurr's embedding used for transmission electron microscopy and UV-microspectrophotometric measurements. The sample material for the confocal Raman imaging analysis was not dehydrated or embedded but simply hand cut and kept in water during measurements. The Raman images based on ratios of integrated intensities for the carbohydrate band (1095 cm^{-1}) and the lignin band (1600 cm^{-1}) (Figure 7.2b, e, and h) did not show the heterogeneous lignin distribution. This is believed to be due to the massive loss of carbohydrates in the decayed S2 cell wall layer which obstructs the image generation based on ratios.

The heterogeneous distribution of lignin in residual material of waterlogged wood decayed by erosion bacteria is confirmed by two earlier studies on *Pinus sylvestris* 50-80 years old (Rehbein et al. 2013) and *Quercus* sp. and *Fraxinus* sp. approximately 4,500 years old and 5,200 years old respectively (Cufar et al. 2008; Nilsson and Klaassen 2008) done with high resolution UV-microspectrophotometry. Both studies showed a similar variety of UV-absorbance with regions of lower absorbance levels than sound S2 layers and regions with absorbance levels as high as cell corners. However, it cannot be ruled out that the very high absorbance levels in the residual material of *Pinus sylvestris* studied by Rehbein et al. (2013) was due or partly due to collapse of the residual material as a result of air drying of the material before analysis.

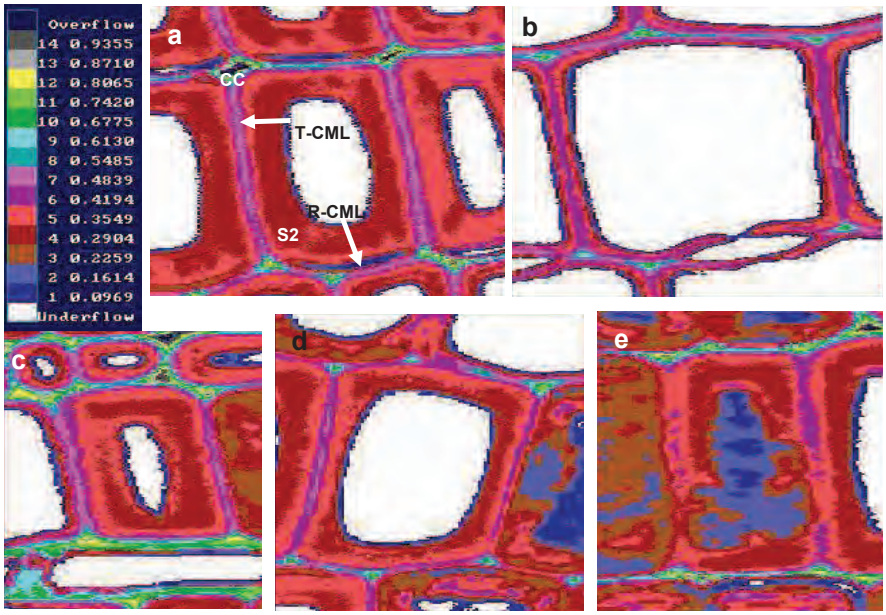

Figure 8.1: UV-microspectrophotometric scanning profiles of Norway spruce; UV-absorbance scale in upper left corner. a) Reference, latewood tracheids from sapwood. b) Reference, earlywood tracheids from sapwood. c) and d) Morphological sound waterlogged archaeological latewood tracheids without erosion bacteria decay. e) Waterlogged archaeological latewood tracheid partly decayed by erosion bacteria in the S2 cell wall layer. CC = cell corner, T-CML = tangential compound middle lamella, R-CML = radial compound middle lamella.

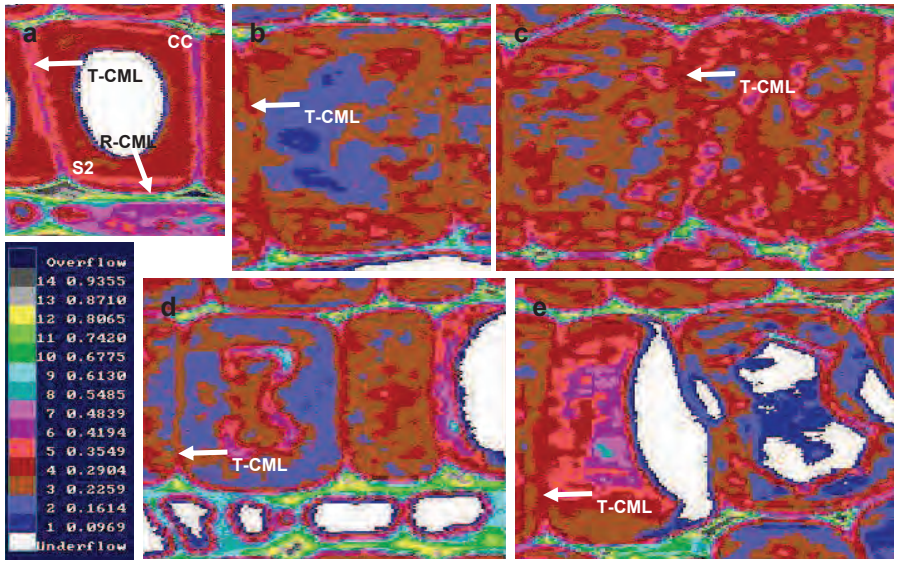

Figure 8.2: UV-microspectrophotometric scanning profiles of Scots pine latewood tracheids; UV-absorbance scale in lower left corner. a) Reference, latewood tracheids from sapwood. b) - e) Four examples of waterlogged archaeological Scots pine tracheids decayed by erosion bacteria. All examined tracheids had heterogeneous UV-absorbance profiles with Type C and D as the most commonly observed; all decayed tracheid had lower UV-absorbance of tangential compound middle lamella (T-CML) than reference tracheids. b) Type C residual material , c) Type D residual material, d) left tracheid: Type D residual material, right tracheid: Type C residual material, e) left tracheid: Type E residual material, right tracheid: Type D residual material.

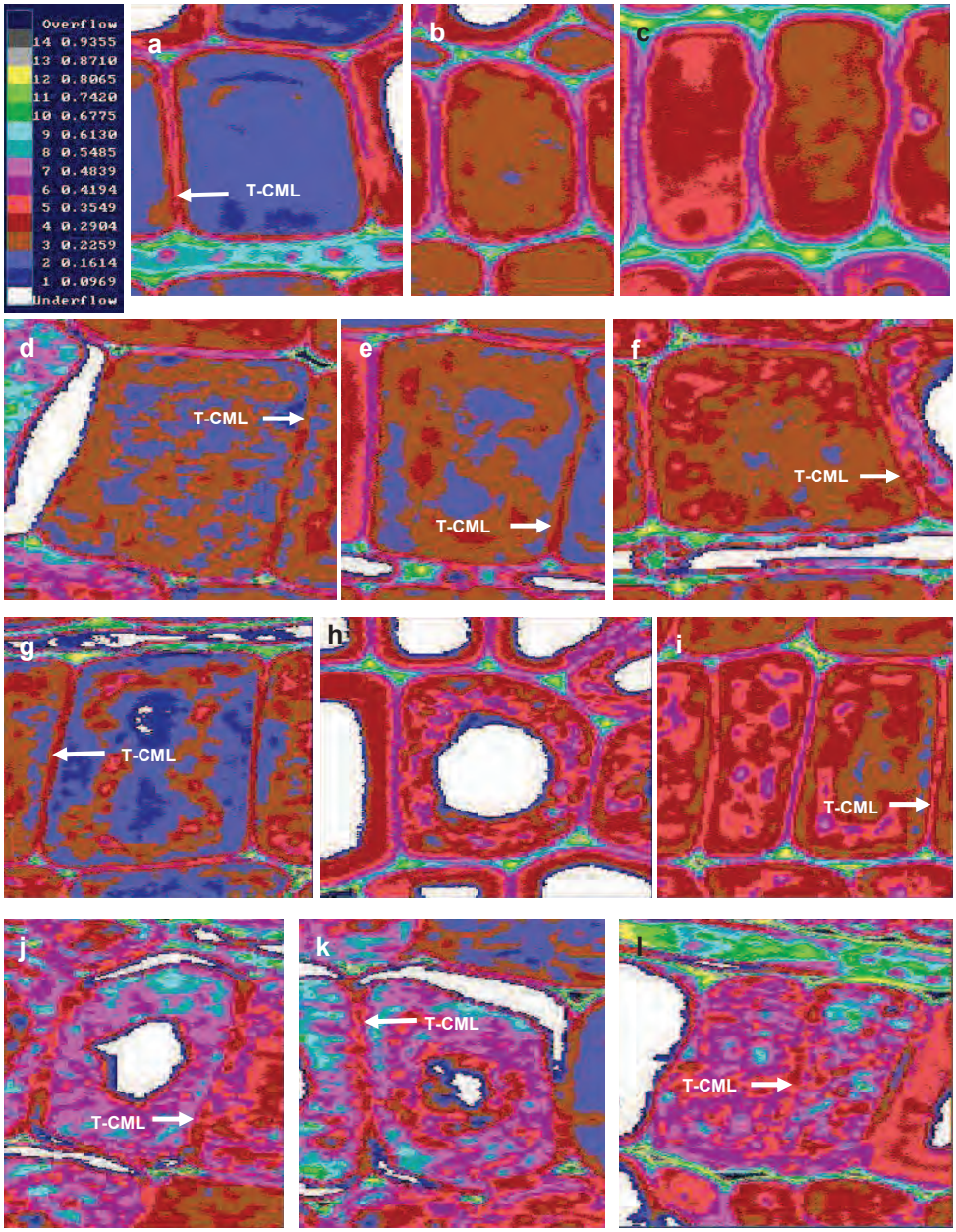

Figure 8.3: UV-microspectrophotometric scanning profiles of waterlogged archaeological Norway spruce latewood tracheids decayed by erosion bacteria; UV-absorbance scale in upper left corner. a) and b) Type A residual material, homogeneous and lower UV-absorbance than sound S2 layers. c) Left tracheid: Type B residual material, homogeneous with UV-absorbance as sound S2 layers, not frequently observed. Right tracheid: Type A. d), e), and f) Three examples of Type C residual material; heterogeneous UV-absorbance with lower UV-absorbance than sound S2 layers. g), h), i) Three examples of Type D residual material, heterogeneous UV-absorbance with some areas of higher UV-absorbance than sound S2 layers, observed in all analysed specimens. j), k), l) Three examples of Type E residual material; heterogeneous UV-absorbance with areas of very high UV-absorbance, mainly seen in the heavily decayed surface layer. k) Tracheids with Type E residual material is situated next to tracheids with Type A/C residual material. a), d), e), f), g), i), j), k), l) show examples of tangential compound middle lamella (T-CML) with lower UV-absorbance than the compound middle lamella in reference material (Figure 8.1a).

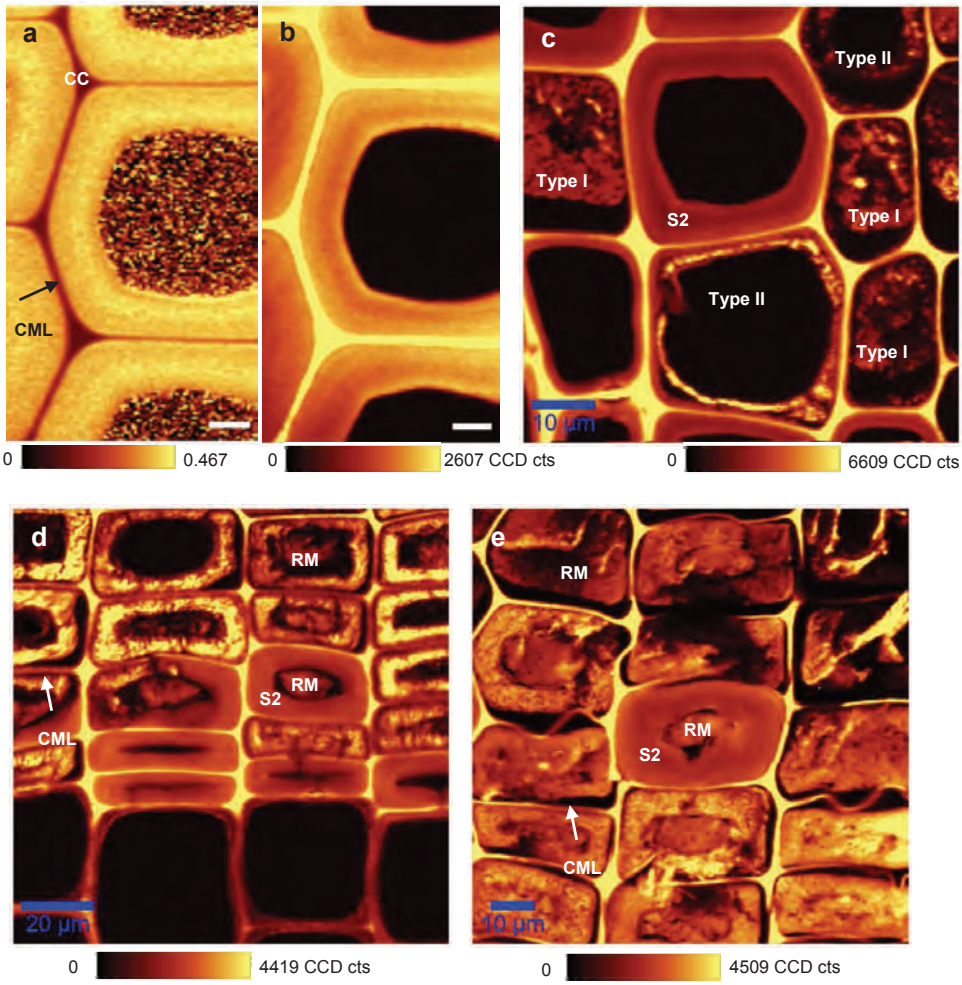

Figure 8.4: Confocal Raman images of Norway spruce xylem. a) and b) Reference, latewood tracheids from sapwood. Scale bars = 5 µm. c)-e) Three specimens from waterlogged archaeological Norway spruce xylem decayed by erosion bacteria. Image a) was generated as a ratio of sum filters from 1080-1190 cm^{-1} (CC and CO, carbohydrates) and from 1540-1720 cm^{-1} (aromatic ring stretching, lignin). Images b)-e) were generated as sum filters of the band at 1600 cm^{-1} (lignin). The reference material showed as expected the highest lignin content in the compound middle and cell corner regions. c) The lignin distribution in sound waterlogged Norway spruce was identical to the distribution in reference material. c), d) and e) Residual material in decayed tracheids showed regions with high, low and intermediate levels of intensity from the aromatic ring stretching band at 1600 cm^{-1}. Some compound middle lamella (CML) regions showed lower intensity from the aromatic ring stretching band at 1600 cm^{-1} than reference tracheids.

Chemical composition of lignin in residual material

Confocal Raman imaging analyses and UV-absorbance line spectra of residual material showed that the aromatic ring structure of the lignin residue is conserved to a high degree (PAPER II and III). This is in agreement with earlier qualitative studies of the lignin composition in waterlogged archaeological wood where little chemical change was found compared to sound reference wood (PAPER I).

The Raman band at 1600 cm^{-1} assigned to lignin was identical to the lignin band in sound S2 layers of waterlogged Norway spruce (Figure 8.5a). However, small variations in the 1600 cm^{-1} band were observed between the different specimens. These variations were not related to decay of the secondary cell wall since the lignin bands were identical in all sound cell wall compartments in the waterlogged wood (S2 and S1 layer, compound middle lamella, and cell corners) and in residual material from the same specimen (Figure 8.5b) (PAPER III). Absence of band broadening, lack of changes in band position, and no evolvement of shoulders all indicates that the chemical composition of the aromatic ring structure of lignin from the S2 layer did not change during erosion bacteria decay. In addition, no spectral changes in the lignin band was observed in Raman spectra extracted from regions with high, low and intermediate intensity contributions from the lignin band within the same specimens, only a marked intensity difference was observed (Figure 8.5c). This observation was also true when Raman spectra from the two visually different (by light microscope) types of residual material were examined (Figure 7.4). The spectra show no spectral difference for the lignin band at 1600 cm^{-1}, but merely an intensity difference.

The UV-absorbance line spectra showed that the λ_{max} at 280 nm characteristic for sound tracheid in waterlogged Norway spruce and reference material did not shift or broaden in spectra of residual material left after erosion bacteria decay. This is true both for randomly selected residual material and residual material with low absorbance (Figure 8.6). This implies that the chemical structure of the aromatic ring system in lignin did not change as a consequence of erosion bacteria decay. The line spectra of the residual material showed a λ_{min} at 257 nm both in the reference material and in the sound S2 layer. This minimum was shifted to 260 nm for the residual material (Figure 8.6). The λ_{min} at 257 nm is not related to the aromatic ring structure in lignin but implies chemical change in UV-absorbing chemical bonds in the material. The two line spectra of residual material are identical, however with a lower absorbance for the tracheids specifically chosen with low absorbance confirming a marked lower amount of aromatic ring structures in this residual material. It was not possible to detect whether depolymerisation had taken place in the lignin fraction of the decayed secondary cell wall layer with either the Raman or the UV-microspectrophotometry technique. To determine if depolymerisation had taken place, and if so, to what degree, it would be necessary to separate the residual material from the residual wood structure e.g. the compound middle lamella, and sound S1, S2, and S3 layers.

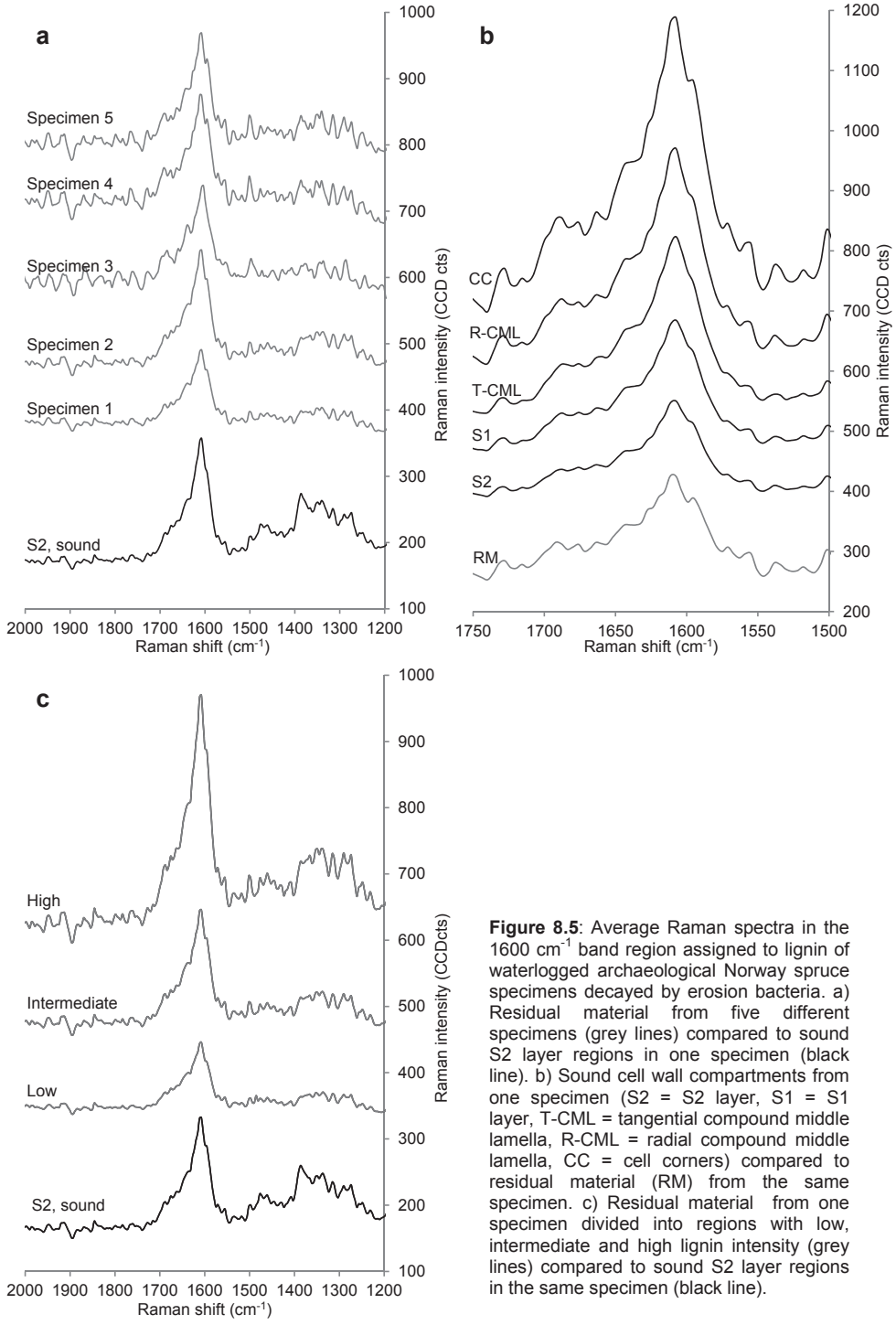

Figure 8.5: Average Raman spectra in the 1600 cm^{-1} band region assigned to lignin of waterlogged archaeological Norway spruce specimens decayed by erosion bacteria. a) Residual material from five different specimens (grey lines) compared to sound S2 layer regions in one specimen (black line). b) Sound cell wall compartments from one specimen (S2 = S2 layer, S1 = S1 layer, T-CML = tangential compound middle lamella, R-CML = radial compound middle lamella, CC = cell corners) compared to residual material (RM) from the same specimen. c) Residual material from one specimen divided into regions with low, intermediate and high lignin intensity (grey lines) compared to sound S2 layer regions in the same specimen (black line).

This was attempted with a laser micro dissection technique with 1µm diameter precision. However, it was not possible due to sample heating and thereby very fast dehydration which destroyed the sample material. It was also attempted to wash the residual material out from thin cross sections of the wood material. However, the residual material was more firmly bound to the wood matrix than expected. Elevated temperatures, continuous shaking, and solvents such as ethanol, acetone and propane did not separate the residual material from the residual wood structure very effectively. Acetone combined with shaking and heating to 50 °C gave a liquid extract with a bright yellow colour. Examination of the cross sections after washing showed intact compound middle lamella and that residual material had been washed out to some degree. The experiments show that the residual material is bound to the residual wood structure. Attempts to dissolve ball milled heavily decayed waterlogged Norway spruce from the surface layer of one pole in dimethyl sulfoxide (DMSO) combined with ultrasonic water and heat (105 °C) was not very effective either. The bright yellow colour of the solution indicated low solubilisation as was the case with washing in acetone as even low amounts of solubilised plant biomass most often gives dark brown solutions. Due to the low solubility and the high molecular weight of lignin from the compound middle lamella compared to the secondary cell wall (Fromm et al. 2003) it is assumed that the solubilised fraction most likely is fractions of residual material. It was possible to run size exclusion chromatography on the solubilised fraction (Appendix A). The result showed that the extract contained lignin fractions with molecular size varying from values comparable to native lignin and values comparable to mono- and dilignols with a higher portion of dimers and monomers (Figure 8.7).

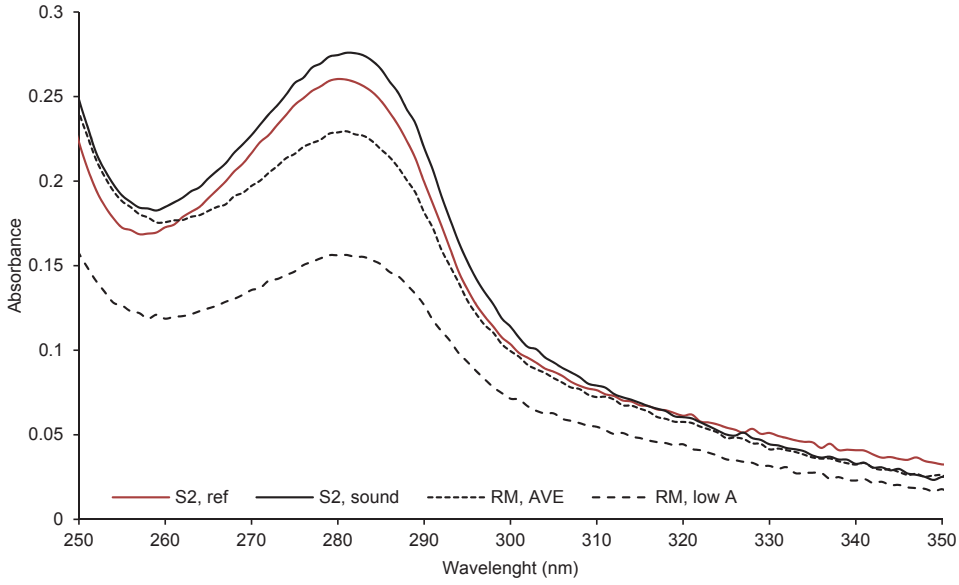

Figure 8.6: UV-absorbance line spectra of Norway spruce from 250-350 nm. Spectra are shown for S2 layers in reference tracheids (S2, ref), S2 layers in sound waterlogged tracheids (S2, sound), residual material randomly taken in decayed tracheids (RM, AVE), and residual material with homogeneous and very low absorbance levels as determined with UV-scanning profiles (RM, low A).

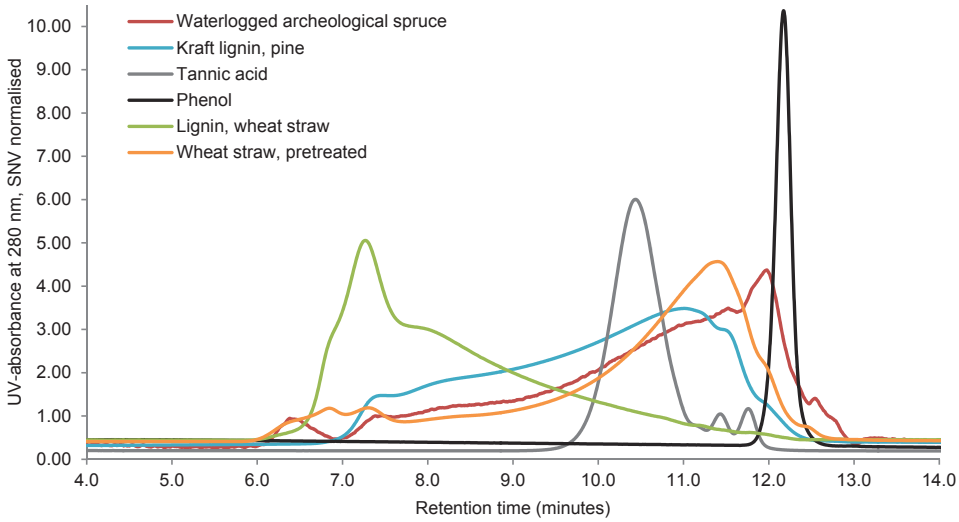

Figure 8.7: SNV normalised size exclusion chromatography spectra of DMSO extracted heavily decayed waterlogged archaeological Norway spruce (red line) and the reference substances: phenol (black line), tannic acid (grey line), Kraft lignin from pine (blue line), organosolve lignin from wheat straw (green line), and pre-treated wheat straw (steam heated to 180-200 °C for 10-20 minutes) (orange line). The molecular size distribution of the heavily decayed DMSO extract of waterlogged archaeological Norway spruce (red line) lie in the range from higher values than tannic acid (grey line) to values as low as phenol (black line).

This indicates that the residual material is depolymerised to some degree. Partial depolymerisation with cleave of ether intermonomeric bonds was also found in lignin extracted from waterlogged hardwood samples from anoxic sediments in the San Rossore Roman Harbour in Pisa (Colombini et al. 2009; Colombini et al. 2009; Giachi et al. 2003; Lucejko et al. 2009).

It is striking how similar the size exclusion chromatography curve for the waterlogged material is to the curves for Kraft lignin and pre-treated wheat straw (steam heated to 180–200 °C for 10–20 min. (Larsen et al. 2012)). Evidence of substantial intermonomeric β-aryl ether cleavage and only minor changes in the aromatic structures have been observed in pre-treated wheat straw lignin (Yelle et al. 2013). This study has shown that lignin from residual material of decayed secondary cell walls has an unchanged aromatic ring structure and the size exclusion chromatography analysis indicate similar depolymerisation behaviour to Kraft pulping processes and wheat straw pre-treatments. Both methods are used to deconstruct the cell wall to gain access to the polysaccharides (fibres). The molecular distribution similarities between the waterlogged wood lignin and Kraft lignin indicates that it is likely that the residual material left after secondary cell wall decay has aggregation behaviour similar to Kraft lignin. Lindströmn (1979) has shown that Kraft lignin form a gel and undergo time depended aggregation. Gel formation is consistent with the observation that the residual material is firmly attached to the residual structure even in thin cross sections. Time depended aggregation is consistent with a higher number of observed tracheids with Type E residual material in the outer

part of the waterlogged poles compared to the lignin distribution closer to the core formed at a later stage.

The single size exclusion analysis reported here is not sufficient to draw solid conclusions. It is of course necessary to prepare a suitable reference of lignin from Norway spruce wood. It is also crucial to find a method to separate the residual material from the compound middle lamella to be able to draw conclusions on the molecular weight distribution of the residual material alone. It would be relatively easy to perform optimising experiments on cross sections with variable solvents, temperatures, and shaking methods, and to control if the compound middle lamella stays intact in the procedure. With an optimized method and patience it would be possible to solubilise enough residual material to run more accurate size exclusion chromatograph. In addition, such material is straight forward to analyse by 2D high resolution-liquid nuclear magnetic resonance (NMR) spectroscopy. This would yield valuable knowledge on the chemical composition of the residual material left after the bacterial decay especially in terms of which linkages have been broken in the decay process.

Lignin metabolism?

No metabolic pathway for lignin has been discovered so far. However, numerous enzymatic systems to deconstruct the lignin to get to the shielded/protected carbohydrate fraction of lignocellulose in plant cell walls exist in oxygen containing ecosystems (Kubicek 2013). Such enzyme systems must also be present in anaerobic plant cell wall degradation. However, the enzymatic pathways are not well described (Chapter 3). Anaerobic biomass/lignocellulose degradation is slow but effectively deconstructs the plant cell wall to metabolise the carbohydrate fraction (Kataeva et al. 2013; van der Lelie et al. 2012) (Chapter 7). Lignin is generally up-concentrated in these environments which points to lignin conservation, but not to what extent the lignin is preserved and if smaller fractions of the lignin polymer is metabolised.

The confocal Raman imaging technique and the UV-microspectophotometric approach have given valuable knowledge on the lignin distribution in wood tracheids decayed anaerobically *in situ*. Unfortunately the two techniques are limited to cross sectional studies, and it cannot be determined if the observed residual material regions with significant lower lignin content than sound cell wall areas is due to metabolic decay or physical movement of the lignin residues within the decayed tracheid (PAPER II).

It is a well-known fact that the density decreases with the degree of degradation (PAPER I). Totally disintegrated waterlogged archaeological wood have densities lower than 100 kg m^{-3} (Gregory and Jensen 2006). The residual wood structure after total disintegration by erosion bacteria will consist of cell corners, compound middle lamella and residual material left after secondary cell wall decay. Is it theoretically possible that all native lignin is preserved in the residual wood structure when densities can reach such low values ($\leq$ 100 kg m^{-3})?

Appendix B shows a simple theoretical calculation of the density of the residual wood structure left after erosion bacteria decay for European ash (*Fraxinus excelsior* L.) and Norway spruce (*Picea abies*). The first calculated scenario simply determines the density if all carbohydrates were degraded and all lignin were preserved in the residual wood structure. However, this is an underestimation of the density as at least some carbohydrates are preserved in the compound middle lamella even in very old and heavily decayed waterlogged wood. The second scenario determines the density of the residual wood structure if all carbohydrates (cellulose and hemicellulose) were preserved in the compound middle lamella.

Table 8.1: Results of simplified theoretical calculations of the density of the residual wood structure left after erosion bacteria decay for European Ash (Fraxinus excelsior) and Norway spruce (Picea abies).

	Fraxinus excilsior	***Picea abies***
Scenario 1: Density of residual wood structure if all lignin is preserved and all carbohydrates are decayed		
Density, max. (kg m^{-3})	206	248
Density, min. (kg m^{-3})	99	79
Density, average (kg m^{-3})	166	104
Scenario 2: Density of residual wood structure if all lignin is preserved and all carbohydrates from compound middle lamella is preserved (as is the case for wood decayed by erosion bacteria)		
Density, max. (kg m^{-3})	267	300
Density, min. (kg m^{-3})	128	95
Density, average (kg m^{-3})	216	125

Both scenarios were calculated based on the maximum and minimum density of the two species available in the literature to determine limiting values, and for an average density value to obtain a most-likely-value. Table 8.1 shows the results.

Both scenarios show higher theoretical density values than the experimentally obtained average densities. In the case of the used minimum density values only Norway spruce wood obtained values just below the experimentally obtained values. It is highly unlikely that the native waterlogged wood in general contain such low densities. It is therefore most likely that lignin is lost from the wood structure to some extent. However, lack of chemical alteration of the aromatic lignin structure in residual material speaks against metabolic decay of lignin by the erosion bacteria consortia. However, the size exclusion chromatography analysis indicates that the S2 cell wall lignin is partly depolymerised into mono- and dimers. Such molecules will be much more susceptible toward loss by physical removal (diffusion) than high molecular weight lignin molecules. This suggests that the loss of lignin accounted for must be due to physical removal of lignin from the residual structure during waterlogging.

Lignin aggregation?

In conclusion the present study has shown that residual material left after erosion bacteria decay of the secondary cell wall contains lignin and/or lignin residues. The most common lignin distribution pattern of residual material in cross sections is a heterogeneous

distribution with values higher, similar to, or lower than native S2 layers. However, regions close to the wood surface contain some tracheids with either very low or very high lignin content in the residual material. Furthermore the chemical composition of the aromatic ring structure in the residual material has not been altered compared to the sound S2 cell wall layers. The observations could be explained as follows: When the waterlogged wood cell wall is deconstructed by the erosion bacteria the lignin and lignin residues will be released into the water filled void space. Due to the hydrophobic nature of the lignin it is highly likely that the free-to-move lignin polymer will aggregate to form micelle like structures (PAPER II). This is confirmed by various studies that point to a prevailing consensus that lignin associates in both aqueous and organic media, but the magnitude and the underlying driving forces behind these processes are still a matter of discussion (Guerra et al. 2007). This would explain the heterogeneous distribution of lignin and regions with lignin content as high as in the middle lamella. However, the lignin is not so hydrophobic that it curls up in small and tight droplets. Void space without lignin present has only been observed in earlywood where the amount of cell wall material is very low compared to the cross sectional area of the lumen. This study indicates that the lignin containing residual material form a gel like structure that is tightly bound to the residual wood structure, however very fragile upon dehydration. Within this layer some movement and aggregation of the lignin polymer takes place. UV-microspectrophotometric studies of heavily decayed tracheids in the surface layer shows a significant number of tracheids with very low and very high UV-absorbance levels which indicates that the lignin aggregation is more advanced here. This suggests that time and/or water flow could play a role in the aggregation of lignin.

Tangential longitudinal direction of decayed waterlogged Norway spruce xylem stained with toluidine blue (Appendix A) was examined with light microscopy in the present study to view the lignin distribution in the longitudinal direction of the wood structure (Figure 8.8). In cross section toluidine blue stains sound secondary cell wall light green-blue, the compound middle lamella a slight darker green-blue and the residual material in different shades of blue (Chapter 5.4). In the longitudinal direction sound secondary cell walls have the same light green-blue colour, and the middle lamella a darker blue colour (Figure 8.8a and b). Longitudinal sections of waterlogged xylem with intermediate decay clearly show tracheids with regions of intact secondary cell wall and regions with residual material (darker blue colour). The blue colour of the residual material is in some regions almost even in colour (Figure 8.8c and d, Figure 5.6c) while it is more heterogeneous in other regions (Figure 8.8e). The more homogeneous distribution was the most commonly observed, but aggregation in some parts of the residual material was found (Figure 8.8f, g, and h). This is a strong indication that the lignin residue in the residual material aggregates at least in some regions. However, it is not conclusive since the specificity of the toluidine blue as a stain for lignin is unknown.

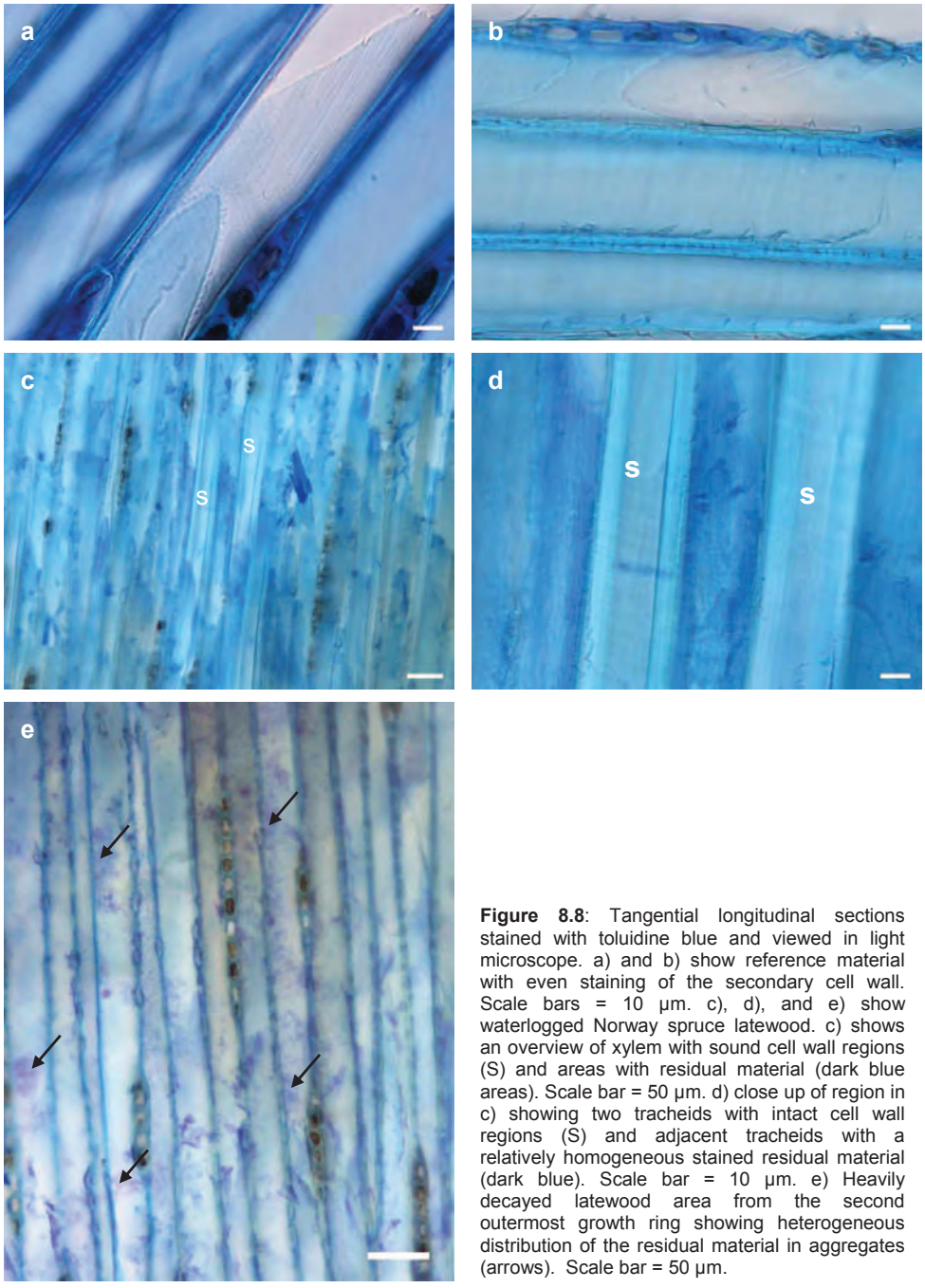

Figure 8.8: Tangential longitudinal sections stained with toluidine blue and viewed in light microscope. a) and b) show reference material with even staining of the secondary cell wall. Scale bars = 10 µm. c), d), and e) show waterlogged Norway spruce latewood. c) shows an overview of xylem with sound cell wall regions (S) and areas with residual material (dark blue areas). Scale bar = 50 µm. d) close up of region in c) showing two tracheids with intact cell wall regions (S) and adjacent tracheids with a relatively homogeneous stained residual material (dark blue). Scale bar = 10 µm. e) Heavily decayed latewood area from the second outermost growth ring showing heterogeneous distribution of the residual material in aggregates (arrows). Scale bar = 50 µm.

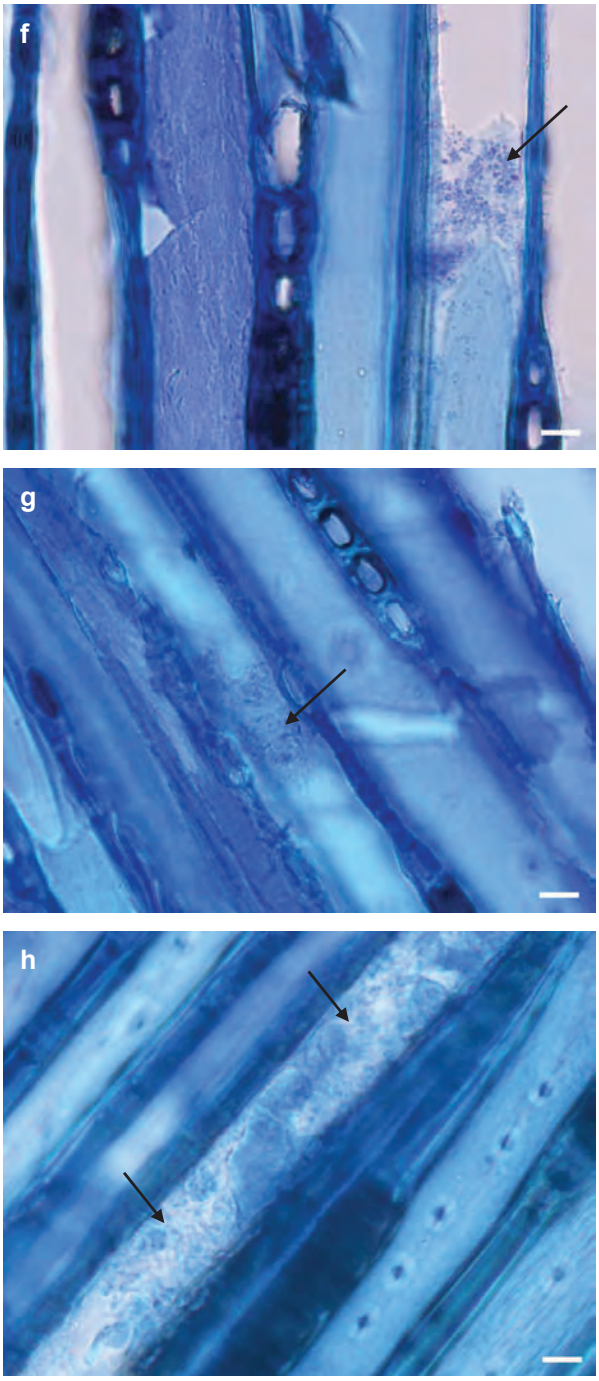

Figure 8.8, continued: Tangential longitudinal sections stained with toluidine blue and viewed in light microscope. f), g), and h) show waterlogged Norway spruce latewood with a decayed tracheid that contain blue stained aggregates (arrows). Scale bars = 10 µm.

Compound middle lamella

Light, scanning electron, and transmission electron microscopy studies have shown that the compound middle lamella is morphologically intact in wood decayed by erosion bacteria (Björdal 2000; Singh and Butcher 1991; Singh et al. 1990)(PAPER I, PAPER II, Chapter 5). However, UV-microspectrophotometric analysis revealed UV-absorbance reduction in the compound middle lamella of decayed tracheids; especially the tangential middle lamella was affected (Figure 8.2b-e, Figure 8.3 d-g and i-l). The topochemical analysis showed that 109 decayed tracheids out of 131 had a lower UV-absorbance level in the tangential compound middle lamella compared to the tangential compound middle lamella of sound tracheids. A majority of the decayed tracheid with lower absorbance levels in the tangential middle lamella still contained a higher UV-absorbance in the compound middle lamella than in the residual material (Figure 8.3). Few decayed tracheids showed the same UV-absorbance of the compound middle and the residual material even though the compound middle lamella was morphologically sound when viewed in light microscope (Figure 8.9).

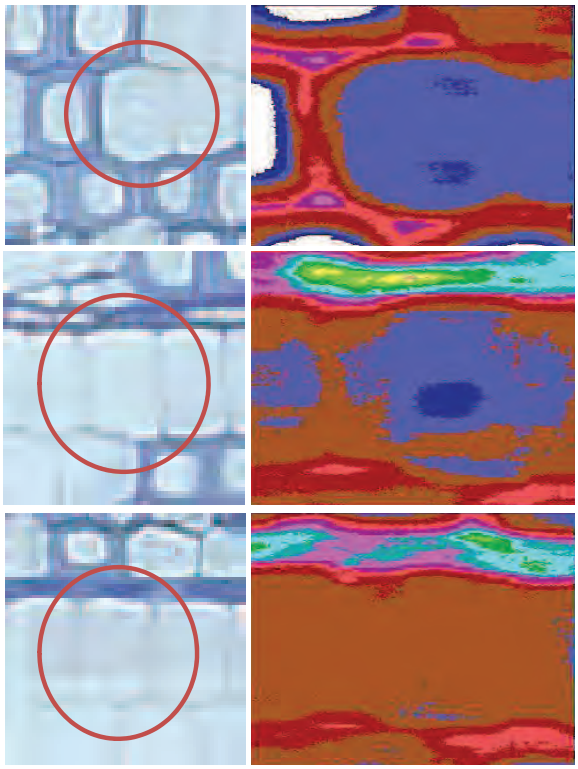

Figure 8.9: Light microscope images stained with toluidine blue of decayed tracheids (left side) showing a morphologically sound compound middle lamella. UV-absorbance profiles (right side) of the same tracheids showing equal UV-absorbance of residual material and compound middle

Reduction in electron density and degradation of lignin in the middle lamella has so far only been reported in the presence of tunnelling bacteria (Kim and Singh 1994; Singh et al. 2003). The observed lowering of the UV-absorbance in the compound middle lamella could be due to measurement artefacts as a consequence of the resolution limit of the apparatus (0.25 µm x 0.25 µm). The average thickness of the S1, S2 and S3 cell wall layers in latewood Norway spruce (*Picea abies*) have been measured to 0.38 µm, 3.7 µm, and 0.14 µm respectively. The primary cell wall plus half of the middle lamella was measured to values between 0.04 µm and 0.16 µm (Fengel and Stoll 1973) (Figure 8.10).

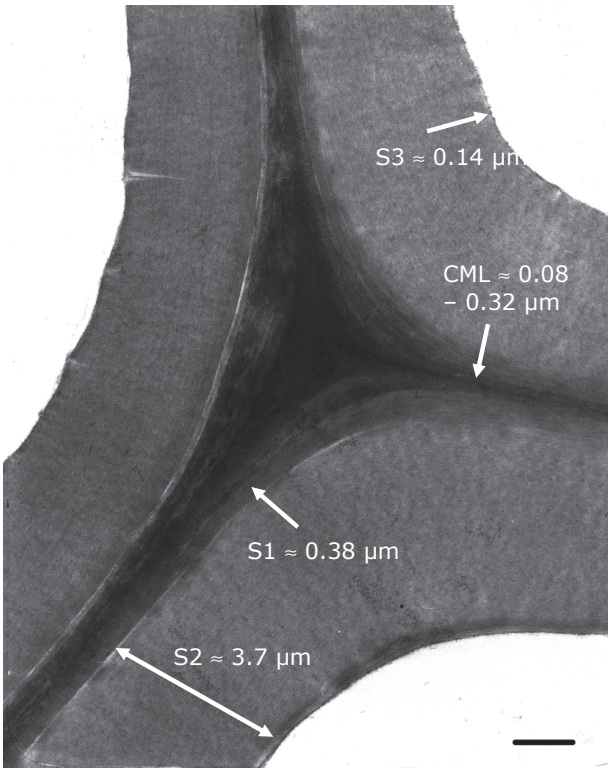

Figure 8.10: Transmission electron microscopy image of cell corner region of latewood Norway spruce obtained in this study. Data for the average thickness of the S1, S2 and S3 cell wall layers and the compound middle lamella (CML) in Norway spruce taken from Fengel & Stoll (1973) is shown in the image.

This means that the whole compound middle lamella region between two tracheids lay in the range from 0.08 µm to 0.32 µm which is less than the resolution limit of the method. Removal of the secondary cell wall layer by bacterial degradation next to the compound middle lamella might therefore lead to a lowering of the UV-absorbance in the compound middle lamella region. However, the observed intact S1 layer weighs against this. The total width of the S1 layer, the compound middle lamella, and the S1 layer in two adjacent tracheids (S1+CML+S1) should lie in the range from 0.84 µm to 1.08 µm which is above the resolution limit of the method. Furthermore the compound middle lamella thickness in black spruce (*P. marina* Mill.) earlywood was found to be 0.40 µm and 0.49 µm in the tangential and the radial direction, respectively (Fergus et al. 1969). This is

more than double the width of the reported thickness in *Picea abies* (Fengel and Stoll 1973). Great variation in compound middle lamella thickness might play an essential role in the observed lowering of UV-absorbance in the compound middle lamella in waterlogged wood decayed by erosion bacteria and it cannot be concluded if this observed change is due to measurement artefacts or decay.

The more limited amount of analysed tracheids with confocal Raman imaging also shows both tangential and radial compound middle lamella areas with lower lignin intensity than seen in the reference material (Figure 8.4d and e). The resolution limit is 0.33 µm with one pixel in the Raman image representing the integrated intensity of the chosen band from one spectrum. Raman images generated as a sum filter from 1080-1190 cm^{-1} (CC and CO stretching vibrations, carbohydrates) illustrates very well that the compound middle lamella thickness is in the border area of the resolution limit of the method. The compound middle lamella with low carbohydrate intensity 'drowns' in signal intensity from the tangential S1 cell wall with very high intensity (Figure 8.11).

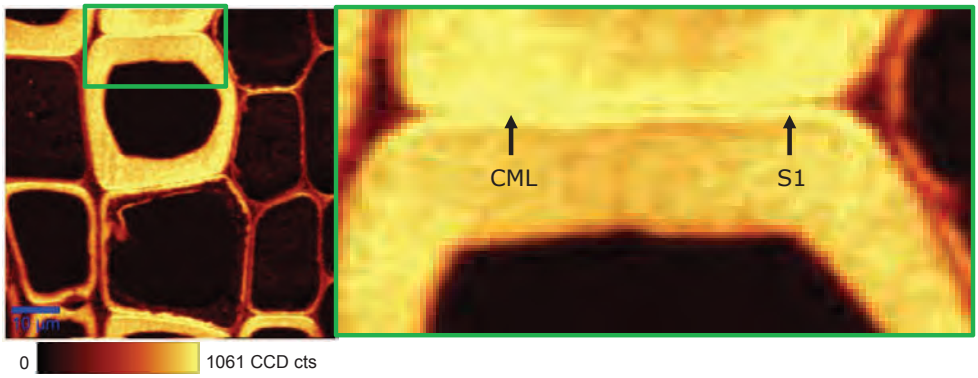

Figure 8.11: a) Confocal Raman image of waterlogged Norway spruce decayed by erosion bacteria generated as a sum filter from 1080-1190 cm^{-1} (CC and CO stretching vibrations, carbohydrates). The S1 layers in the tangential direction of the wood have a very high intensity related to orientation of the microfibrils and the laser polarization direction. b) Detail of a) showing how the compound middle lamella (CML) with low carbohydrate intensity 'drowns' in the high signal from the S1 cell wall.

9 Conclusions and perspectives

9.1 Conclusions

The traditional analytical approach to chemical analysis of wood can give valuable information on degree of degradation and chemical differences between for instance biotic and abiotic decay types in waterlogged wood - if representative sample material is selected carefully with the aid of light microscope investigations. However, the traditional analytical approach has the limitation that the sample material covers large sample areas. The chemical composition of the individual cell wall compartments is thereby averaged. Knowledge of the chemical composition at the ultrastructural level with a high spatial resolution is important for understanding the degraded waterlogged wood material and the decay mechanisms acting here. This study has proven it possible to obtain spatially resolved chemical information on waterlogged archaeological wood at the sub-cellular level by a combination of high resolution imaging and micro-spectroscopic techniques. The confocal Raman imaging and UV-microspectrophotometry used in this study gave spatially resolved information on the molecular structure with a resolution of 0.25 µm and 0.33 µm, respectively. This made it possible to separate the chemical composition of the residual material from the sound cell wall compartments. It is a novel approach to study the chemical composition of waterlogged archaeological wood. The chemical analysis was obtained on cross sections of sample material and thereby on the biopolymers as they are situated in the wood cell wall *in situ.* The techniques offer an opportunity to study the composition of the biopolymers in their native state. This is preferred to some of the more traditional chemical and spectroscopic analysis where the biopolymers are isolated from the cell wall prior to analysis and therefore altered to some degree.

Numerous publications on the chemical composition of waterlogged wood do not consider the decay type and degree of degradation as well as the contribution of abiotic and biotic decay factors on the investigated waterlogged wood material. This makes it impossible to compare data and results from different studies. In addition, wood species, original wood properties, and site specific abiotic decay factors influence the chemical material characteristics. The present study showed that the waterlogged environment contributed with minor chemical changes to the wood structure. This effect was separated from the chemical changes of erosion bacteria decay by comparing analyses of ultrastructural sound xylem and sound cell wall compartments with native reference material. In addition this study was novel in the way sample collection was carried out. The majority of previous studies performed on chemical composition of waterlogged wood have been carried out due to the significance of the find and not selected due to the material or site characteristics. In the present study great care was taken in sample selection, collection, and post-excavation storage to be able to study the chemical alterations due to erosion bacteria decay without interference from other microbial wood degraders.

The present work gives new insight into the chemical composition of the residual structure in softwood tracheids left after erosion bacteria decay in waterlogged anoxic environments. The S2 cell wall layer is effectively deconstructed and all carbohydrates metabolised. The S1 cell wall layer is conserved to a high degree and the S3 layer is only partly decayed. The residual wood structure of totally disintegrated wood can therefore be observed as a skeleton composed of cell corners, the thin compound middle lamella and S1 cell wall layer with an amorphous residual material often filling up both native cell wall regions and the lumen. The residual material consists of lignin or lignin-like substances. The aromatic ring structure is preserved but the lignin is most likely partly depolymerised in the aliphatic polymer regions into monomer, dimers and oligomers of varying molecular size. The residual material seems to form a gel like structure with aggregates of lignin substance that in some cases have lignin concentrations as high as in cell corners. This residual material "gel" seems to be intramolecular bound and firmly attached to the residual wood skeleton. However, it provides no physical strength to the wood structure and it is very sensitive to dehydration. In case of an intermediate decay stage the waterlogged wood will consist of alternating sound and decayed tracheids when viewed in cross section. This is not due to alternating sound and decayed tracheids but merely a two dimensional visualisation of alternating regions of intact and decayed S2 cell wall regions in the longitudinal direction of individual tracheids. The cell wall region in a given point of a tracheid is either decayed or intact; no intermediate decay stages with partly preserved carbohydrates seem to be present. Morphological intact cell wall regions have shown to contain minor abiotic changes of the wood polymers. The lignin and carbohydrate content and distribution are identical to cell walls in reference tracheids. However, the lignin polymer show possible minor hydrolysis and oxidation but preservation of the aromatic ring structure whereas the hemicellulose show evidence of hydrolysis of ester bonds in lignin-carbohydrate complexes and acetyl groups attached to glucomannan. This has implications for the supramolecular structure of the biopolymers and thereby the mechanical behaviour of the residual cell wall regions. However, the abiotic decay is minor and insignificant compared to erosion bacteria decay in terms of physical alteration of the wood structure. Therefore, the abiotic decay has the greatest impact in relation to wood material with a high proportion of morphological sound cell wall material.

Microscopic and micro-spectroscopic analyses have some limitations as is the case with the more traditional analytic approach. Very small sample areas are examined even with a high number of replicas. Obviously there is a trade-off between the resolution of the spatial resolved chemical information and the amounts of sample material investigated. This limitation should not be underestimated since both the wood material and the wood decay feature natural variations. Variability between individual samples within the same wood sample and between different samples from the same location is to be expected. This study shows a similar lignin distribution within three different Norway spruce poles from the same waterlogged site and in Scotch pine and Norway spruce both decayed solely by erosion bacteria but excavated from two different waterlogged sites. This

indicates that the results obtained on lignin and carbohydrate distribution on the Norway spruce material will have some similarities with wood from other burial environments. Another limitation to the chemical imaging approach is that the techniques can only be used for cross sections. This results in two dimensional visualisation of a three dimensional decay pattern. Furthermore, the longitudinal direction should be a better choice in case of two dimensional examinations since the erosion bacteria follows the almost horizontal aligned microfibril angle in the S2 cell wall layer. However, interpretation of even simple stained longitudinal sections for the light microscope is not straight forward. The cross sectional studies performed in this study are still very valuable if the two-dimensional limitation is considered when interpreting the results.

The low density of heavily decayed waterlogged wood unveil that apart from the metabolic decay of the structural carbohydrates from the cell wall some lignin must be lost as well. However, lack of degradation of the aromatic ring structure in the lignin indicates that lignin is not used as a carbon source by the bacteria. The lignin is most likely lost by means of physical processes. One likely explanation is that smaller fractions such as monomers and dimers are removed by diffusion controlled by water flow at the waterlogged site. Despite the lack of metabolic decay of lignin the bacteria are able to deconstruct the cell wall to gain access to the polysaccharides. However, in Norway spruce wood the bacteria prefer tracheids to parenchyma and epithelia cells. Within the tracheids the bacteria prefer the S2 cell wall layer over the S1 layer, the S3 layer, the compound middle lamella, bordered pit regions, and the lignified outer S2 layer in compression wood. This strongly indicates that the content, chemical composition and conformation of lignin plays a significant role in the decay resistance of some cell types and cell wall compartments. However, the chemical composition and conformation of the structural carbohydrates such as the microfibril angle might also play a role in the recalcitrant nature of some cell types and cell wall compartments. It is still an open question which enzymatic processes are responsible for cell wall deconstruction in anaerobic decay communities. The bacteria need enzymatic tools to be able to gain access to the structural carbohydrates they feed on. This study shows that depolymerisation of the lignin polymer is most likely involved. Furthermore this study suggests that enzymatic deconstruction of the lignocellulosic cell wall material to gain access to the polysaccharides is the rate limiting step in the decay process as the cell wall is either degraded or intact and the residual material does not contain structural carbohydrate remnants; the carbohydrates are consumed by the bacteria as soon as they are released from the material.

9.2 Significance for conservation

The main task when conserving waterlogged archaeological wood is to bring the wood from a wet to a dry state suitable for display, research, and storage. A handful of suitable water or solvent based techniques such as polyethylene glycol impregnation followed by freeze drying or internal coating of the wood structure with melamine have been developed in the last 60 years (http://www.rgzm.de/kur/). However, the different methods

have disadvantages such as high cost, long treatment times, limitation to the size of the objects, health hazards, and crack developments due to heterogeneous decay. This drives the search for new treatment methods. Especially low cost conservation strategies for large-sized objects with a heterogeneous decay profile are needed.

The chemical imaging methods used in this study are performed on highly specialised equipment and are not suited for routine checks of type of decay and degree of degradation prior to conservation treatments. This advanced approach is however valuable in basic material and degradation research and is crucial in the understanding of the wood material. Wood is a highly complex material and not even fully understood in un-altered state. The biotic and abiotic decay in waterlogged submerging environments likewise. The decay profiles in waterlogged wood material vary greatly both at the macroscopic and microscopic level. At the macroscopic level the wood structure can be totally disintegrated from surface to core, almost intact from surface to core, or contain varying amounts of sound and totally disintegrated regions with an in-between region of intermediate decayed xylem. From a conservation perspective it is important to understand these macroscopic differences at the microscopic level. At the microscopic level the different decay types can be divided into the three categories discussed below:

1. Totally disintegrated tracheids
2. Tracheids with no erosion bacteria decay
3. Tracheids with both sound and decayed cell wall regions

Category 1: Waterlogged wood material with totally disintegrated tracheids will consists of a network of intact middle lamella with or without a sound S1 cell wall layers and an amorphous residual material with lignin and lignin-like substances and possible remnants of intact cell S3 wall layers. The wood skeleton possesses no strength and is only kept in shape by the water filling up the structure. The whole structure will collapse if subjected to air drying since the capillary forces of the evaporating water are greater than the fragile wood structure. This type of material require an impregnation agent that is able to fill up the decayed areas and the lumen or chemically lock/coat the remaining cell wall components to physically hinder collapse of the remaining wood skeleton. Several impregnation substances that are water soluble and solid at room temperature are able to fulfil this. The impregnation agent can diffuse into the wood in the aqueous phase and solidify upon water evaporation. Due to the lack of secondary cell walls even high molecular weight substances have easy access to the wood structure. If the process is purely a matter of filling up the void space to physically hinder collapse the chemical structure of the residual wood structure is less important. However, the nature of the amorphous lignin-rich residual material could play a role in the diffusion rate and chemical compatibility of an impregnation agent since this study has shown that it seems to form a gel that is firmly attached to the residual wood structure. Further investigation of the chemical composition and physical properties of the residual material could lead to

the use of the residual material for binding of an impregnation agent to gain strength and thereby hinder collapse. In case of chemical bonding between the wood material and the impregnation agent (e.g. a coating) it could play a major role whether the S1 cell wall layer is preserved or not. The compound middle lamella and the S1 cell wall layer have very different supramolecular structure and thereby very different potential binding sites. Further investigation into parameters that determines S1 cell wall layer preservation is highly interesting. From the present study it is hypothesised that the supramolecular structure is a considerable factor in the recalcitrance of the S1 cell wall layer and that the supramolecular structure of the S1 cell wall layer to some degree depends on the wood species.

Category 2: Waterlogged wood material that consists of sound tracheids with no erosion bacteria decay will shrink upon drying when bound water is evaporated from the cell wall. It is the same physical process as observed when drying recent wood. However, this study has shown that abiotic decay plays a minor role in the waterlogged wood material. Small changes in the chemical composition of the biopolymers will have an influence on the physical properties of the material even though the polymers have not changed position within the cell wall. The breaking of ester linkages will lead to a higher proportion of hydroxyl groups in the cell wall and thereby a higher number of sites available for hydrogen bonding with water. The cell wall can therefore bind more water and the cell wall will shrink more than recent wood upon drying. In addition, the breakage of ester linkages between the carbohydrate and lignin matrix will very likely lead to a less rigid wood structure. Further investigation into abiotic wood decay in waterlogged anoxic environments to determine factors controlling the chemical processes and the extent of the decay is interesting and relevant. From the present study it is hypothesised that this varies between different submerging environments and different wood species. To avoid shrinkage in the sound waterlogged wood structure impregnation agents must be able to replace the water in the cell thus preventing shrinkage when water evaporates. This has proven not to be an easy task. The molecules have to be small to be able to enter the cell wall. In addition, the molecules have to have a higher affinity to the cell wall than water. If not the water from the ambient air will replace the impregnation substance. This would lead to leakage of the impregnation substance from the wood structure if the substance is liquid at room temperature. Another challenge is that well preserved heartwood such as oak and pine has a very low diffusion potential since the wood structure is closed due to tylose and pit closure, respectively; even long impregnation periods with low molecular substances are not very effective.

Category 3: The intermediate decay zone between totally disintegrated and sound xylem consists of tracheids with both decayed and sound cell wall regions within single tracheids. How the individual tracheids will react upon drying will both depend on the proportion of decayed cell wall regions and the distribution of decayed and intact regions in the tracheids. The physical reaction of the individual tracheids towards drying has a direct influence on the macroscopic behaviour of the wood material. With this in mind

impregnation agents suitable for this type of wood material have to fulfil the two very different physical tasks of hindering both collapse and shrinkage. This is not an easy task since demands such as long service life, resistance to chemical, physical and microbial decay, aesthetic, chemically and physical changes of the wood, destruction of research potential, reversibility of the treatment, health hazards, and cost have to be considered too.

This study presents a low number of samples and studied sites comparable to the many inherent irregularities in the wood material. It is of interest to investigate how variable the residual wood structure is between different wood species and between different submerging environments. The techniques used in the present study are highly suitable for this task. A larger number of samples including both softwoods and hardwoods from waterlogged environments as variable as marine and freshwater sediments, bogs, and waterlogged soils will most likely give the opportunity to locate some similarities and differences that are species and site specific. This might lead to the ability to predict a likely chemical composition of the residual wood structure on cell wall level with help from more readily available equipment such as light microscope and FT-IR analysis.

This study only considered erosion bacteria decay. However, soft rot fungi are often present in waterlogged archaeological wood at least in the surface layer, and often in combination with erosion bacteria decay. In heavily decayed wood xylem the ultrastructure of soft rot decay is very similar to erosion bacteria decay. The fungi do not degrade the compound middle lamella and also leaves behind an amorphous residual material. It is expected that the chemical composition at the ultrastructural level is different from erosion bacteria decay since the enzymatic systems used for deconstruction and utilisation of the cell wall polymers are different due to the oxygen dependent respiration by the fungi. It is therefore highly relevant to study similarities and differences of the chemical ultrastructure between the wood residual structure left after erosion bacteria and soft rot decay. This could be done in three-step project. Firstly by identifying the most dominant soft rot species associated with different waterlogged environments; secondly by degradation of wood samples with pure strains in the laboratory; thirdly by studying the chemical composition at the ultrastructural level in a similar manner as was done in this study. This would identify how the chemical structure differs between the two decay types and if this has any implications for the conservation strategies.

9.3 Significance for anaerobic biomass degradation

Waterlogged anoxic ecosystems are extreme environments with low biotic activity. This leads to very slow decay rates of plant litter. The waterlogged environments are therefore large carbon sinks in regard to the global carbon cycle. Understanding the anaerobic biomass degradation in natural ecosystems is important in relation to quantification of the carbon input and output to these environments. A more clarified knowledge of the decay systems could lead to better estimates of the effect of wetland areas for the carbon balance. Understanding the complex interactions in waterlogged anoxic or near anoxic

ecosystems are more critical than ever due to the ongoing climate changes. The reported preservation of waterlogged wood 65 million years old (Obst et al. 1991) suggest that the terminal stage of anaerobic lignocellulose degradation is the compound middle lamella skeleton containing some residual material. Whereas the terminal stage for aerobic decay of plant litter is formation of humus substances (Berg et al. 2014). The difference between aerobic and anaerobic lignocellulose degradation pathways has a great implication for the chemical composition of the carbon stored in the waterlogged ecosystems. The present study has by use of ultrastructural and chemical approach added new insight to the knowledge on biomass decay in extreme anoxic environments.

Bacterial degradation is the principle degradation route but the present study has shown that abiotic decay processes also play a minor role in the extreme slow decay rates and very long submerging periods. One central question in this respect is how a temperature increase will affect the decay rates in waterlogged anoxic and near anoxic environments. It is not known if elevated temperatures of two to five degrees will have significant effect on the decay rate and thereby on the carbon release. It would be very valuable to put an effort into identification of the erosion bacteria consortia in different types of ecosystems. This would make it possible to study anaerobic decay rates of lignocellulose under different climate scenarios. The most promising approach is by use of RNA techniques combined with ultrastructural studies of the plant cell wall.

Results from the present study confirm that natural anaerobic bacteria are able to deconstruct softwood lignocellulose. The bacteria have a preference for the S2 cell wall layer in softwood tracheids. Other cell types and cell wall compartments are more recalcitrant. This preference for some cell types and cell wall compartments does not seem to be caused by accessibility but rather by differences in cell wall architecture. The relative lignin content plays an important role in this aspect, but the supramolecular organisation and chemical composition also seem to have an impact on the decay resistance of some cell wall compartments. The compound middle lamella is for example highly decay resistant. The lignin content is not only higher but also chemically different from the preferred S2 cell wall. The compound middle lamella lignin does not only have a higher molecular weight but also a less ordered supramolecular arrangement compared to lignin in the S2 cell wall layer. The more recalcitrant nature of the S1 cell wall layer compared to the S2 layer point to the fact that the conformation and chemical composition of the hemicellulose and/or the microfibril arrangement also play a role in the recalcitrant nature of some cell wall compartments. It would be highly interesting to further investigate the impact of other plant cell wall characteristics than lignin in anaerobic deconstruction of plant cell walls. This knowledge will help clarify the reasons for differences in the recalcitrant nature of different cell types and plant organs. This could be useful in optimizing commercial enzyme blends for different feedstock to obtain a higher hydrolysis yield when turning structural carbohydrates from biomass into sugar monomers. The present study has shown that ultrastructural studies and chemical imaging are valuable tools for understanding cell wall deconstruction in native cell wall material. In some cases this approach could be more valuable than research performed on model

materials. Furthermore this study showed due to the very slow decay rate of erosion bacteria that it is valuable to study intermediate decay stages and not only the terminal stage in native material. This approach could also be used within biomass science of much faster decay processes if it is possible to stop the enzymatic decay process and examine the material before the terminal decay stage has taken place.

This study showed that the carbohydrate fraction of attacked cell wall compartments is utilised highly effectively. This suggests that the erosion bacteria have a number of different enzymes that together have the capacity to hydrolyse cellulose and all types of hemicellulose situated in the S2 cell wall layer of the wood tracheids. Furthermore the results of the study indicate that lignin is not metabolised by the bacteria. But the bacteria do most likely possess enzyme systems that are able to open up the cell wall structure to allow access of cellulases to the structural carbohydrates. In industrial processing of biomass for biomaterials and biofuels it is necessary to pre-treat the material with for example a steam treatment to be able to use cellulases effectively. The present study show that the lignin residue left after bacterial decay of the cell wall did not change the chemical composition of the aromatic ring system. However, an initial size exclusion chromatographic analysis indicated that the lignin polymer was partly depolymerised as is the case for pre-treated wheat straw and Kraft lignin. This indicates that it is necessary to at least partly depolymerise lignin for cellulases systems to physically gain access to the structural carbohydrates in the cell wall. This fits with the protective function of lignin and the proposed model for organisation of the wood polymers presented in Chapter 2.4. However, it cannot be ruled out that abiotic decay mechanisms are responsible for the depolymerisation. This does not however seem very plausible as lignin depolymerisation under anoxic conditions must be expected to be a very slow process. But it should be fairly simple to clarify this by examination of the lignin structure in modern wood samples waterlogged under sterile conditions.

Light microscope investigations in the longitudinal direction have shown that adjacent intact and decayed cell wall regions form a diamond- or V-shaped pattern. This pattern could be caused by the simple fact that the erosion bacteria are aligned along the microfibrils as they decay the cell wall. Erosion bacteria are often found in clusters producing parallel erosion grooves. This scenario will likely produce V-shapes in the cell wall in the zone between decayed and sound cell wall material. It is however also possible that this decay pattern contain information on the enzymatic strategy used by the bacteria. Brunecky et al. (2013) have found that the anaerobic thermophilic bacteria strain *Caldicellulosiruptor bescii* secretes free cellulases that contain multiple catalytic domains. One of these, CelA, has been shown to form angled ends in Avicel particles and in addition it forms cavities in the surface instead of the normal surface ablation observed in cellulose digestion by cellulases. This pattern has some resemblance to the decay pattern of erosion bacteria decay seen in light microscope. Transmission electron microscopy of early stage erosion bacteria decay in the longitudinal direction could most likely give a better understanding of the enzymatic systems used by the erosion bacteria. Cellulosomes have been observed in association with erosion bacteria but like

Caldicellulosiruptor bescii the bacteria might possess the ability to secrete free cellulases with multiple catalytic sites.

Transmission electron microscopy performed in the present study showed that that the border between decayed and sound cell wall regions is abrupt and that the residual material in this border zone is similar in microscopic and chemical appearance. This indicates that the enzymatic deconstruction of the lignocellulosic cell wall is the rate limiting step in the decay process. It would be interesting to go deeper into the lignin depolymerisation enzyme system that the bacteria most likely possess. It could be valuable to get a deeper understanding of anaerobic lignin depolymerisation. Such an enzymatic system active under anoxic conditions must be different from fungal lignin oxidation systems.

10 References

Abe, H., and Funada, R. (2005): Review - The orientation of cellulose microfibrils in the cell walls of tracheids in conifers. *Iawa Journal*, 26(2), 161-174.

Agarwal, U. (2006): Raman imaging to investigate ultrastructure and composition of plant cell walls: distribution of lignin and cellulose in black spruce wood (*Picea mariana*). *Planta*, 224(5), 1141-1153.

Agarwal, U. P. (1999): An overview of Raman Spectroscopy as Applied to Lignocellulosic Materials. In: D. S. Argyropoulos (ed.). *Advances in Lignocellulosics Characterization*. Atlanta, Tappi Press, pp. 201-225.

Agarwal, U. P., and Atalla, R. H. (1986): In-situ Raman microprobe studies of plant cell walls: Macromolecular organization and compositional variability in the secondary wall of *Picea mariana* (Mill.) B.S.P. *Planta*, 169(3), 325-332.

Agarwal, U. P., and Ralph, S. A. (1997): FT-Raman spectroscopy of wood: Identifying contributions of lignin and carbohydrate polymers in the spectrum of black spruce (*Picea mariana*). *Applied Spectroscopy*, 51(11), 1648-1655.

Agarwal, U. P., and Ralph, S. A. (2008): Determination of ethylenic residues in wood and TMP of spruce by FT-Raman spectroscopy. *Holzforschung*, 62(6), 667-675.

Akin, D. E. (2008): Plant cell wall aromatics: influence on degradation of biomass. *Biofuels Bioproducts & Biorefining-Biofpr*, 2(4), 288-303.

Anon (2012): Nationella Laboratoriet för Vedanatomi och Dendrokronologi, rapport nr 2012:15, Lund University.

Appelqvist, C and Björdal, C.G. (2011): Wood degraders in the Baltic Sea. In: C. G. Björdal and D. Gregory (eds.). *WreckProtect. Decay and protection of archaeological wooden shipwrecks*. Oxford, Archaeopress Ldt, pp. 57-72.

Balakshin, M., Capanema, E., Gracz, H., Chang, H.-m., and Jameel, H. (2011): Quantification of lignin–carbohydrate linkages with high-resolution NMR spectroscopy. *Planta*, 233(6), 1097-1110.

Balakshin, M. Y., Capanema, E. A., and Chang, H.-m. (2007): MWL fraction with a high concentration of lignin-carbohydrate linkages: Isolation and 2D NMR spectroscopic analysis. *Holzforschung*, 61(1), 1-7.

Barbour, R. J., and Leney, L. (1986): Microstructural Analysis of Red Alder (*Alnus rubra* Bong) from a 2500 Year Old Archaeological Wet Site. In: *Biodeterioration 6. 6th International Biodeterioration Symposium*, Washington DC 1984. Slough, United Kingdom.

Bardage, S., Donaldson, L., Tokoh, C., and Daniel, G. (2004): Ultrastructure of the cell wall of unbeaten Norway spruce pulp fibre surfaces. *Nordic Pulp & Paper Research Journal*, 19(4), 448-452.

Bardet, M., Foray, M. F., Maron, S., Goncalves, P., and Trân, Q.-K. (2004): Characterization of wood components of Portuguese medieval dugout canoes with high-resolution solid-state NMR. *Carbohydrate Polymers*, 57(4), 419-424.

Bardet, M., Gerbaud, G., Giffard, M., Doan, C., Hediger, S., and Pape, L. L. (2009): 13C high-resolution solid-state NMR for structural elucidation of archaeological woods. *Progress in Nuclear Magnetic Resonance Spectroscopy*, 55(3), 199-214.

Barnes, R. J., Dhanoa, M. S., and Lister, S. J. (1989): Standard Normal Variate Transformation and De-Trending of Near-Infrared Diffuse Reflectance Spectra. *Applied Spectroscopy*, 43(5), 772-777.

Bayer, E. A., Chanzy, H., Lamed, R., and Shoham, Y. (1998): Cellulose, cellulases and cellulosomes. *Current Opinion in Structural Biology*, 8(5), 548-557.

Bayer, E. A., Henrissat, B., and Lamed, R. (2008): The Cellulosome: A Natural Bacterial Strategy to Combat Biomass Recalcitrance. In: M. E. Himmel (ed.). *Biomass Recalcitrance. Deconstructing the Plant Cell Wall for Bioenergy*. Oxford, Blackwell Publishing, pp. 407-435.

Beguin, P., and Aubert, J. P. (1994): The Biological Degradation of Cellulose. *FEMS Microbiology Reviews*, 13(1), 25-58.

Benner, R., Maccubbin, A. E., and Hodson, R. E. (1984): Anaerobic Biodegradation of the Lignin and Polysaccharide Components of Lignocellulose and Synthetic Lignin by Sediment Microflora. *Applied and Environmental Microbiology*, 47(5), 998-1004.

Berg, B., and McClaugherty, C. (2014): Plant Litter. Decomposition, Humus Formation, Carbon Sequestration. Berlin, Springer-Verlag.

Björdal, C. G. (2000). Waterlogged archaeological wood. Biodegradation and its implications for conservation, Swedish University of Agricultural Science, Uppsala.

Björdal, C. G. (2012): Evaluation of microbial degradation of shipwrecks in the Baltic Sea. *International Biodeterioration & Biodegradation*, 70, 126-140.

Björdal, C. G., Daniel, G., and Nilsson, T. (2000): Depth of burial, an important factor in controlling bacterial decay of waterlogged archaeological poles. *International Biodeterioration & Biodegradation*, 45(1-2), 15-26.

Björdal, C. G., and Nilsson, T. (2008): Reburial of shipwrecks in marine sediments: a long-term study on wood degradation. *Journal of Archaeological Science*, 35(4), 862-872.

Björdal, C. G., Nilsson, T., and Bardage, S. (2005): Three-dimensional visualisation of bacterial decay in individual tracheids of Pinus sylvestris. *Holzforschung*, 59(2), 178-182.

Björdal, C. G., Nilsson, T., and Daniel, G. (1999): Microbial decay of waterlogged archaeological wood found in Sweden Applicable to archaeology and conservation. *International Biodeterioration & Biodegredation*, 43(1-2), 63-73.

Blanchette, R. A. (1995): Degradation of the Lignocellulose Complex in Wood. *Canadian Journal of Botany-Revue Canadienne de Botanique*, 73, S999-S1010.

Blanchette, R. A., and Hoffmann, P. (1994): Degradation Processes in Waterlogged Archaeological Wood. In: *Proceedings of the 5th ICOM Group on Wet Organic Archeological Materials*. Portland/Maine 1993. Bremerhaven.

Blanchette, R. A., Nilsson, T., Daniel, G., and Abad, A. (1990): Biological Degradation of Wood. In: Rowell, R. M. & Barbour, R. J. (eds.): *Archaeological Wood. Properties, Chemistry, and Preservation*. Developed from a symposium sponsored by the Cellulose, Paper and Textile Division at the 196th National Meeting of the American Chemical Society, Los Angeles, California, September 25-September 30 1988. Advances in Chemistry Series 225. American Chemical Society. Washington D.C. Pp. 141-174.

Bojesen-Koefoed, I. (2013): Re-conservation of wood treated with alum in the 1920s - challenges and strategies. In: Strætkvern,K. and Williams, E. (eds.): *Proceedings of the 11th ICOM-CC Group on Wet Organic Archaeological Materials Conference*, Greenville, North Carolina 2010. Eds. The International Council of Museums (ICOM). pp. 497-502.

Borgin, K., Faix, O., and Schweers, W. (1975a): The effect of aging on lignins of wood. *Wood Science and Technology*, 9(3), 207-211.

Borgin, K., Parameswaran, N., and Liese, W. (1975b): The effect of aging on the ultrastructure of wood. *Wood Science and Technology*, 9(2), 87-98.

Boutelje, J. B., and Bravery, A. F. (1968): Observations on the bacterial attack of piles supporting a Stockholm building. *Journal of the Institute of Wood Science*, 20(4/2), 47-57.

Brändström, J., Bardage, S. L., Daniel, G., and Nilsson, T. (2003): The structural organisation of the S1 cell wall layer of Norway spruce tracheids. *IAWA Journal*, 24(1), 27-40.

Braovac, S., and Kutzke, H. (2012): The presence of sulfuric acid in alum-conserved wood – Origin and consequences. *Journal of Cultural Heritage*, 13(3), S203-S208

Brunecky, R., Alahuhta, M., Xu, Q., Donohoe, B. S., Crowley, M. F., Kataeva, I. A., Yang, S.-J., Resch, M. G., Adams, M. W. W., Lunin, V. V., Himmel, M. E., and Bomble, Y. J. (2013): Revealing Natures's Cellulase Diversity: The Digestion Mechanism of *Caldicellulosiruptor bescii* CelA. *Science*, 342, 1513-1516.

Brunow, G., and Lundquist, K. (2010): Funktional groups and bonding patterns in lignin (including the lignin-carbohydrate complexes). In: C. Heitner, D. R. Dimmel, and J. A. Schmidt (eds.). *Lignin and Lignans. Advances in Chemistry*. Boca Raton, CRC Press, pp. 267-299.

Capretti, C., Macchioni, N., Pizzo, B., Galotta, G., Giachi, G., and Giampaola, D. (2008): The characterization of waterlogged archaeological wood: the three Roman ships found in Naples (Italy). *Archaeometry*, 50, 855-876.

Christensen, B. B. (1970): The Conservation of Waterlogged Wood in the National Museum of Denmark.With a report on the methods chosen for the stabilization of the timbers of the Viking ships from Roskilde Fjord, and a report on experiments carried out in order to improve these methods, Copenhagen: The National Museum of Denmark.

Colombini, M. P., Lucejko, J. J., Modugno, F., Orlandi, M., Tolppa, E. L., and Zoia, L. (2009): A multi-analytical study of degradation of lignin in archaeological waterlogged wood. *Talanta*, 80(1), 61-70.

Colombini, M. P., Lucejko, J. J., Modugno, F., and Ribechini, E. (2009): Characterisation of archaeological waterlogged wood by direct exposure mass spectroscopy (DE-MS) and pyrolysis-gas chromatography/mass spectroscopy (PY-GC/MS). In: Strætkvern, K. and Huisman, D.J. (eds.): *Proceedings of the 10th ICOM Group on Wet Organic Archaeological Materials Conference*, Amsterdam 2007. Amersfoort, Rijksdienst voor Archaeologie, Cultuurlandschap en Monumenten. Pp. 35-41.

Cufar, K., Gricar, J., Zupancic, M., Koch, G., and Schmitt, U. (2008): Anatomy, cell wall structure and topochemistry of waterlogged archaeological wood aged 5,200 and 4,500 years. *IAWA Journal*, 29(1), 55-68.

Daniel, G., and Nilsson, T. (1998): Developments in the Study of Soft Rot and Bacterial Decay. In: A. Bruce and J. W. Palfreyman (eds.). *Forest Products Biotechnology*. London, Taylor & Francis, pp. 37-62.

Daniel, G., Nilsson, T., and Pettersson, B. (1991): Poorly and non-lignified regions in the middle lamella cell corners of birch (*Betula verrucosa*) and other wood species. *IAWA Bulletin*, 12(1), 70-83.

Decker, S. R., Siika-aho, M., and Viikari, L. (2008): Enzymatic Depolymerization of Plant Cell Wall Hemicelluloses. In: M. E. Himmel (ed.). *Biomass Recalcitrance. Deconstructing the Plant Cell Wall for Bioenergy*. Oxford, Blackwell Publishing, pp. 352-373.

Dence, C. W., and Lin, S. Y. (1992): Introduction. In: S. Y. Lin and C. W. Dence (eds.): Methods in Lignn Chemistry. Berlin, Springer-Verlag, pp. 110-121.

Dimmel, D. R. (2010): Overview. In: C. Heitner, D. R. Dimmel, and J. A. Schmidt (eds.). *Lignin and Lignans. Advances in Chemistry*. Boca Raton, CRC Press, pp. 1-10.

Donaldson, L. A. (1987): S3 lignin concentration in radiata pine tracheids. *Wood Science and Technology*, 21(3), 227-234.

Eriksson, K.-E. L., Blanchette, R. A., and Ander, P. (1990): *Microbial and enzymatic degradation of wood and wood components*, Berlin: Springer-Verlag.

Fackler, K., and Schwanninger, M. (2012): How spectroscopy and microspectroscopy of degraded wood contribute to understand fungal wood decay. *Applied Microbiology and Biotechnology*, 96(3), 587-599.

Fackler, K., Stevanic, J. S., Ters, T., Hinterstoisser, B., Schwanninger, M., and Salmen, L. (2010): Localisation and characterisation of incipient brown-rot decay within spruce wood cell walls using FT-IR imaging microscopy. *Enzyme and Microbial Technology*, 47(6), 257-267.

Fackler, K., and Thygesen, L. G. (2013): Microspectroscopy as applied to the study of wood molecular structure. *Wood Science and Technology*, 47(1), 203-222.

Faix, O. (1991): Classification of Lignins from Different Botanical Origins by FT-IR Spectroscopy. *Holzforschung*, 45, 21-27.

Feist, W. C., and Hon, D. N.-S. (1984): Chemistry of Weathering and Protection. In: R. Rowell (ed.). *The Chemistry of Solid Wood*. Washington D.C., American Chemical Society, pp. 401-451.

Fengel, D. (1969): The ultrastructure of cellulose from wood. *Wood Science and Technology*, 3(3), 203-217.

Fengel, D., and Stoll, M. (1973): Über die Veränderungen des Zellquerschnitts, der Dicke der Zellwand und der Wandschichten von Fichtenholz-Tracheiden innerhalb eines Jahrringes. *Holzforschung*, 27(1), 1-7.

Fengel, D., and Wegener, G. (2003): *Wood. Chemistry, Ultrastructure, Reactions*, Remangen: Kessel Verlag.

Fergus, B. J., Procter, A. R., Scott, J. A. N., and Goring, D. A. I. (1969): The distribution of lignin in sprucewood as determined by ultraviolet microscopy. *Wood Science and Technology*, 3(2), 117-138.

Florian Mary-Lou, E. (1981): Analyses of different states of deterioration of terrestical waterlogged wood. Conservation implication of the analyses. A review. In: *ICOM Committee for Conservation 6th Triennial Meeting*, Ottawa 1981. ICOM Committee for Conservation. Working Group: Waterlogged Wood. pp. 81/7/9-1 – 81/7/9-19.

Fors, Y., Grudd, H., Rindby, A., Jalilehvand, F., Sandström, M., Cato, I., and Bornmalm, L. (2014): Sulfur and iron accumulation in three marine-archaeological shipwrecks in the Baltic Sea: The Ghost, the Crown and the Sword. *Scientific reports*, 4: 4222.

Fors, Y., Jalilehvand, F., and Sandström, M. (2011): Analytical Aspects of Waterlogged Wood in Historical Shipwrecks. *Analytical Science*, 27, 785-792.

Fromm, J., Rockel, B., Lautner, S., Windeisen, E., and Wanner, G. (2003): Lignin distribution in wood cell walls determined by TEM and backscattered SEM techniques. *Journal of Structural Biology*, 143(1), 77-84.

Fujita, M., and Harada, H. (2001): Ultrastructure and Formation of Wood Cell Wall. In: D. N.-S. Hon and N. Shiraishi (eds.). *Wood and cellulosic chemistry*. New York, Marcel Dekker, Inc., pp. 1-49.

Fukazawa, K. (1992): Ultraviolet Microscopy. In: S. Y. Lin and C. W. Dence (eds.). *Methods in Lignin Chemistry*. Berlin, Springer-Verlag, pp. 110-121.

Gelbrich, J., Carsten, M., and Militz, H. (2009): Evaluation of bacterial wood degradation by Fourier-Transform-Infrared (FTIR) measurements. In: *International Conference on Wooden Cultural Heritage: Evaluation of Deterioration and Management of Change. Cost Action IE0601 "Wood Science for Conservation of Cultural Heritage"*, Hamburg, Germany 2009.

Gelbrich, J., Mai, C., and Militz, H. (2008): Chemical changes in wood degraded by bacteria. *International Biodeterioration & Biodegradation*, 61(1), 24-32.

Giachi, G., Bettazzi, F., Chimichi, S., and Staccioli, G. (2003): Chemical characterisation of degraded wood in ships discovered in a recent excavation of the Etruscan and Roman harbour of Pisa. *Journal of Cultural Heritage*, 4(2), 75-83.

Giachi, G., and Pizzo, B. (2009): A chemical characterisation of the decay of waterlogged archaeological wood. In: Strætkvern, K, and Huisman, D.J. (eds.): *Proceedings of the 10th ICOM Group on Wet Organic Archaeological Materials Conference*, Amsterdam 2007. pp. 21-33.

Gierlinger, N., Keplinger, T., and Harrington, M. (2012): Imaging of plant cell walls by confocal Raman microscopy. *Nature Protocols*, 7(9), 1694-1708.

Gierlinger, N., Luss, S., König, C., Konnerth, J., Eder, M., and Fratzl, P. (2010): Cellulose microfibril orientation of Picea abies and its variability at the micron-level determined by Raman imaging. *Journal of Experimental Botany*, 61(2), 587-595.

Gierlinger, N., and Schwanninger, M. (2007): The potential of Raman microscopy and Raman imaging in plant research. *Spectroscopy: An International Journal*, 21(2), 69-89.

Goldstein, I. S. (1984): Degradation of Wood by Chemicals. In: R. Rowell (ed.). *The Chemistry of Solid Wood*. Washington D.C., American Chemical Society, pp. 575-586.

Greaves, H. (1971): The bacterial factor in wood decay. *Wood Science and Technology*, 5(1), 6-16.

Gregory, D., and Jensen, P. (2006): The importance of analysing waterlogged wooden artefacts and environmental conditions when considering their in situ preservation. *Journal of wetland archaeology*, 6, 65-81.

Guerra, A., Gaspar, A. R., Contreras, S., Lucia, L. A., Crestini, C., and Argyropoulos, D. S. (2007): On the propensity of lignin to associate: A size exclusion chromatography study with lignin derivatives isolated from different plant species. *Phytochemistry*, 68(20), 2570-2583.

Hames, B., Ruiz, R., Scarlata, C., Sluiter, J., and Templeton, D. (2008). Preparation of Samples for Compositional Analysis. Laboratory Analytical Procedure (LAP). National Renewable Energy Laboratory, Colorado, USA.

Harmsen, L., and Nissen, T. V. (1965): Timber Decay caused by Bacteria. *Nature*, 206(4981), 319-319.

Harris, P. J., and Stone, B. A. (2008): Chemistry and Molecular Organization of Plant Cell Walls. In: M. E. Himmel (ed.). *Biomass Recalcitrance. Deconstructing the Plant Cell Wall for Bioenergy*. Oxford, Blackwell Publishing, pp. 61-93.

Hatcher, P. G., Breger, I. A., and Earl, W. L. (1981): Nuclear magnetic resonance studies of ancient buried wood I. Observations on the origin of coal to the brown coal stage. *Organic Geochemistry*, 3(1-2), 49-55.

Hather, J. G. (2000): The Identification of the Northern European Woods. A guide for archaeologists and conservators, London: Archetype Publications Ltd.

Hedges, J. I. (1990): The Chemistry of Archaeological Wood. In: R. M. Rowell and R. J. Barbour (eds.). *Archaeological Wood. Propeties, Chemistry, and Preservation*. Washington, DC, American Chemical Society, pp. 111-140.

Hedges, J. I., Cowie, G. L., Ertel, J. R., James Barbour, R., and Hatcher, P. G. (1985): Degradation of carbohydrates and lignins in buried woods. *Geochimica et Cosmochimica Acta*, 49(3), 701-711.

Helms, A. C. (2008). *Bacterial Diversity in Waterlogged Archaeological Wood*. PhD thesis. Copenhagen, The National Museum of Denmark / DTU Biosys. 152 pp.

Helms, A. C., Camillo Martiny, A., Hofman-Bang, J., Ahring, K., and Kilstrup, M. (2004): Identification of bacterial cultures from archaeological wood using molecular biological techniques. *International Biodeterioration & Biodegradation*, 53(2), 79-88.

Herbst, C.F. (1861): Om bevaring af oldsager af træ fundne i tørvemoser. *Antiquarisk tidsskrift*, 1858-60, 174-176.

Hoffmann, P. (1981): Chemical wood analysis as a means of characterizing archaeological wood. In: Grattan, D. W., and McCawley, J. C. (eds.): Proceedings of the ICOM Waterlogged Wood Working Group Conference, Ottawa 1981. International Council of Museums (ICOM), Committee for Conservation, Waterlogged Wood Working Group.

Hoffmann, P., and Jones, M. A. (1990): Structure and Degradation Process for Waterlogged Archaeological Wood. *Archaeological Wood*. Washington, DC, American Chemical Society, pp. 35-65.

Holt, D. M. (1983): Bacterial degradation of lignified wood cell walls in aerobic aquatic habitats: Decay patterns and mechanisms proposed to account for their formation. *Journal of the Institute of Wood Science*, 9(5), 212-223.

Holt, D. M., and Jones, E. B. (1983): Bacterial degradation of lignified wood cell walls in anaerobic aquatic habitats. *Applied and Environmental Microbiology*, 46(3), 722-727.

Huisman, D. J., Manders, M. R., Kretschmar, E. I., Klaassen, R. K. W. M., and Lamersdorf, N. (2008): Burial conditions and wood degradation at archaeological sites in the Netherlands. *International Biodeterioration & Biodegradation*, 61(1), 33-44.

Iiyama, K., Kasuya, N., Tuyet, L. T. B., Nakano, J., and Sakaguchi, H. (1988): Chemical Characterization of Ancient Buried Wood. *Holzforschung*, 42(1), 5-10.

Jane, F. W. (1970): *The Structure of Wood*: Adam & Charles Black.

Jensen, P., Bojesen-Koefoed, I., Meyer, I., and Strætkvern, K. (Year): The Cellosolve-Petroleum Method. In: Hoffmann, P.; Daley,T. & Grant, T. (eds.): *Proceedings of the 5th ICOM Group on Wet Organic Archaeological Materials Conference*. Portland/Maine 1993. Bremerhaven. Pp. 523-535.

Jensen, P., and Jensen, J. B. (2006): Dynamic model for vacuum freeze-drying of waterlogged archaeological wooden artefacts. *Journal of Cultural Heritage*, 7(3), 156-165.

Jespersen, K. (1981): Conservation of waterlogged wood by use of tertiary butanol, PEG and freeze-drying. In: *Conservation of waterlogged wood. International symposium on the conservation of large objects of waterlogged wood*. Amsterdam 1979. The Hague, Netherlands National Commission for UNESCO, pp. 69-76.

Kataeva, I., Foston, M. B., Yang, S. J., Pattathil, S., Biswal, A. K., Poole, F. L., Basen, M., Rhaesa, A. M., Thomas, T. P., Azadi, P., Olman, V., Saffold, T. D., Mohler, K. E., Lewis, D. L., Doeppke, C., Zeng, Y. N., Tschaplinski, T. J., York, W. S., Davis, M., Mohnen, D., Xu, Y., Ragauskas, A. J., Ding, S. Y., Kelly, R. M., Hahn, M. G., and Adams, M. W. W. (2013): Carbohydrate and lignin are simultaneously solubilized from unpretreated switchgrass by microbial action at high temperature. *Energy & Environmental Science*, 6(7), 2186-2195.

Killham, K. (1994): *Soil ecology*, Cambridge: Cambridge University Press.

Kim, Y. S. (1990): Chemical Characteristics of Waterlogged Archaeological Wood. *Holzforschung*, 44(3), 169-172.

Kim, Y. S., and Singh, A. (1994): Ultrastructural Aspects of Bacterial Attacks on A Submerged Ancient Wood. *Mokuzai Gakkaishi*, 40(5), 554-562.

Kim, Y. S., and Singh, A. P. (1999): Micromorphological characteristics of compression wood degradation in waterlogged archaeological pine wood. *Holzforschung*, 53(4), 381-385.

Kim, Y. S., and Singh, A. P. (2000): Micromorphological characteristics of wood biodegradation in wet environments: A review. *Iawa Journal*, 21(2), 135-155.

Kim, Y. S., Singh, A. P., and Nilsson, T. (1996): Bacteria as Important Degraders in Waterlogged Archaeological Woods. *Holzforschung*, 50(5), 389-392.

Kirk, T. K., and Cowling, E. B. (1984): Biological Decomposition of Solid Wood. In: R. Rowell (ed.). *The Chemistry of Solid Wood*. Washington D.C., American Chemical Society, pp. 455-487.

Klaassen, R. K. W. M. (2008a): Bacterial decay in wooden foundation piles - Patterns and causes: A study of historical pile foundations in the Netherlands. *International Biodeterioration & Biodegradation*, 61(1), 45-60.

Klaassen, R. K. W. M. (2008b): Water flow through wooden foundation piles: A preliminary study. *International Biodeterioration & Biodegradation*, 61(1), 61-68.

Klaassen, R. K. W. M., and van Overeem, B. S. (2012): Factors that influence the speed of bacterial wood degradation. *Journal of Cultural Heritage*, 13(3), S129-S134.

Ko, J. J., Shimizu, Y., Ikeda, K., Kim, S. K., Park, C. H., and Matsui, S. (2009): Biodegradation of high molecular weight lignin under sulfate reducing conditions: Lignin degradability and degradation by-products. *Bioresource Technology*, 100(4), 1622-1627.

Koch, G., and Kleist, G. (2001): Application of Scanning UV Microspectrophotometry to Localise Lignins and Phenolic Extractives in Plant Cell Walls. *Holzforschung*, 55(6), 563-567.

Kollmann, F. F. P., and Côté, W. A. J. (1968): *Principles of Wood Science and Technology. I. Solid Wood.*, Berlin, Springer-Verlag. 592 pp.

Kretschmar, E. I., Gelbrich, J., Militz, H., and Lamersdorf, N. (2008): Studying bacterial wood decay under low oxygen conditions. Results of microcosm experiments. *International Biodeterioration & Biodegradation*, 61(1), 69-84.

Kubicek, C. P. (2013): *Fungi and Lignocellulosic Biomass*, Ames, Iowa: Wiley-Blackwell.

Kutscha, N. P., and Gray, J. R. (1972): The suitability of certain stains for studying lignification in balsam fir, Abies balsamea (L.) Mill. *Life Sciences and Agriculture experiment Station Technical Bulletin*, 53, 5-50.

Landy, E. T., Mitchell, J. I., Hotchkiss, S., and Eaton, R. A. (2008): Bacterial diversity associated with archaeological waterlogged wood: Ribosomal RNA clone libraries and denaturing gradient gel electrophoresis (DGGE). *International Biodeterioration & Biodegradation*, 61(1), 106-116.

Lange, J. (1999): Kulturplanternes indførselshistorie i Danmark indtil midten af 1900-tallet, Frederiksberg: DSR Forlag.

Larsen, J., Haven, M. O., and Thirup, L. (2012): Inbicon makes lignocellulosic ethanol a commercial reality. *Biomass & Bioenergy*, 46, 36-45.

Liese, J. (1950): Zerstörung des Holzes durch Pilze und Bakterien. In: F. Mahlke, E. Troschel, and J. Liese (eds.). *Holzkonservierung*. Berlin, Springer-Verlag, pp. 44-111.

Lindströmn, T. (1979): The colloidal behaviour of kraft lignin. *Colloid and Polymer Science*, 257(3), 277-285.

Lucejko, J. J. (2010). Waterlogged Archaeological Wood: Chemical study of wood degradation and evaluation of consolidation treatments. PhD thesis. Pisa University, VDM Verlag Dr. Müller.

Lucejko, J. J., Modugno, F., Ribechini, E., and del Rio, J. C. (2009): Characterisation of archaeological waterlogged wood by pyrolytic and mass spectrometric techniques. *Analytica Chimica Acta*, 654(1), 26-34.

Lundquist, K. (1992): Wood. In: S. Y. Lin and C. W. Dence (eds.). *Methods in Lignin Chemistry*. Berlin, Springe-Verlag, pp. 65-69.

Macchioni, N., Capretti, C., Sozzi, L., and Pizzo, B. (2013): Grading the decay of waterlogged archaeological wood according to anatomical characterisation. The case of the Fiave site (N-E Italy). *International Biodeterioration & Biodegradation*, 84, 54-64.

MacLeod, I. D., and Richards, V. L. (Year): The Impact of Metal Corrosion Products on the Degradation of Waterlogged Wood Recovered from Historic Shipwreck Sites. In: Hoffmann, P; Grant, T.; Spriggs, J.A. & Daley, T. (eds.): *Proceedings of the 6th ICOM Group on Wet Organic Archaeological Materials Conference*, York 1996. Bremerhaven. pp. 331-353.

MacLeod, I. D., and Richards, V. L. (Year): Wood Degradation on Historic Shipwreck Sites: The Use of FT-IR Spectroscopy to Study the Loss of Hemicellulose. In: Hoffmann, P; Grant, T.; Spriggs, J.A. & Daley, T. (eds.): *Proceedings of the 6th ICOM Group on Wet Organic Archaeological Materials Conference*, York 1996. Bremerhaven. pp. 203-225.

Marchessault, R. H. (1962): Application of infra-red spectroscopy to cellulose and wood polysaccharides. Pure and Applied Chemistry. Wood chemistry Symposium, Montreal, Canada, 9-11 August 1961. City, pp. 107-129.

Modugno, F., Lucejko, J. J., Ribechini, E., Colombini, M. P., and Del Rio, J. C. (2009): Characterization of archaeological waterlogged wood by mass spectrometric techniques. In: *italic 5. Science & Technology of Biomasses: Advances and Challenges.From forest and agricultural biomasses to high added value products: Processes and materials*, Villa Monasterio, Varenna (Como), Italy. Pp. 27-30

Nilsson, T., and Björdal, C. (2008a): Culturing wood-degrading erosion bacteria. *International Biodeterioration & Biodegradation*, 61(1), 3-10.

Nilsson, T., and Björdal, C. (2008b): The use of kapok fibres for enrichment cultures of lignocellulose-degrading bacteria. *International Biodeterioration & Biodegradation*, 61(1), 11-16.

Nilsson, T., Björdal, C., and Fällman, E. (2008): Culturing erosion bacteria: Procedures for obtaining purer cultures and pure strains. *International Biodeterioration & Biodegradation*, 61(1), 17-23.

Nilsson, T., and Daniel, G. (1986): Ligniolytic activity of wood degrading-bacteria. In: *Proceedings of the 3rd International Conference on Biotechnology in the Pulp and Paper Industry.* Stockholm 1986. Pp. 54-57

Nilsson, T., and Klaassen, R. K. W. M. (2008): Abiotic or bacterial degradation? *Iawa Journal*, 29(3), 336-338.

O'Brien, T. P., Feder, N., and McCully, M. E. (1964): Polychromatic staining of plant cell walls by toluidine blue O. *Protoplasma*, 59(2), 368-373.

Obst, J. R., McMillan, N. J., Blanchette, R. A., Christensen, D. J., Faix, O., Han, J. S., Kuster, T. A., Landucci, L. L., Newman, R. H., Pettersen, R. C., Schwandt, V. H., and Wesolowski, M. F. (1991): Characterization of Canadian Artic Fossil Woods. In: R. L. Christie and N. J. McMillan (eds.). *Tertiary Fossil Forests of the Geodetic Hills, Axel Heiberg Island, Arctic Archipelago*. pp. 123-146.

Ødum, S. (1968): Udbredelse af træer og buske i Danmark. *Botanisk Tidsskrift*, 64(36), 7-8.

Pan, D. R., Tai, D. S., Chen, C. L., and Robert, D. (1990): Comparative-Studies on Chemical-Composition of Wood Components in Recent and Ancient Woods of Bischofia-Polycarpa. *Holzforschung*, 44(1), 7-16.

Pareek, S., Azuma, J. I., Matsui, S., and Shimizu, Y. (2001): Degradation of lignin and lignin model compound under sulfate reducing condition. *Water Science and Technology*, 44(2-3), 351-358.

Pavia, D. L., Lampman, G. M., Kriz, G. S., and Vyvyan, J. R. (2009): *Introduction to spectroscopy*, Belmont, USA: Brooks/Cole.

Pavlikova, H., Sykorova, I., Cerny, J., Sebestova, E., and Machovic, V. (1993): Spectroscopic study of degraded woods from the Elbe river valley. *Energy & Fuels*, 7(3), 351-356.

Pedersen, N. B., Jensen. P., Botfeldt, K. (2013): A strategy for testing impregnation agents for waterlogged archaeological wood – examination of azelaic acid as an impregnation agent. In: Strætkvern, K. and Williams, E. (eds.): Proceedings of the 11th ICOM-CC Group on Wet Organic Archaeological Materials Conference. Greenville 2010. Internationl Council of Museums (ICOM), Committee for Conservation. Pp. 185-206.

Pelletier, M. J., and Pelletier, C. C. (2010): Spectroscopic Theory for Chemical Imaging. *Raman, Infrared, and Near-Infrared Chemical Imaging*. John Wiley & Sons, Inc., pp. 1-20.

Petrou, M., Edwards, H., Janaway, R., Thompson, G., and Wilson, A. (2009): Fourier-transform Raman spectroscopic study of a Neolithic waterlogged wood assemblage. *Analytical and Bioanalytical Chemistry*, 395(7), 2131-2138.

Pizzo, B., Pecoraro, E., and Macchioni, N. (2013): A New Method to Quantitatively Evaluate the Chemical Composition of Waterlogged Wood by Means of Attenuated Total Reflectance Fourier Transform Infrared (ATR FT-IR) Measurements Carried Out on Wet Material. *Applied Spectroscopy*, 67(5), 553-562.

Rehbein, M., Koch, G., Schmitt, U., and Huckfeldt, T. (2013): Topochemical and transmission electron microscopic studies of bacterial decay in pine (*Pinus sylvestris* L.) harbour foundation piles. *Micron*, 44(0), 150-158.

Richter, S., Müssig, J., and Gierlinger, N. (2011): Functional plant cell wall design revealed by the Raman imaging approach. *Planta*, 233(4), 763-772.

Saariaho, A. M., Jaaskelainen, A. S., Nuopponen, M., and Vuorinen, T. (2003): Ultra violet resonance Raman spectroscopy in lignin analysis: Determination of characteristic vibrations of p-hydroxyphenyl, guaiacyl, and syringyl lignin structures. *Applied Spectroscopy*, 57(1), 58-66.

Saka, S. (2001): Chemical Composition and Distribution. In: D. N.-S. Hon and N. Shiraishi (eds.). *Wood and cellulosic chemistry*. New York, Marcel Dekker, Inc., pp. 51-81.

Salmén, L. (2004): Micromechanical understanding of the cell-wall structure. *Comptes Rendus Biologies*, 327(9-10), 873-880.

Salmén, L., and Burgert, I. (2009): Cell wall features with regard to mechanical performance. A review. *Holzforschung*, 63(2), 121-129.

Salmén, L., Olsson, A. M., Stevanic, J. S., Simonovic, J., and Radotic, K. (2012): Structural organisation of the wood polymers in the wood fibre structure. *Bioresources*, 7(1), 521-532.

Sandak, A., Sandak, J., Zborowska, M., and Pradzynski, W. (Year): Characterization of archeological oak (*Quercus* sp.) with mid and near infrared spectroscopy. *Presented at International Conference on Wooden Cultural Heritage: Evaluation of Deterioration and Management of Change. COST Action IE0601 "Wood Science for Conservation of Cultural Heritage"*.

Sandak, A., Sandak, J., Zborowska, M., and Pradzynski, W. (2010): Near infrared spectroscopy as a tool for archaeological wood characterization. *Journal of Archaeological Science*, 37(9), 2093-2101.

Scheller, H. V., and Ulvskov, P. (2010): Hemicelluloses. *Annual Review of Plant Biology*, 61, 263-289.

Schmidt, O., and Liese, W. (1994): Occurrence and Significance of Bacteria in Wood. *Holzforschung*, 48(4), 271-277.

Schmidt, O., Moreth, U., and Schmitt, U. (1995): Wood degradation by a bacterial pure culture. *Material und Organismen*, 29(4), 289-293.

Schmidt, O., Nagashima, Y., Liese, W., and Schmitt, U. (1987): Bacterial Wood Degradation Studies under Laboratory Conditions and in Lakes. *Holzforschung*, 41(3), 137-140.

Schmitt, U., and Melcher, E. (2004): Section staining with potassium permanganate for transmission electron microscopy: A useful tool for lignin localisation. In: U. Schmitt, P. Ander, J. R. Barnett, A. M. C. Emons, G. Jeronimiidis, P. Saranpää, and S. Tschegg (eds.). *Wood Fibre Cell Walls: Methods to Study their Formation, Structure and Properties*. Uppsala, Swedish University of Agricultural Science, pp. 105-117.

Schniewind, A. P. (1990): Physical and Mechanical Properties of Archaeological Wood. *Archaeological Wood*. Washington, DC, American Chemical Society, pp. 87-109.

Schwanninger, M., Rodrigues, J. C., Pereira, H., and Hinterstoisser, B. (2004): Effects of short-time vibratory ball milling on the shape of FT-IR spectra of wood and cellulose. *Vibrational Spectroscopy*, 36(1), 23-40.

Scott, J. A. N., and Goring, D. A. I. (1970): Lignin Concentration in the S_3 Layer of Softwood. *Cellulose Chemistry and Technology*, 4, 83-93.

Singh, A., Daniel, G., and Nilsson, T. (2002a): High variability in the thickness of the S3 layer in *Pinus radiata* tracheids. *Holzforschung*, 56(2), 111-116.

Singh, A., Daniel, G., and Nilsson, T. (2002b): Ultrastructure of the S2 layer in relation to lignin distribution in Pinus radiata tracheids. *Journal of Wood Science*, 48(2), 95-98.

Singh, A., Schmitt, U., Möller, R., Dawson, B., and Koch, G. (2006): Ray tracheids in *Pinus radiata* are more highly resistant to soft rot as compared to axial tracheids: relationship to lignin concentration. *Wood Science and Technology*, 40(1), 16-25.

Singh, A. P. (1997a): Initial pit borders in *Pinus radiata* are resistant to degradation by soft rot fungi and erosion bacteria but not tunnelling bacteria. *Holzforschung*, 51(1), 15-18.

Singh, A. P. (1997b): The ultrastructure of the attack of *Pinus radiata* mild compression wood by erosion and tunnelling bacteria. *Canadian Journal of Botany-Revue Canadienne de Botanique*, 75, 1095-1102.

Singh, A. P., and Butcher, A. J. (1991): Bacterial degradation of wood cell walls: a review of degradation patterns. *Journal of the Institute of Wood Science*, 12(3), 143-157.

Singh, A. P., and Daniel, G. (2001): The S2 layer in the tracheid walls of *Picea abies* wood: Inhomogeneity in lignin distribution and cell wall microstructure. *Holzforschung*, 55(4), 373-378.

Singh, A. P., Kim, Y. S., Wi, S. G., Lee, K. H., and Kim, I. J. (2003): Evidence of the degradation of middle lamella in a waterlogged archaeological wood. *Holzforschung*, 57(2), 115-119.

Singh, A. P., Nilsson, T., and Daniel, G. F. (1990): Bacterial attack of *Pinus Sylvestris* wood under near anaerobic conditions. *Journal of the Institute of Wood Science*, 11(6), 237-249.

Sluiter, A., Hames, B., Ruiz, R., Scarlata, C., Sluiter, J., and Templeton, D. (2005a). Determination of Ash in Biomass. Laboratory Analytical Procedure (LAP). National Renewable Energy Laboratory, Colorado, USA.

Sluiter, A., Hames, B., Ruiz, R., Scarlata, C., Sluiter, J., and Templeton, D. (2010). Determination of Structural Carbohydrates and Lignin in Biomass. Laboratory Analytical Procedure (LAP). National Renewable Energy Laboratory, Colorado, USA.

Sluiter, A., Ruiz, R., Scarlata, C., Sluiter, J., and Templeton, D. (2005b). Determination of Extractives in Biomass. Laboratory Analytical Procedure (LAP). National Renewable Energy Laboratory, Colorado, USA.

Sun, L., Simmons, B. A., and Singh, S. (2011): Understanding Tissue Specific Compositions of Bioenergy Feedstocks Through Hyperspectral Raman Imaging. *Biotechnology and Bioengineering*, 108(2), 286-295.

Sun, L., Varanasi, P., Yang, F., Loque, D., Simmons, B. A., and Singh, S. (2012): Rapid determination of syringyl: Guaiacyl ratios using FT-Raman spectroscopy. *Biotechnology and Bioengineering*, 109(3), 647-656.

Tate, R. L. (2000): *Soil microbiology*, New York: John Wiley & Sons, Inc.

Terashima, N., Kitano, K., Kojima, M., Yoshida, M., Yamamoto, H., and Westermark, U. (2009): Nanostructural assembly of cellulose, hemicellulose, and lignin in the middle layer of secondary wall of ginkgo tracheid. *Journal of Wood Science*, 55(6), 409-416.

Terashima, N., Yoshida, M., Hafren, J., Fukushima, K., and Westermark, U. (2012): Proposed supramolecular structure of lignin in softwood tracheid compound middle lamella regions. *Holzforschung*, 66(8), 907-915.

Thieme, H., and Maier, R. (1995): *Archäologische Ausgrabungen im Braunkohlentagebau Schöningen*, Hannover: Verlag Hahnsche Buchhandlung.

Thomassen, T. (1977): Træ og træmaterialer. Teknologisk Institut. Træteknik. 174 pp.

Thygesen, A., Oddershede, J., Lilholt, H., Thomsen, A. B., and Stahl, K. (2005): On the determination of crystallinity and cellulose content in plant fibres. *Cellulose*, 12(6), 563-576.

Thygesen, L. G., and Gierlinger, N. (2013): The molecular structure within dislocations in *Cannabis sativa* fibres studied by polarised Raman microspectroscopy. *Journal of Structural Biology*, 182(3), 219-225.

Tirumalai, V. C., Agarwal, U. P., and Obst, J. R. (1996): Heterogeneity of lignin concentration in cell corner middle lamella of white birch and black spruce. *Wood Science and Technology*, 30(2), 99-104.

van der Lelie, D., Taghavi, S., McCorkle, S. M., Li, L. L., Malfatti, S. A., Monteleone, D., Donohoe, B. S., Ding, S. Y., Adney, W. S., Himmel, M. E., and Tringe, S. G. (2012): The Metagenome of an Anaerobic Microbial Community Decomposing Poplar Wood Chips. *Plos One*, 7(5).

Vicuña, R. (1988): Bacterial degradation of lignin. *Enzyme and Microbial Technology*, 10(11), 646-655.

Wei, H., Xu, Q., Taylor II, L. E., Baker, J. O., Tucker, M. P., and Ding, S. Y. (2009): Natural paradigms of plant cell wall degradation. *Current Opinion in Biotechnology. Energy biotechnology / Environmental biotechnology*, 20(3), 330-338.

Westermark, U., Lidbrandt, O., and Eriksson, I. (1988): Lignin distribution in spruce (*Picea abies*) determined by mercurization with SEM-EDXA technique. *Wood Science and Technology*, 22(3), 243-250.

Wiley, J. H., and Atalla, R. H. (1987): Band assignments in the raman spectra of celluloses. *Carbohydrate Research*, 160, 113-129.

Wilson, D. B. (2008): Aerobic Microbial Cellulase Systems. In: M. E. Himmel (ed.). *Biomass Recalcitrance. Deconstructing the Plant Cell Wall for Bioenergy*. Oxford, Blackwell Publishing, pp. 374-392.

Wilson, K., and White, D. J. B. (1986): *The Anatomy of Wood*: Stobart & Son.

Wilson, M. A., Godfrey, I. M., Hanna, J. V., Quezada, R. A., and Finnie, K. S. (1993): The degradation of wood in old Indian Ocean shipwrecks. *Organic Geochemistry*, 20(5), 599-610.

Wittköpper, M. (s.a.): Current developments in the preservation of archaeological wet wood with melamine/amino resins at the Romisch-Germanisches Zentralmuseum (online). http://www2.rgzm.de/navis/Conservation/ConservationUK.htm. Date of visit 25.05.2014.

Yelle, D. J., Kaparaju, P., Hunt, C.G., Hirth, K., Kim H., Ralph, J., and Felby, C. (2013): Two-Dimensional NMR Evidence for Cleavage of Lignin and Xylan Substituents in Wheat Straw Through Hydrothermal Pretreatment and Enzymatic Hydrolysis. *Bioenergy Research*, 6:211–221.

Young, L. Y., and Frazer, A. C. (1987): The Fate of Lignin and Lignin-Derived Compounds in Anaerobic Environments. *Geomicrobiology Journal*, 5(3-4), 261-293.

Zabel, R. A., and Morrell, J. J. (1992): *Wood Microbiology. Decay and Its Prevention*, San Diego: Academic Press, Inc.

Zeikus, J. G., Wellstein, A. L., and Kirk, T. K. (1982): Molecular Basis for the Biodegradative Recalcitrance of Lignin in Anaerobic Environments. *Fems Microbiology Letters*, 15(3), 193-197.

Zimmermann, W. (1990): Degradation of lignin by bacteria. *Journal of Biotechnology*, 13(2-3), 119-130.

Appendix A

This appendix contains experimental methods, which are not described in PAPER II and PAPER III.

Chapter 4: Light microscopy of sample material to determine wood species

To identify diagnostic characteristics of the three softwood poles from Kgs Nytorv and the softwood pole from Nibe 20-50 µm cross sections, tangential longitudinal sections, and radial longitudinal sections were cut from each pole on a microtome (Thermo Scientific Microm HM 450). In addition, similar sections of recent *Picea abies* (L.) Karst, *Larix* sp, and *Pinus sylvestris* L. were cut as reference material. Sections were either viewed unstained or stained with Safranin O (5 × 10-5 M Safranin O in 0.01 M acetate buffer containing 20 % ethanol). The slides were viewed by light microscope (Zeizz Axioplan) using 5x, 10x, and 20x magnifications.

Chapter 5 and Chapter 8: Light microscopy of sample material

To determine type of degradation and degree of degradation of the three softwood poles from Kgs Nytorv and the softwood pole from Nibe cross sections and tangential longitudinal sections were hand cut with a razor blade. Sections were cut at a distance of 0 mm, 10 mm, 20 mm and 40 mm from the surface from each pole. Some sections were stained with either 1% w/V safranine O in 96% ethanol, 0.1 % w/V safranine O in water, or 0.1 % w/V toluidine blue O in 0.1 M benzoate buffer (pH 4.4) to highlight the micro morphology of the wood xylem. Some sections were stained with 0.1 % w/V aniline blue in 50% lactic acid to highlight fungal hyphae. The section was either examined with a Zeiss Axioplan light microscope or Nikon Eclipse wide field microscope at 2.5x, 10x, 20x, and 40x magnifications.

Chapter 5: Scanning electron microscopy of sample material

Small block 50x50x50 mm^3 were cut with a razor blade from the sapwood of the Scots pine pole and from the surface layer and 10 mm below the surface from the Norway spruce sample material. The wood blocks were dehydrated in a series of acetone water solutions with concentration of 30 %, 50 %, 70 %, and 95 % for 10 minutes each. The samples were stored in 100 % acetone overnight at 5 °C. The samples were critical point dried, mounted on an aluminium stub each and sputter coated with a gold/palladium mixture. The samples were view in a FEI Quanta 200 scanning electron microscope with a traditional tungsten gun and an ET detector for detection of secondary electrons.

Sample preparation

50-100 g of waterlogged archaeological wood from the three Norway spruce poles and the Scots pine pole (Chapter 4) was cut into chips (100 µm) at a sliding microtome (Thermo Scientific Microm HM 450). The Norway spruce sample material included the whole degradation gradient from the heavily decayed surface area to sound xylem approximately two cm from the pith. The Scots pine sample material included xylem from the whole disc from heavily decayed surface to sound core. The material did not include visible compression wood. The wood chips were dried in an oven at 45 °C overnight before small batches of wood chips were milled in a coffee mill for 2 x 30 seconds. The mill was cooled between each batch to avoid heating of the wood. The coarse milled wood was further milled in a ball mill (Retsch MM 2000 steal ball mill) for 2 x 10 minutes at 50 rpm. The total solids of the milled wood material were determined on an automatic infrared moisture analyser (Sartorius MA 30) in duplicate. The procedure was modified from (Hames et al. 2008).

Determination of extractives

A Soxhlet apparatus was assembled with 3.5 g glass beads (3 mm in diameter) in each Soxhlet boiling flask. An extraction thimble for each sample was numbered with a pencil, oven dried overnight at 45 °C and weighted. 3-10 g of milled wood was put into each tarred extraction thimble and the weight recorded to the nearest 0.1 mg. The thimble was put into the Soxhlet tube and the material was moistened with demineralised water. 400 ± 5 mL demineralised water was added to the Soxhlet boiling flasks and the heating mantle switched on. The material was extracted with approximately two siphon cycles per hour for 24 hours. The Soxhlet apparatus was then turned off and cooled before all water in the system was combined and 50 ml of liquid was saved for carbohydrate analysis. 400 ± 5 mL ethanol (96 %) was added to the Soxhlet boiling flasks and the extraction was repeated for 24 hours with approximately four siphon cycles per hour. The Soxhlet apparatus was turned off and cooled before the solid material was washed with approximately 100 mL fresh ethanol. The thimble holding the sample material was air dried in fume hood overnight and then in oven at 45 °C overnight. The weight of thimble and material was recorded to the nearest 0.1 mg and the total solids of the extracted wood material were determined on an automatic infrared moisture analyser (Sartorius MA 30) in duplicate. The procedure was modified from (Sluiter et al. 2005b).

Monosaccharide content of the liquid from the hot water extraction was done by mixing 1000 µl water extract with 50 µl fucose standard solution (internal standard, 2.000 g/L) in an Eppendorf tube. Five standards containing 250, 100, 50, 25, 12.5, and 5 mg/L of each of the monosaccharides D-glucose, D-xylose, L-arabinose, D-mannose and D-galactose were prepared. 1000 µl of each standard solution was mixed with 50 µl fucose standard solution (internal standard, 2.000 g/L). The samples and standards were mixed well and transferred into HPLC vials. The monosaccharaide content (D-glucose, D-xylose, L-arabinose, D-mannose and D-galactose) was measured on a Dionex ICS5000-system

equipped with a CarboPac-PA1 column and using PAD-detection (Dionex, Sunnyvale, CA, USA). The flow rate was 1.0 ml/min and the eluent was MilliQ-water for 35 min followed by an increase to 200 mM NaOH for 10 min and a final equilibration with MilliQ-water for 10 min. The procedure was modified from (Sluiter et al. 2010).

Determination of Klason lignin and structural carbohydrates

0.3000 g oven dried sample material was put into 100 mL tared red cap glass bottles holding a Teflon coated magnet and cap in triplicate. 3.00 mL of 72 % H_2SO_4 was added and the bottles placed in water bath at 30 °C for 1 hour while stirred at 150 rpm. Then 84.00 mL MilliQ water was added to each glass bottle. The bottles were autoclaved at 121 °C for 1 hour with the six standards prepared as described below, cooled overnight and weighted.

A sugar stock solution was prepared from the monosaccharaides D-glucose anhydrate (30.0007 g), D-xylose (10.0003 g), L-arabinose (5.0003 g), D-mannose (9.9960 g) and D-galactose (4.9999 g) (standards from Sigma Aldrich, USA) in 1.0000 L MilliQ water. From this sugar stock solution six standards (S1-S6) were prepare in 100 mL tared red cap glass bottles according to the following: (standards from Sigma Aldrich, USA)

S1: 10.00 mL stock solution, 3.00 mL 72% H_2SO_4, 74.00 g MilliQ water
S2: 5.00 mL stock solution, 3.00 mL 72% H_2SO_4, 79.00 g MilliQ water
S3: 2.50 mL stock solution, 3.00 mL 72% H_2SO_4, 81.50 g MilliQ water
S4: 1.50 mL stock solution, 3.00 mL 72% H_2SO_4, 82.50 g MilliQ water
S5: 0.50 mL stock solution, 3.00 mL 72% H_2SO_4, 83.50 g MilliQ water
S6: 0.25 mL stock solution, 3.00 mL 72% H_2SO_4, 83.75 g MilliQ water

The autoclaved samples was filtered using a vacuum system and fritted glass crucibles that had been heated in in a muffle furnace at 550 °C for 3 hours, cool in a desiccator and weighed to 4 decimals just prior to use. 15 mL of the liquid filtrate was collected for sugar analysis. The bottles were rinsed with 30-50 ml water and any remaining solid is transferred to the filter crucible. The fritted glass crucibles were dried in an oven at 105 °C overnight and the exact mass recorded. The crucible was then heated in a muffle furnace at 550 °C for 3 hours and cooled to room temperature in a desiccator before recoding the exact mass. Ash free Klason lignin content was then calculated.

5.0 ml of liquid filtrate from the samples or 5.0 mL solution from the six standards were neutralised by adding using 0.20 g Ca_2CO_3 in 10 ml centrifugation tubes. The samples were gently mixed before centrifuged. 50 µl of supernatant from samples or standards were mixed with 950 µl of MilliQ water and 50 µl of fucose standard solution (internal standard, 2.000 g/L) in Eppendorf tubes. The samples were mixed well and filtered through a 0.45 µm filter into HPLC vials. The monosaccharaide content (D-glucose, D-xylose, L-arabinose, D-mannose and D-galactose) was measured on a Dionex ICS5000-system equipped with a CarboPac-PA1 column and using PAD-detection (Dionex,

Sunnyvale, CA, USA). The flow rate was 1.0 ml/min and the eluent was MilliQ-water for 35 min followed by an increase to 200 mM NaOH for 10 min and a final equilibration with MilliQ-water for 10 min. The procedure was modified from (Sluiter et al. 2010).

Determination of total ash

1.000 g of oven dried sample material (in duplicate) was put in a crucible that had been heated in a muffle furnace at 550 °C for 3 hours, cooled in a desiccator and weighed to 4 decimals just prior to use. The crucible was then heated in a muffle furnace at 550 °C for 3 hours and cooled to room temperature in a desiccator before recoding the exact mass. The procedure was modified from (Sluiter et al. 2005a)

Chapter 6: ATR-FTIR analysis

Wood specimens were cut in radial longitudinal direction with a thickness of approximately 1 mm 0-5 mm, 10-15 mm, and 20-25 mm from the surface in two areas on the three waterlogged archaeological Norway spruce poles (Chapter 4). Each position was sampled in triplicate (a total of 18 specimens from each pole). Five specimens were cut in radial longitudinal direction from *Picea abies* sapwood as reference material. ATR-FTIR analyses were conducted with a Thermo Scientific Nicolet 6700 FT-IR, Smart Golden gate ATR from 4000 cm^{-1} to 600 cm^{-1} with 50 scans and a resolution of 4.0 cm^{-1} at 25 °C. A background was taken with the same parameters, however with 100 scans. Spectra were normalized by standard normal variate (SNV) transformation, a data pre-treatment that scales and centres each spectrum and removes scattering effects (Barnes et al. 1989).

Chapter 8: Size exclusion chromatography

Sample preparation

20 g of heavily decayed waterlogged archaeological wood from the outer 0-5 mm of one Norway spruce pole (65087) (Chapter 4) was grated on a kitchen grater and air dried for two days. The dry material was ball milled in a ball mill (Retsch MM 2000 steal ball mill) for 2 x 10 minutes at 50 rpm.

Dissolution of sample material

A small amount of sample material was mixed with a 0.05 M lithium bromide in 9:1 DMSO:H_2O solution in an Eppendorf tube and kept in ultrasonic water for one hour. The Eppendorf tube was centrifuged at 12000 rpm for two minutes. The supernatant was transferred into a HPLC vial and loaded into the HPLC apparatus.

Size exclusion chromatography

The size exclusion chromatographic system contained a 300 mm column, 5 µm PolarSil analytical 100Å (Polymer Standard Service) equipped with a UV detector set at 280 nm. The samples were run at 40 °C with a flow of 1 mL/minute and 0.05 M lithium bromide in 9:1 DMSO:H_2O as eluent.

The following standards were run in addition to the waterlogged sample material with the same parameters: Phenol (94.11 g mol^{-1}) and tannic acid (1,701.20 g mol^{-1}). In addition, Kraft lignin from pine, organosolve lignin from wheat straw, and pre-treated wheat straw (heated to 180–200 °C for 10–20 min with steam) were used as reference materials.

Appendix B

This appendix contains simple theoretical calculations on the density of the residual wood structure left after erosion bacteria decay. Table B1 and Table B2 show data, abbreviations, and results for European Ash (*Fraxinus excelsior*) and Norway spruce (*Picea abies*).

Table B1: Data and abbreviations used for simplified theoretical calculation of the density of the residual wood structure left after erosion bacteria decay in European Ash (Fraxinus excelsior) and Norway spruce (Picea abies).

Data	Abbreviation	*Fraxinus excilsior*	*Picea abies*
Density of totally disintegrated wood (kg m^{-3})	ρ_{WAW}	≤100	≤100
Density, max. (kg m^{-3})	$\rho_{WOOD,\ max}$	803	910
Density, min. (kg m^{-3})	$\rho_{WOOD,\ min}$	385	290
Density, average (kg m^{-3})	$\rho_{WOOD,\ ave}$	650	380
Percentage lignin content of wood (%)	m_{lignin}/m_{wood}	25.6	27.3
Percentage cellulose content of wood (%)	$m_{cellulose}/m_{wood}$	37.9	46.0
Percentage hemicellulose content of wood (%)	m_{hemi}/m_{wood}	36.0	23.6
Percentage cellulose content in compound middle lamella (%)	$m_{cellulose}/m_{CML}$	-	≅ 3
Percentage hemicellulose content in compound middle lamella (%)	m_{hemi}/m_{CML}	-	≅ 18

Data from Fengel and Wegener (2003) and Kollmann and Côté (1968)

Calculations

1. Density of residual wood structure if all lignin is preserved and all carbohydrates are decayed ($\rho_{lignin,\ wood}$): $\rho_{lignin,wood} = \rho_{wood}\,(m_{lignin}/m_{wood})$

2. Density of residual wood structure if all lignin is preserved and all carbohydrates from compound middle lamella is preserved as is the case for wood decayed by erosion bacteria ($\rho_{wood,erosion}$):

   Density of lignin in whole wood structure ($\rho_{lignin,\ wood}$):

   $$\rho_{lignin,wood} = \rho_{wood}\,(m_{lignin}/m_{wood})$$

   Density of cellulose in compound middle lamella ($\rho_{cellulose,CML}$):

   $$\rho_{cellulose,CML} = \rho_{wood}\,(m_{cellulose}/m_{wood})(\ m_{cellulose}/m_{CML})$$

   Density of hemicellulose in compound middle lamella ($\rho_{hemicellulose,CML}$):

   $$\rho_{hemicellulose,CML} = \rho_{wood}\,(m_{hemiellulose}/m_{wood})(\ m_{hemicellulose}/m_{CML})$$

$$\rho_{wood,erosion} = \rho_{lignin,wood} + \rho_{cellulose,CML} + \rho_{hemicellulose,CML}$$

Table B2: Results for simplified theoretical calculation of the density of the residual wood structure left after erosion bacteria decay for European Ash (Fraxinus excelsior) and Norway spruce (Picea abies).

Results	***Fraxinus excilsior***	***Picea abies***
Density of residual wood structure if all lignin is preserved and all carbohydrates are decayed		
Density, max. (kg m^{-3})	206	248
Density, min. (kg m^{-3})	99	79
Density, average (kg m^{-3})	166	104
Density of residual wood structure if all lignin is preserved and all carbohydrates from compound middle lamella is preserved as is the case for wood decayed by erosion bacteria		
Density, max. (kg m^{-3})	267	300
Density, min. (kg m^{-3})	128	95
Density, average (kg m^{-3})	216	125

PAPERS I-III

Paper I

Pedersen, N.B., Björdal, C.G., Jensen, P., Felby, C. (2013): Bacterial Degradation of Archaeological Wood in Anoxic Waterlogged Environments. In: Stability of Complex Carbohydrate Structures. Biofuel, Foods, Vaccines and Shipwrecks. Harding, S.E. (ed.). The Royal Society of Chemistry. Special Publication No. 341. pp 160-187.

Paper II

Pedersen, N.B., Schmitt, U., Koch, G., Felby, C., Thygesen, L. G. (2014): Lignin distribution in waterlogged archaeological Picea abies (L.) Karst degraded by erosion bacteria. Holzforschung, Volume 68, Issue 7, pp 791-798. De Gruyter Holzforschung, Walter De Gruyter GmbH Berlin Boston, 2014. Copyright and all rights reserved.

Paper III

Pedersen, N.B., Gierlinger, N., Thygesen, L. G. (2015): Bacterial and abiotic decay of waterlogged archaeological Picea abies (L.) Karst studied by confocal Raman imaging and ATR-FTIR spectroscopy. Holzforschung, Volume 69, Issue 1, pp 103-112. De Gruyter Holzforschung, Walter De Gruyter GmbH Berlin Boston, 2015. Copyright and all rights reserved.

The papers are not included in this version of the thesis due to copyright.

FORMER ISSUES

Maj 2013	Landskabsbyens æstetik. En undersøgelse af fikmmediet som redskab til belysning af forstadens omgivelseskarakter *Mads Farsø* ISBN 978-87-7903-614-7
August 2013	Smallholder tree farming systems for livelihood enchancement and carbon storage *James Michael Roshetko* ISBN 978-87-7903-629-1
August 2013	Translating Harbourscape. Site-specific Design Approaches in Contemporary European Harbour Transformation *Lisa Diedrich* ISBN 978-87-7903-626-6
January 2014	Changing heathlands in a changing climate. Climate change effects on heathland plant communities *Johannes Ransijn* ISBN 978-87-7903-644-4
April 2014	Deriving harmonised forest information in Europe using remote sensing methods. Potentials and limitations for further applications *Lucia Maria Seebach* ISBN 978-87-7903-651-2
May 2014	Health Promoting Pocket Parks in a Landscape Architectural Perspective *Karin Kragsig Peschardt* ISBN 978-87-7903-658-1
August 2014	Adaptive properties of Adansonia digitata L. (Baobab) & Parkia biglobosa (Jacq.) R.Br. (African Locust Bean) to drought stress *Zoéwindé Henri-Noël Bouda* ISBN 978-87-7903-665-9
October 2014	Cemeteries–Organisation, management and innovation. Diffusion of maintenance specifications in Danish national church cemetery administrations *Christian Philip Kjøller* ISBN 978-87-7903-673-4
November 2014	Parks, People and Places. Place-based governance in urban green space maintenance *Julie Frøik Molin* ISBN 978-87-7903-675-8

November 2014 Assessing forest resources in Denmark using wall-to-wall remote sensing data
Johannes Schumacher
ISBN 978-87-7903-677-2

December 2014 Vegetation dynamics and community assembly in post-agricultural heathland
Sebastián Kepfer Rojas
ISBN 978-87-7903-671-0

March 2015 Improving and conserving sahelian fruits trees: a case study of *Parkia biglobosa* (Jacq.) Benth
Moussa Ouedraogo
ISBN 978-87-7903-693-7

May 2015 Microscopic and spectroscopic characterisation of waterlogged archaeological softwood from anoxic environments
Nanna Bjerregaard Pedersen
ISBN 978-87-7903-707-6

PhD Thesis May 2015
ISBN 978-87-7903-707-6

Nanna Bjerregaard Pedersen

Microscopic and spectroscopic characterisation of waterlogged archaeological softwood from anoxic environments

DEPARTMENT OF GEOSCIENCES AND
NATURAL RESOURCE MANAGEMENT

UNIVERSITY OF COPENHAGEN

ROLIGHEDSVEJ 23
DK-1958 FREDERIKSBERG

TLF +45 35 33 15 00
IGN@IGN.KU.DK
WWW.IGN.KU.DK